Development of nano/micro hybrid susceptor sheet for induction heating applications

Vom Fachbereich für Maschinenbau und Verfahrenstechnik

der Technischen Universität Kaiserslautern

zur Erlangung des akademischen Grades

Doktor-Ingenieur (Dr.-Ing.)

genehmigte

Dissertation

von

Herrn

M. Sc. Muhammad Muddassir

aus Pakistan

2016

D 386

Table of Contents

Table of Figures

Abstract

Thermoplastic composite materials are being widely used in the automotive and aerospace industries. Due to the limitations of shape complexity, different components need to be joined. They can be joined by mechanical fasteners, adhesive bonding or both. However, these methods have several limitations. Components can be joined by fusion bonding due to the property of thermoplastics. Thermoplastics can be melted on heating and regain their shape on cooling. This property makes them ideal for joining through fusion bonding by induction heating. Joining of non-conducting or non-magnetic thermoplastic composites needs an additional material that can generate heat by induction heating.

Polymers are neither conductive nor electromagnetic so they don't have inherent potential for inductive heating. A susceptor sheet having conductive materials (e.g. carbon fiber) or magnetic materials (e.g. nickel) can generate heat during induction. The main issues related with induction heating are non-homogeneous and uncontrolled heating.

In this work, it was observed that to generate heat with a susceptor sheet depends on its filler, its concentration, and its dispersion. It also depends on the coil, magnetic field strength and coupling distance. The combination of different fillers not only increased the heating rate but also changed the heating mechanism. Heating of 40°C/ sec was achieved with 15wt.-% nickel coated short carbon fibers and 3wt.-% multi-walled carbon nanotubes. However, only nickel coated short carbon fibers (15wt-.%) attained the heating rate of 24°C/ sec. In this study, electrical conductivity, thermal conductivity and magnetic properties testing were also performed. The results also showed that electrical percolation was achieved around 15wt.-% in fibers and (13-6)wt.-% with hybrid fillers. Induction heating tests were also performed by making parallel and perpendicular susceptor sheet as fibers were uni-directionally aligned. The susceptor sheet was also tested by making perforations.

The susceptor sheet showed homogeneous and fast heating, and can be used for joining of non-conductive or non-magnetic thermoplastic composites.

Kurzfassung

Thermoplastische Materialien finden ein breites Anwendungsspektrum in der Auto-mobil- und Luftfahrtindustrie. Langfaser- und Glasmattenverstärkte Thermoplaste werden zur Herstellung verschiedener Komponenten herangezogen. Die Größe der Komponenten wird jedoch durch den Herstellungsprozess eingeschränkt. Durch die Einschränkung der geometrischen Komplexität wird die Verbindung von thermoplas-tischen Komponenten zu einem kritischen Prozessschritt. Thermoplaste können durch mechanische Schrauben oder durch Kleben miteinander verbunden werden. Diese Fügeverfahren bringen mehrere Einschränkungen und nachteilige Effekte mit sich. Mechanische Schrauben erhöhen das Gewicht, die Spannungskonzentration um Löcher, die Anzahl an Delaminationen und ermöglichen Korrosion an der Verbin-dung. Das Kleben benötigt eine umfangreiche Vorbehandlung der Oberfläche und lange Aushärtezeiten und bringt Schwierigkeiten bei der Überprüfung der Grenzflä-che mit sich. Fusions-Bonden und Schweißen stellen eine gute Alternative dar, um die Probleme zu überwinden. Mit diesen Verfahren kann nicht nur das Gewicht und die Prozesszeit verringert werden, sondern ebenso der Aufwand für eine Oberflä-chenvorbehandlung reduziert werden. Beim Fusions-Bonden gibt es mehrere Mög-lichkeiten Wärme zu generieren. Diese sind: Ganzkörpererwärmung, Erwärmung durch Reibung, Elektromagnetische Erwärmung und zweistufige Verfahren. Bei der elektromagnetischen Erwärmung bei der der Fügeprozess über ein elektromagneti-sches Feld realisiert wird spricht man von induktivem Erwärmen bzw. induktivem Schweißen. Die Verbindung zweier nichtleitender oder unmagnetischer thermoplasti-scher Materialien kann über eine Suszeptorfolie realisiert werden. Polymere sind we-der leitfähig noch elektromagnetisch und zeigen daher kein inhärentes Potential für eine induktive Erwärmung. Eine Suszeptorfolie mit leitfähigen (z.B. Kohlenstofffa-sern) oder magnetischen Materialien (z.B. Nickel) kann zur induktiven Erwärmung dienen, jedoch müssen elektrisch leitfähige Fasern eine Voraussetzung erfüllen, z.B. die Bildung geschlossener elektrischer Netzwerke.

Das Verbinden leitfähiger Thermoplaste kann durch deren Leitfähigkeit über indukti-ve Erwärmung erfolgen. Der größte Nachteil der leitfähigen Thermoplaste liegt in der thermisch bedingten Entstehung von Defekten in der Faser-Matrix Grenzfläche. Für spezielle Anwendungen kann eine Suszeptorfolie verwendet werden. Diese Suszep-torfolie sollte eine elektrische und/oder magnetische Suszeptibilität besitzen, um Wärme über die genannten Prozesse wie magnetische Hystereseverluste oder ohm-

sche Verluste durch die Erwärmung von Fasern und Knotenpunkten, zu generieren. Die Suszeptorfolie ermöglicht durch eine schnelle und homogene Erwärmung einen schnellen Prozess.

In dieser Arbeit wurden die Materialien für die Suszeptorfolie auf der Grundlage ihres Potentials für eine induktive Erwärmung ausgewählt. Ausgewählt wurden Nickel beschichtete Kohlenstofffasern (NiSCF), Nickel beschichtete Graphitpartikel (NiCGP), Multiwall Carbon Nanotubes (MWNTs) und Permalloy Flocken. Die Fasern waren in der Größenordnung von Millimetern und die Partikel in der Größenordnung von Mikrometern. Die Fasern hatten entsprechend ein hohes Aspektverhältnis und die Partikel ein niedriges Aspektverhältnis. Polypropylen (PP) wurde als thermoplastische Matrix aufgrund der Kosten und einfachen Verarbeitbarkeit ausgewählt. Die elektrische und thermische Leitfähigkeit sowie die magnetischen Eigenschaften wurden gemessen und mit der induktiven Erwärmbarkeit korreliert. Unterschiedliche Gewichtsanteile und Kombinationen der genannten Materialien wurden untersucht.

Suszeptorfolien wurden über Aufschmelzen und Mischen hergestellt. Dazu wurden ein Doppelschneckenextruder und ein kleiner Extruder im Labormaßstab verwendet. Dünne Suszeptorfolien wurden über einen Kalander verarbeitet, jedoch wurden die Folien für den Labormaßstab in der Heißpresse hergestellt. In den Suszeptorfolien, die über den Kalander hergestellt wurden, wurden die Fasern parallel zur Verarbeitungsrichtung ausgerichtet. Bei den Labormaßstabs Folien wurden die Fasern stochastisch verteilt. Die Experimente zur induktiven Erwärmung wurden mit einer kreisförmigen Flachspule an einem selbst entwickelten Versuchsstand durchgeführt. Die Versuche wurden ebenfalls in Abhängigkeit der Frequenz durchgeführt. Die Einflüsse der Füllstoffkonzentration und der Frequenz wurden analysiert. Infrarot-Thermographie wurde zur Temperaturmessung und -visualisierung verwendet.

Die Ergebnisse aus den Versuchen zur induktiven Erwärmung der mit Fasern gefüllten Suszeptorfolien (NiSCF) wiesen auf eine schnelle und homogene Erwärmung hin. Hier wurde ein steiler Anstieg der Temperatur beobachtet. Die Folien mit Partikeln und hybriden Füllstoffen (Partikel und Fasern) zeigten ebenfalls ein hohes Potential für die induktive Erwärmung, jedoch konnte hier kein steiler Anstieg in der Temperatur beobachtet werden. In den Suszeptorfolien mit Fasern konnte eine induktive Erwärmung durch magnetische Hysterese und Wirbelstromverluste beobachtet werden. Durch die Nickelbeschichtung konnte eine Erwärmung über magnetische Hysterese und durch die elektrisch leitfähigen Fasern eine Erwärmung durch Wir-

belstromverluste erzielt werden. Wirbelstromverluste führen im Vergleich zur magnetischen Hysterese zu einer schnellen Temperaturerhöhung. Es konnte damit gezeigt werden, dass die Fasern einen kombinierten Effekt aufzeigten. Die mit Partikeln gefüllten Suszeptorfolien zeigten nur magnetische Hysterese. Die Folien mit hybriden Füllstoffen zeigten ebenfalls einen kombinierten Erwärmungseffekt, jedoch war der Effekt durch die magnetische Hysterese aufgrund des hohen Nickelgehaltes größer als bei den Partikeln und Fasern.

Multiwall Carbon Nanotubes wurden mit den Fasern in unterschiedlichen Konzentrationen hinzugefügt. Die Suszeptorfolie mit MWNTs und Fasern zeigte im Vergleich zu den Fasern und hybriden Füllstoffen eine sehr gute Erwärmung. Der Anstieg in der Temperatur war vergleichbar mit dem bei den Fasern. Der Mechanismus zur Erwärmung war hauptsächlich auf Wirbelstromverluste zurückzuführen, jedoch gab es einen kleinen Anteil an magnetischer Hysterese. Wärmebilder der mit Fasern und MWNTs gefüllten Suszeptorfolien bestätigten, dass ohmsche Verluste den dominanten Mechanismus zur Erwärmung bildeten.

Die Suszeptorfolien mit unterschiedlichen Konzentrationen an Permalloy Flocken und Fasern wurden ebenfalls hergestellt. Aufgrund der hohen magnetischen Permeabilität dieser Flocken konnte bei hohen Frequenzen eine gute Erwärmung erzielt werden.

Die Maschineneinstellungen zur induktiven Erwärmung beeinflussen die Erwärmung. Ebenso beeinflussen die Materialeigenschaften die Erwärmung. Elektrische Leitfähigkeit, thermische Leitfähigkeit, magnetische Permeabilität und Wärmekapazität wurden gemessen, um deren Einfluss auf die Erwärmung zu analysieren. Die elektrische Leitfähigkeit der mit Fasern gefüllten Suszeptorfolien war größer als die der mit hybriden Partikeln gefüllten Folien. Im Gegensatz dazu waren die magnetischen Eigenschaften (z.B. Remanenz x Koerzitivität) der hybriden Füllstoffe am höchsten. Die hohen magnetischen Werte bei den hybriden Füllstoffen zeigten, dass die magnetische Hysterese einen großen Einfluss auf die Erwärmung hat. Ebenso zeigte die elektrische Leitfähigkeit der Fasern einen großen Einfluss auf die Erwärmung. Die Ergebnisse zur thermischen Leitfähigkeit waren aufgrund der geringen Füllstoffkonzentration unklar, jedoch zeigten die Ergebnisse zur Wärmekapazität, dass die Heiz- und Abkühlraten mit ansteigender Füllstoffkonzentration verbessert werden konnten.

Abbreviations and Variables

Abbreviations

PP	Polypropylene
NiCSCF	Nickel coated short carbon fibers
NiCGP	Nickel coated graphite particles
MWNTs	Multiwall carbon nanotubes
Emf	Electromotive force
AC	Alternating current
DC	Direct current
CNT	Carbon nanotubes
VSM	Vibratory sample magnetometer
PAN	Polyacrylic nitrile
SCF	Short Carbon Fibers
IR	Infrared
SEM	Scanning electron microscopy
ESD	Electrostatic discharge
EMI	Electromagnetic interference
RFI	Radiofrequency interference

Variables

Tm	[°C]	Melting Temperature
Tg	[°C]	Glass transition temperature
ρ_f	[Ohm/m]	Specific Resistivity of fiber
A_f	[mm]	Area of fiber
l_f	[mm]	Length of fiber
d_f	[mm]	Diameter of fiber
Ω	[rad/s]	Angular frequency
$\varepsilon_\circ$	[F/m]	Permittivity of vacuum
emf	[volt]	Electromotive force
dV_f	[volt]	Potential difference
R_{id}	[Ω]	Junction dielectric impedance
K	[Ω]	Dielectric constant
T_{cu}	[°C]	Curie Temperature
B	[T]	Flux density
M	[emu/g]	Magnetization (Mass)
H	[T]	Magnetization force
Hc	[A/m]	Coercivity
Br	[T]	Remanence
J	[T]	Polarization
μ	[-]	Magnetic Permeability
$\mu_\circ$	[-]	Magnetic Permeability of vacuum
μ_r	[-]	Relative Magnetic Permeability
δ	[m]	Penetration Depth
P	[Ohm-m]	Resistivity
R	[Ω]	Resistance
Σ	[S/m]	Electrical conductivity
T	[-]	Fitted Constant
φ_f	[vol%]	Filler Concentration
φ_c	[vol%]	Critical Filler Concentration
Q	[W]	Heatflux
ΔT	[K]	Temperature difference
Δx	[m]	Thickness
K	[W/mK]	Thermal Conductivity
F	[J/gK]	Specific Thermal Capacity

f	[1/ sec]	Frequency
I	[A]	Current
H	[A/m]	Magnetic field strength
L	[H]	Inductance
T	[°C]	Temperature
$Qind$	[Joules]	Inductive heat generated

1. Introduction

Composite materials are a fast growing industry due to various advantages over metals. Different properties and their comparison with metals and composite materials can be seen in figure 1. Composite have low density and thermal expansion, high stiffness, strength and superior fatigue. Compositelightweight structures are replacing the metals [1]. Composite materials consist of a matrix and reinforcement. Thermosetting and thermoplastic polymer matrices are being used in fiber composites. Both of these thermosets and thermoplastic have different characteristics. Continuous fiber reinforced thermoplastic composites are being used due to many advantages in comparison to the widely used thermoset composites. Thermoplastics have high fracture toughness and damage tolerance, ease of shape forming, significantly low cycle times, low manufacturing cost and fast production [2] properties. Finally they have long shelf life of raw materials [3] [4].
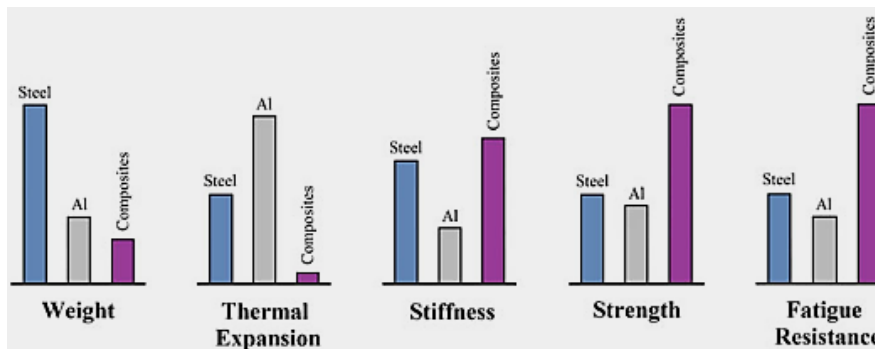
Figure 1: Comparison between conventional materials and composite materials[5]

Continuous reinforced fiber composites have lightweight and high specific properties and are suitable for aerospace, automotive, construction and engineering applications. Leading aerospace and automobile companies have increased the use of composite materials. Boeing is using 50% composite materials in their Dreamliner 787[6] and Airbus in A350-900XWB, is using more than 50%[7] and getting advantage of weight reduction as well as less fuel consumption. Similarly, automotive industry uses glass mat reinforced thermoplastic and long fiber reinforced thermoplastic to manufacture different components[8] [9] [10] [11]. Automotive industry is also targeting fuel efficient and cost effective cars with reliability and added features[12]. BMW has introduced various components of composite materials in their cars and got advantage of weight saving and less fuel consumption. In their models i3 and i8, they have saved up to 12-20% weight[13].

It is difficult to produce parts of complex geometries, with continuous thermoplastic composites [14].The process for continuous thermoplastic fiber reinforced composites starts with textile fibers and polymers, passing through impregnation and consolidation process[15].Later on these semi-finished sheets are shaped by thermoforming process[16]. Finally manufacturing of complex structures and large parts can be done by joining technology application. Therefore, introducing the joining operation within the processing cycle, various complex components can be developed. Joints can be of classified, (i) joints that can open by external force to destroy the joint (ii) partial detachable joints for repair purpose (iii) bolted joint can be opened with external force however without destroying the joint.
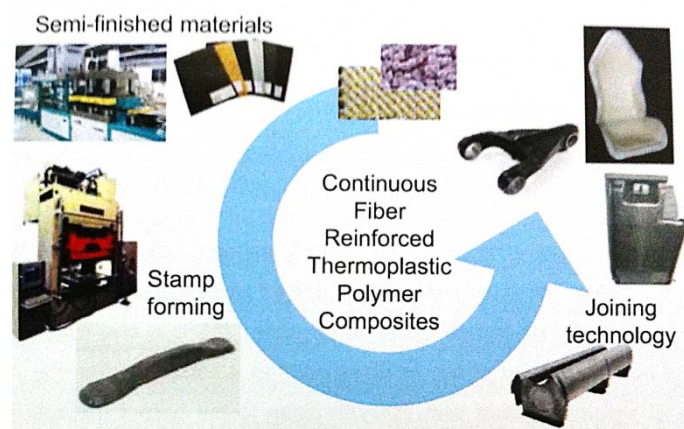
Figure 2: Processing chain for continuously reinforced thermoplastic composites[15]

In figure 2, processing cycle can be seen that starts from impregnation and consolidation and in next step these semi-finished sheets are transformed into different shaped parts. In last step, these parts are joined with other metal or thermoplastic parts.

There are different conventional joining technologies already being used since long time; however they are not ideal for thermoplastic composites. Mechanical fastening and adhesive bond are the two most widely and established joining methods[17] [18] [19], however other methods like combined mechanical and adhesive joint, co-curing process and stitching, are also being used as per desired structure.

Following are the disadvantages of the above mentioned joining methods.

Mechanical fastening (disadvantages)

- Fastening systems increases the weight
- Making holes and cut-out creates stress concentration around holes.
- If holes are being made by drilling delamination can take place.

- Fasteners and composite have different coefficient of thermal expansion therefore thermally induced stress can occur.
- Galvanic corrosion at joints in case of aluminum bolts and CFRP
- It's cost of titanium fasteners.

Adhesive bonding (disadvantages)

- Extensive surface preparation [20].
- Long curing times [21].
- It's quality assurance effort.

Keeping the above mentioned problems associated with mechanical fastening and adhesive bonding, there should be such a method for joining that it can take place without these drawbacks. Joining of thermoplastic composites can be done by fusion bonding. Fusion bonding or welding is a well-established technology[22] [23]. This technique is based on melting and reconsolidation of joining partners at the bond line, however to generate heat near bonding partners may be different[24] [25]. Fusion bonding technique not only eliminates the above mentioned drawbacks but also has advantages for rapid bonding, automation of process and reprocessing. Although mechanical fastening is a well-established technique, nevertheless fusion bonding is also capable to produce high strength joints that are comparable to other techniques[23]. Fusion bonding is further classified on the basis of heat generation at bondline e.g. induction welding, ultrasonic welding and resistance welding. Induction heating is considered to be most suitable technique that has advantages of fast heating at bondline, contact less heating, and low negative thermal effects on the polymers. Due to contact less heating process, geometrically complex parts can be heated which is difficult in other techniques. Fusion bonding can be performed in static as well as dynamic mode. In dynamic mode, relative movement between the sample and the coil can be made. Sample holding platform can be used as moving while coil remain static to form a continuous welding process [26].

In fusion bonding, sub-categories have different advantages. However, the main advantage of induction welding is the ability of process automation and energy saving[27] [28]. In non-conducting and non-magnetic materials, external heating elements are required to generate the heat. For these external elements, they should fulfill various requirements to obtain fast and homogenous heating. These external elements can be susceptor sheet of same thermoplastic matrix. The susceptor sheet should have adequate thickness and filler concentration of heating elements that can generate fast heating.

Motivation and Scope of the Work

Joining of composites materials by conventional techniques has several disadvantages. In alternative technique that can overcome these disadvantages is needed. However, selecting a method for joining depends on various aspects that should be considered. For example structural material, manufacturing process limitations, weight, repair, transportation of assembly, surface preparation and environmental exposure. To make large or complex parts, the most cost effective method involves molding two or more parts and joining them together[22].

The joining method should be fast, reliable, industrially feasible and have no adverse effect on environment. Further, it should be possible that process can be automated for continuous process. Fusion bonding by induction heating is a contact less and robust technique that is suitable for electrically conductive or magnetic materials[23]. Materials that are susceptible to electromagnetic field can be joined however non-conductive and non-magnetic materials cannot be joined. For such materials, an additional joining sheet is required that can serve as conductive or magnetic material to generate the heat. For the susceptor sheet that can serve as heat generation and joining add should fulfill various properties that can make a good joint in non-conductive and non-magnetic thermoplastic composites.

Various researchers have used various fillers to develop a fast and controlled heat generation susceptor sheet. For an efficient and economical susceptor sheet, it should be lightweight, better electrical conductivity in case of eddy current losses or high magnetic permeability for magnetic hysteresis losses, should form closed electrical loops in case of short carbon fibers, and high thermal conductivity for heating homogeneity. For faster heating heat capacity should be minimized along with surface morphology that can reduce the shielding effect. An added advantage of magnetic materials for automatic heating cutoff by Curie temperature can be obtained however Curie temperature should be in the melting range of polymer[29].

To develop a susceptor sheet that can generate fast and homogeneous heating, materials should be applied that are electrically conductive and magnetic and that can generate heating by combined effect of eddy currents losses and magnetic hysteresis losses. Ferromagnetic materials are higher in density therefore the filler concentration should not be too high, so that the overall density of susceptor sheet stays lower. However, small strip will be used for joining so it will not be effect the joint weight. Different materials like particles or fibers are commercially available and can be used to increase the electrical conductivity of susceptor sheets if used above the percolation threshold. Particles are available in micron sizes i.e. have low aspect ra-

tio and need higher concentration to achieve percolation threshold. Carbon fibers are available in millimeters range i.e. in length, therefore have high aspect ratio and need less amount to achieve percolation. Metal coated fibers can have higher electrical conductivity as compared with non-coated carbon fibers; therefore they have a combined effect of electrically conductive and magnetic properties. Filler concentration of fibers should be above percolation threshold in order to develop a conductive network. At first, heating effects of coated particles and coated carbon fibers were incorporated in polypropylene were investigated. Later on combined effect of particles and fibers were used to obtain better heating effects. For improvement in heating, multi-wall carbon nanotubes were added with coated fibers that reduced the required filler loading and enhanced the conductive network for electrical conductivity. MWNTs may increase the contact resistance and inter tube resistance will help to increase the heating rate. Specific heat capacity is also an important parameter. It can be influenced by addition of metallic fillers. Nickel coated graphite particles and Permalloy flakes have good and high magnetic permeability respectively and were introduced to improve the heating as well as heat capacity. A homogeneous heating was achieved that was not possible with metallic coated particles. Metallic coated graphite particles and permalloy flakes have higher densities. This restricts their use in order to keep the overall density of the composite part within an acceptable range.

The main objectives of this study are

- Development of an optimized susceptor sheet that can be used to join non-conducting thermoplastic composite parts.
- Definition of the critical properties of filler materials for induction heating and optimization of process parameters.
- Identification of the relationship of electrical conductivity and heating performance of different susceptor sheet with respect to filler concentration.
- Optimization of induction generator and component parameters on heating like frequency, generator power and coupling distance
- Heating behavior with respect to the structure of the susceptor sheet.

2. State of the Art

Thermoplastic have various advantages over thermoset. One important advantage of thermoplastic is that they are recyclable however thermosets are not [30]. The ability of thermoplastics to become soft and melt upon heating and re-solidify upon cooling makes them useful in joining using different methods. Fusion bonding of thermoplastic composites is a joining process that can join two components of thermoplastic composites together by fusion and consolidation [31] [32] [33]. The fusion of the joining parts occurs by contacting the joining surface and later by diffusion of macromolecules the bonding line disappears. Fusion can take place by providing the heating at joint and fusion bonding process consists of surface preparation, heating the polymer at the joint interface and consolidation.

Surface preparation is carried out prior to the joining process to remove dirt and contaminants that can affect the bond strength of joint. In fusion bonding, it is not as critical as in adhesive bonding [25]. Usually it is carried out to remove dirt and contamination, however some margin exist in fusion bonding, moreover, only those parts that make the joint need to be cleaned.
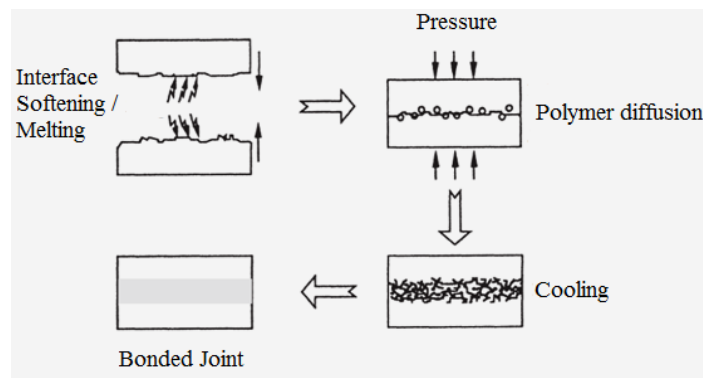
Figure 3: Fusion bonding process [34]

Sufficient heating of the thermoplastic polymer at the bond line is necessary to bring the polymer into molten state, so that melted polymer chains can inter-diffuse and generate a joint strong. Thermoplastic matrices must be heated above their glass transition temperature Tg (for amorphous polymers) or the crystalline melting point Tm (for semi-crystalline polymers) to bring into molten state. There are various heating methods available for fusion bonding of composites [34]. During fusion bonding, preferred heating methods are those that generate heat near bondline [35].

Fusion bonding techniques can be classified into four different classes on the basis of heat generation. These are bulk heating, frictional heating, electromagnetic heating, and two-stage techniques (thermal techniques). They are further divided into sub-classes by the heating mechanism. Bulk heating is sub-divided in co-consolidation, hot melt adhesives, and dual resin bonding. Frictional heating is sub-divided in spin welding, vibration welding, and ultrasonic welding. Electromagnetic heating is sub-divided in induction welding, microwave heating, dielectric heating and resistance welding. Finally two-stage techniques are sub-divided in hot plate welding, hot gas welding and radiant welding. In figure 4, the different heating techniques are illustrated.

Bulk heating techniques such as autoclaving, compression molding or diaphragm forming are available for performing co-consolidation, however the drawbacks associated with this heating technique is that the entire part is exposed to the melting temperature. This requires complex tooling to apply the same pressure on the entire part. Frictional heating is also widely used, however during movements; microstructure may deteriorate and fiber breakage may occur [36]. In two stage heating technique, surface temperature drops during heating and forging process. Later on pressure is applied that may cause unwanted flow in the higher temperature region.
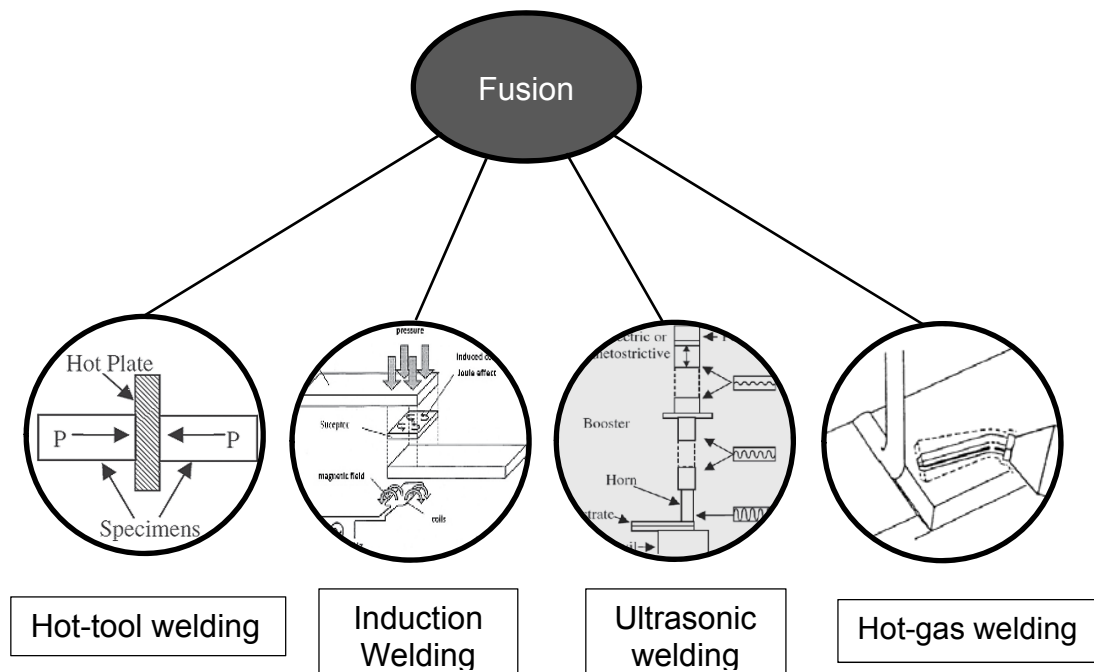
Figure 4: Fusion bonding heating techniques.

Electromagnetic heating has the main advantage that only the joining interface is brought to heating and not to the entire structure. Short cycle times are possible. From these mentioned processes, frictional heating gives the highest heating rate therefore the shortest cycle times and thinnest melt or softened layers. The two stage

process that gives slow heating rate therefore long cycle times and thickest melt lay-
ers, whereas electromagnetic heating gives medium heating rates therefore takes
medium range cycle times [32].

There are various types of electromagnetic heating available, however, most de-
manding are those that heat at or near bond-line [35] and not the whole joint assem-
bly, and those with fast and homogeneous heat generation, which and can be adopt-
ed to continuous automated systems. Other interrelated aspects are joining speed
and distribution of heat within the bond line. A suitable process can be selected out of
these processes depending on heating efficiency and size of joint. For example con-
ventional ovens can be used from small to large component joints, however, they
have a low efficiency. Joining by laser technique has a very high efficiency however it
is applicable only to small component joints.
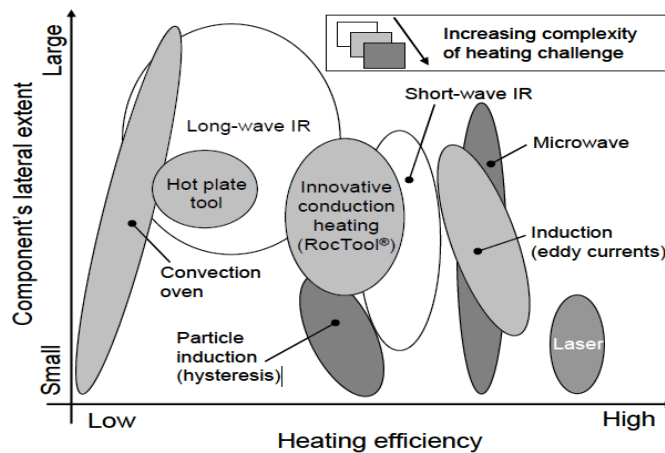
Figure 5: Heating approaches categories according to their size, efficiency, and adaptability
to complex problems for thermoplastic materials [37]

The consolidation of joined parts is the sub-divided into pressing, inter-chain diffusion
and cooling. After heating, polymer chains are in the molten state and pressure
should be applied so that they can be brought in contact and diffuse [32]. Usually
gases are present within the bond line that should be removed by applying pressure,
and parts that need to be joined should remain in contact, preventing the joint from
delamination. When molten polymer sheets are in close contact, entanglement of
polymer chains helps to improve the joint strength. The intermolecular diffusion pro-
cess consists of five phases [38].First three phases are the part of pressing and re-
maining two phases are diffusion part. These five phases are (a) surface rearrange-
ment (b) surface approach (c) wetting (d) diffusion (e) randomization.
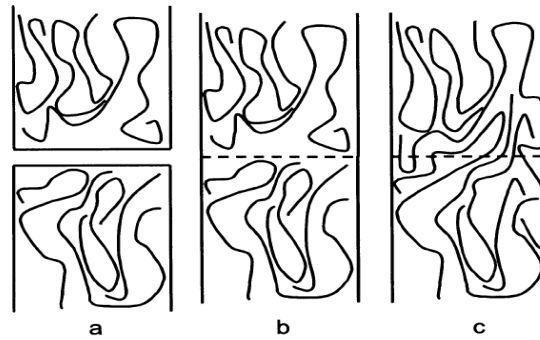
Figure 6: Healing of a polymer-polymer interface showing: a. two distinct interfaces; b. achievement of intimate contact; c. collapse of the interface through inter-diffusion [34]

Cooling is the last part of consolidation in fusion bonding. As the melting takes place during heating, amorphous polymers melt at glass transition temperature and semi-crystalline polymers melt at crystalline melting temperature, re- solidification takes place during cooling. Amorphous polymers retain their molecular orientation and semi-crystalline polymer tends to re-crystallize. In the cooling step, residual stress by thermal gradient may persist [32].

2.1.   Induction Heating (Theory)

The electromagnetic induction's basic principle was described by English physicist Michael Faraday [39] in 1830 during laboratory experiment and later on German physicists Heinrich Lenz and J. Henry made important contributions on this research, and finally C. Maxwell [40] evaluated the equations mathematically for electromagnetic phenomena. The basic phenomenon of induction heating is that when an alternating voltage is applied to an induction coil, resulting in an alternating current in the coil circuit, a time variable electromagnetic field in coil surrounding is generated. This alternating electromagnetic field has the same frequency as the coil current. The electromagnetic field induces eddy currents if the adjacent material is conductive, or creates magnetic polarization if the material is ferromagnetic. Combined effect may take place if the material has a dual nature. When electrically conductive or ferro-magnetic materials [41] are exposed to an alternating electromagnetic filed, heating can be obtained by joule losses and magnetic polarization effects respectively. Conductive materials generate heat due to joule effect [42] and ferromagnetic materials by magnetic hysteresis loss. Hysteresis loss generates heat due to friction of magnetic dipoles [43]. In conductive fibers filled composites heating occurs due to induced eddy currents flowing along global conductive loops, and in each conductive loop a drop in voltage occurs due to the electrical impedance. This volumetric heat generation depends on intrinsic properties of the composite. For a generalized manner,

electrical conductivity, magnetic permeability, hysteresis loss, permittivity, and magnetic susceptibility are the key properties of electrical and ferromagnetic materials.
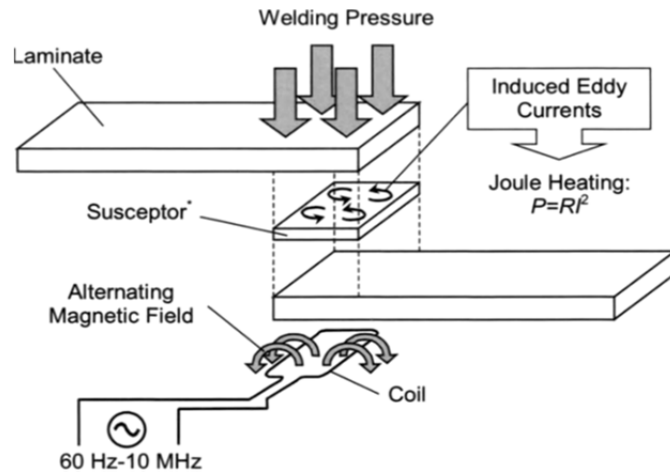
Figure 7: Induction welding set-up for lap shear specimens [44]

In figure 7, the joining of a lap shear specimen by induction heating is shown. When alternating current passes through the coil, it generates a magnetic field that induces eddy currents in the susceptor sheet. Heating is obtained due to joule losses and melts the polymer. Pressure is applied to make contact between the joining surfaces to bond.

2.2.   Induction Heating Mechanisms

The Induction heating mechanism in conductive susceptor materials depends on the structure of fillers and processing of the susceptor sheet. Three main heating mechanisms are fiber heating, junction heating by dielectric hysteresis and junction heating by contact resistance heating. Fiber heating produces heat due to joule losses, junction heating due to dielectric hysteresis effect and junction heating due to contact resistance. On the other hand, inappropriate current distribution, can lead to inhomogeneous heating of the material. Important are the skin effect, proximity effect and ring effect.

In figure 8, the important heating mechanisms can be seen. Heating due to intrinsic resistance of fibers takes place by joule losses. At cross-over point dielectric and contact resistance are illustrated.
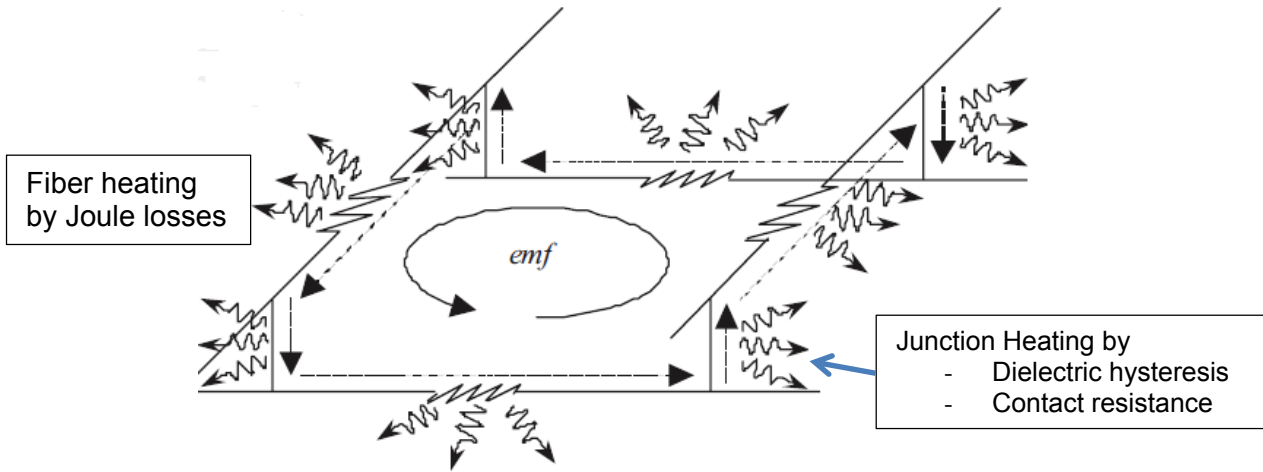
Figure 8: Fiber heating mechanisms [45]

2.2.1. Fiber Heating

When alternating electromagnetic fields are generated and conductive fibers are ex-posed to them, heating is obtained by inherent resistance of fibers due to joule loss-es. It depends on fiber resistivity, fiber length and cross-sectional area. A contact re-sistance of $10^3\Omega$ was suggested as threshold for the dominance of fiber heating[45].
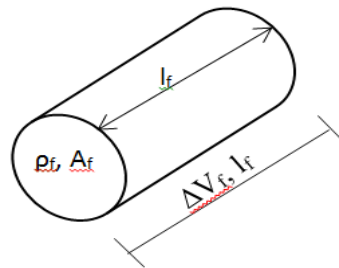
Figure 9: Fiber heating as intrinsic heating [45]

In figure 9, the intrinsic heating of fiber depends on fiber resistivity, area and length of the fiber. Resistance of the fiber can be calculated by equation (2-1)

$$R_f = \rho_f\, l_f\, /\, A_f \qquad\qquad (2\text{-}1) \qquad\qquad [45]$$

2.2.2. Junction Heating (Dielectric hysteresis)

Junction heating is based on the fibers cross-over. These junctions are typically available in prepreg based laminates. If fibers are not in direct contact, the junction heating dominates. When fibers are separated by thin layers of polymer matrix and no direct contact exists a capacitive effect can be observed, as charges accumulates

on both ends, voltage drops and heat is generated [45]. Matrix between fibers acts as dielectric and can be modeled as a capacitor (C_{jd}) and resistor (R_{jd}) in parallel and heating obtained due to dielectric losses as in equation (2-2), where R_{jd} is junction dielectric impedance, h is fiber-fiber separation distance, ω is angular frequency, ε is the permittivity of vacuum, K is the dielectric constant, tanδ the dissipation factor and d_f the fiber diameter.

$$R_{jd} = \frac{h}{\omega \, \varepsilon_o \, K \, (\tan\delta) d^2 f} \qquad (2\text{-}2) \quad [45]$$

Heat Generation depends on the frequency as well as on matrix dielectric properties (dielectric constant and dissipation factor) and fiber-fiber separation distance [45], however to maximize the dielectric heating effect of cross ply or angle ply laminates, Gillespie et al [46] worked and finalized these conditions that ply thickness above and below the interface and fiber volume fraction should be maximized, as well as fiber
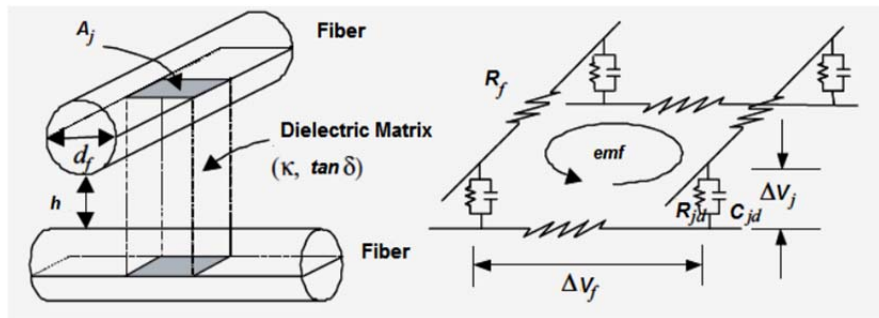
Figure 10: Junction Heating –Dielectric Heating[41]

diameter and inter-ply resin thickness should be minimized. In addition to above mentioned conditions, dielectric properties of polymers have also influence on heating mechanisms. In figure 10, dielectric heating sketch can be seen. In this sketch, fiber-fiber cross-over that are separated by polymer can be seen. They form capacitive effect and heating depends on dielectric properties of polymer. The effect of dielectric properties of polymers on heating was investigated by Fink et al [47].

2.2.3. Junction heating–contact resistance heat

This is the third heating mechanism. It is due to fiber contact at cross over points as in angled plies; heat is generated by contact resistance [45]. In non-unidirectional composites several cross-over points exist and voltage drops at fiber junction occur, generates heat. Heating can be obtained if the closed electrical loops are present,

this may be within plies or between adjacent plies. If fibers are not in direct contact, heating can be obtained, however fibers should be close enough so that electrons can jump [48].
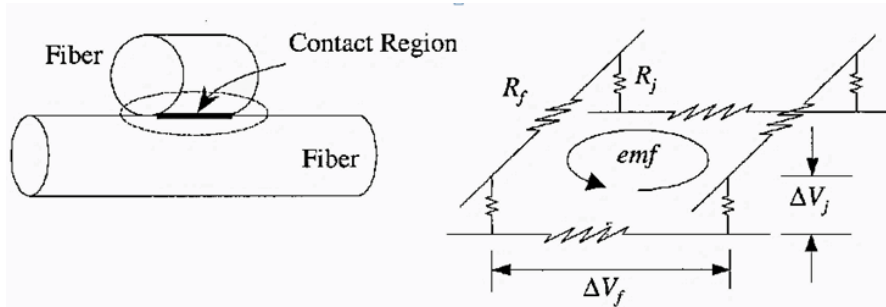
Figure 11: Fiber junction heating – contact resistance [45]

Heat generation depends on the contact resistance at the fiber junctions as in equation (2-3)

$$R_j = R_{jc} \qquad\qquad (2\text{-}3)$$

Where R_j is resistance at junction and R_{jc} is contact resistance at the junctions.

2.2.4. Hysteresis loss

Heating can be obtained by induction heating process using ferromagnetic particles. When ferromagnetic materials are exposed to alternating magnetic field, heating occurs due to magnetic hysteresis losses [49]. These losses are the result of friction due to movements of magnetic dipoles which tend to realign themselves with the alternating magnetic field. If ferromagnetic material is not present as in case of carbon fibers, hysteresis will not exist, however ferromagnetic coated fibers are being used in this work, therefore combined heating effects will be present.
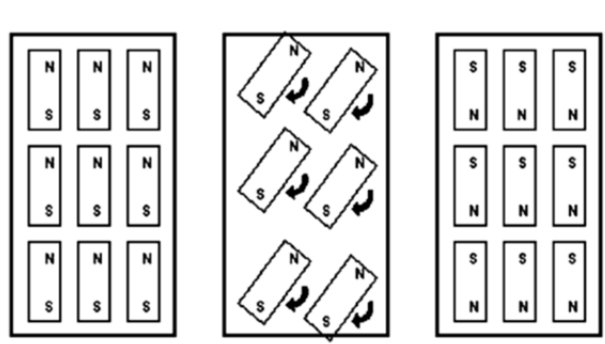
Figure 12: Hysteresis Loss

Ferromagnetic materials generate heat under alternating magnetic field; however there comes a point where ferromagnetic materials become non-ferromagnetic. At this point, material stops releasing heat even if a strong magnetic field is applied. This point is known as Curie temperature and abbreviated as T_{cu}[50]. This temperature can be used for an automatic control of heat generation of ferromagnetic materials. The heating behavior of ferromagnetic particles filled polymer films depends on particle size, weight fraction, applied magnetic field and frequency. If the ferromagnetic particles filler concentration exceeds the percolation threshold, eddy currents can be generated and heating could be due to joule losses.

2.2.5. Combined effect (Joules loss and Hysteresis loss)

If ferromagnetic particles are used for induction heating, hysteresis losses will be the main heating mechanism, however, if they are used above the percolation threshold, there is a possibility that they may heat also due to joule losses, if they fulfil the requirement of a closed electrical loop. Several researchers used metal mesh as susceptor to study the combined effect of joule losses and magnetic hysteresis losses, however, a metal mesh can lead to inhomogeneous heating due to the non-uniformity of the magnetic field [51]. Other problems associated with metal mesh were poor adhesion, stress concentrations, and differences in thermal expansions generate residual stresses. Perforated susceptor sheet of metal coated fibers filled thermoplastic can work better than metal mesh screen. Former will not only reduce the density but also overcome the problems of poor adhesion and thermal expansion.

The hysteresis curve explains the history of magnetization reversal. Figure 13 is a typical hysteresis curve showing magnetic flux density or magnetization versus magnetic field strength (i.e. B or M vs H) The hysteresis loop area gives quantitative measures of the energy obtained from hysteresis loss [52], larger the hysteresis loop area higher the heating [53].
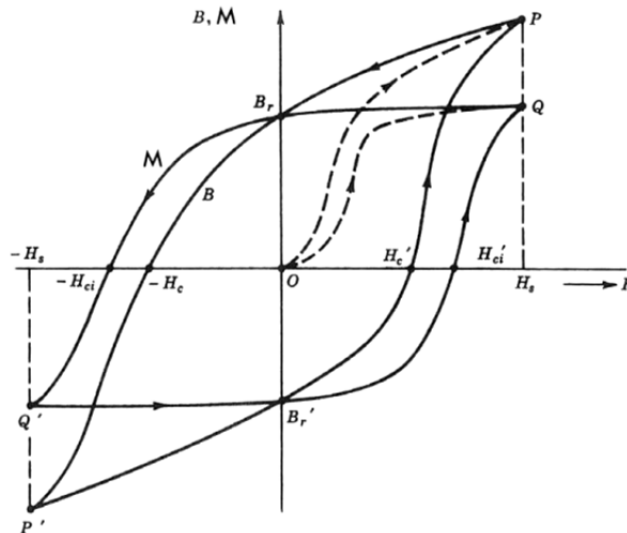
Figure 13: Hysteresis loop of a ferromagnetic material [46]

For the induction heating of particles, hysteresis loss is the dominant heating mechanism; however the magnetic hysteresis loss stands much behind the heating obtained by eddy current losses [29].Heat is generated according to Joules law, see equation (2-4)

$$P = I^2 R \qquad\qquad (2\text{-}4)$$

The heat generation due to the individual mechanisms can be described with equation (2-4), using the appropriate resistance value, see equations mentioned above eq:(2-1, 2-2, & 2-3). The induced current has to be determined from Faraday's law of induction. For specific calculation about the heat generation needs numerical methods; however equation (2-5) gives an approximation [29]

$$P = \frac{4 \ \pi \ f^2 \mu^2 H^2 \ A^2}{R} \qquad (2\text{-}5)$$

2.3.   Skin Effect

During induction heating, a temperature gradient over the laminate thickness arises due to the limited penetration of the electromagnetic field. This is known as skin effect, where the field intensity decreases over the thickness. In conductive or magnetic materials, electromagnetic waves stay near the surface region and temperature difference develops due to induced currents' penetration limitation. The skin effect is dependent on the induced currents and it is generated by electromagnetic fields, therefore it is related with frequency, the electrical resistivity, and the magnetic permeability of the absorbing material.
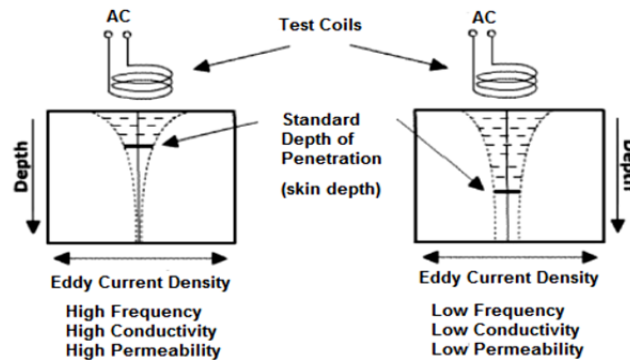
Figure 14: Skin depth at two different materials [54]

The skin depth 'δ' can be determined by following equation (2-6), 'ρ' electrical resistivity (Ohm-m), 'μ' magnetic permeability (H/m), and 'f' frequency (Hz).

$$\delta = \sqrt{\frac{\rho}{\pi \ \mu \ f}} \qquad (2\text{-}6)$$

Increasing the frequency increases more power and have better heating results conversely high frequency reduces the penetration of electromagnetic field to certain depth i.e. skin depth [55]. Skin depth limits the heat generation to surface area at

higher frequencies. For ferromagnetic like nickel powder and nickel coated fibers, relative magnetic permeability of 5,80 and 1,38 has been reported having filler concentrations of 67vol% and 20vol% respectively [56]. For non-ferromagnetic materials like carbon fiber reinforced thermoplastic, magnetic permeability was reported as equal to air (1,256 x 10^{-6} H/m) [55]. Yamashita et al. [57] measured the susceptibility value as ratio of parallel to normal aligned fibers and got higher values in aligned fibers. The low penetration depth at high frequencies confines the heat energy to the surface regions of the part.

2.4. Mechanism of electrical conduction in polymer composites

Materials can be classified on the basis of their resistivity as insulators and conductors. Polymeric materials have high resistivity and come into the category of insulators and metals have very low resistivity and come into the category of conductors. Various fillers can be introduced in polymers to reduce their resistivity and can be used for various applications as their resistivity decreases with respect to the filler. The intrinsic conductivity of fillers, their aspect ratio, interactions between polymer and filler surface, their distribution and orientation are critical parameters to obtain the conductivity and their percolation threshold [58] [59].

Figure 15: Volume resistivity (Ohm/cm) [60]

In figure 15, the volume resistivity with respect to various materials is shown. Unfilled polymers are insulation and as the filler concentration increases, resistivity decreases. Electrostatic discharge (ESD), electromagnetic interference (EMI) and radiofrequency interference (RFI) shielding also needs electrical conductive materials. Finally, pure metal have very low resistivity.

Percolation threshold is the critical filler concentrations where transition takes place from insulator to conductor. At percolation, the electrical conductivity of the composite significantly increases due to the formation of conductive pathway. Percolation was first described by Flory and Stockmayer. Figure 16, shows the insulative and conductive transition as filler concentration effect. Contact resistance between the filler becomes important when filler concentration goes above percolation. Therefore, electron transfer takes place by direct contact between the filler. However when fillers are separated by thing polymer layer, conductivity is mainly due to tunneling effect[61].
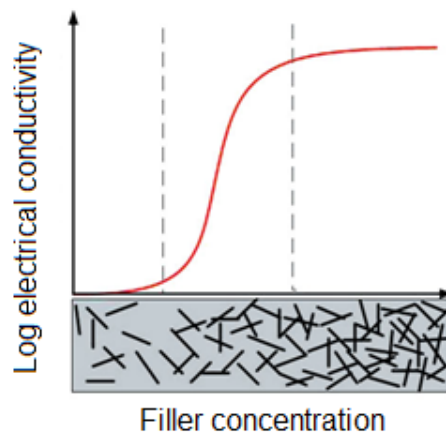
Figure 16: Filler concentration vs electrical conductivity for describing

The electrical conductivity of composites depends on the intrinsic conductivity of polymer and fillers. Polymer have very low electrical conductivities in the range of 10^{-14} to 10^{-17} S/cm, however different fillers have higher conductivities. For example, carbon black has conductivity of 10^2 S/cm, graphite 10^5 S/cm and pitch based carbon fibers have 10^3 S/cm [62] [63] [64]. Nano fillers have exceptionally high electrical conductivity and MWNTs conductivity lies in the range of 10^4-10^8 $\Omega^{-1}m^{-1}$[61].The problem associated with these Nano fillers is their dispersion in the polymer matrix. Polymer filler bond interface should also be optimized. Carbon nanotubes have gained interest as functional fillers due to production on industrial scale and reduction in price. Due to their high aspect ratio, percolation threshold can be obtained between 1-2wt% [66] or even at lower filler concentration, depending on processing.

The electrical conductivity can also be affected by fillers shape and size. If particles size of the filler decreased, conductivity of composite also decreased and similarly the shape of particles can also change the conductivity. The aspect ratio, which is the length to width ratio, plays another important role that helps to use fewer amounts of

filler, as high aspect ratios fillers reach percolation with small amounts [67] [68]. Conversely, fillers having a low aspect ratio need large amounts of fillers to reach percolation. Dani et al. studied short carbon fiber and thermoplastic matrix and found the percolation threshold at 20vol% in injection direction and 16vol% on hot press samples [69].

Polymer and filler interaction during composite preparation also becomes important when there is a good bonding. This helps to avoid isolation of fillers in the polymer composites. Processing techniques also have influence on electrical conductivity. High aspect ratio fillers when processed through extruder and injection molding tend to align themselves in processing direction; therefore composites prepared by using these techniques have a higher conductivity in processing direction [70]. Matrix viscosity also plays an important role and helps to align fibers in the injection molding direction. Drubetski et al. investigated the effect of viscosity using a matrix having two different viscosities [71]. High viscosity has MFI of 1.75 and low viscosity has MFI of 25.

The conductivity of the composite materials changes as the filler concentration is increased. It can be described in a logarithmic scale by using the relationship given in the equation (2.7).

$$\sigma = A(\varphi - \varphi_C)^t \qquad\qquad\qquad (2\text{-}7)$$

where 'σ' is the conductivity of the composite measured in Siemens per meter, 'φ' is the volume fraction of filler, 'φ_C' is the critical volume fraction at percolation, 'A' and 't' are fitted constants.

2.5.   Thermal Conductivity

Thermal conductivity is an important property of materials describes the transport of energy from one place to another by energy carriers. In induction heating, high thermal conductivity increases the heating homogeneity. Heat transfer occurs through three mechanisms: radiation, convection, and conduction. Conduction is the main mechanism of heat transfer within solids and can be is calculated using Equation 2.8[72] [73] [74].

$$Q / A = -K (\Delta T)/ \Delta x \qquad\qquad\qquad (2\text{-}8)$$

where K is the thermal conductivity (W /m-K), 'Q' Heat Flux (W), 'A' cross sectional area of the sample (m^2), 'ΔT'temperature difference (K), 'Δx'thickness (m) and negative sign in equation shows temperature reduction from hot to cold surface. From this

equation, it can be seen that heat transfer depends on the intrinsic thermal conductivity (K) of the materials and a temperature gradient. In solids two main methods of heat transport exist: electron transport and phonon transport. In pure metals, electron transport is the dominant transport mechanism. Both electron and phonon transport the heat energy can be significant in metal alloys. In dielectric materials, like polymers, the dominant method of heat conduction is by phonons [72] [73].

Thermal conductivity of polymers has been conventionally enhanced by the addition of thermally conductive fillers. Graphite, carbon black, carbon fibers, CNTs, ceramic or metal particles are the readily available fillers used to enhance the conductivity [75] [76], however large variation in measurements are reported due to various factors. These factors may include filler purity, crystallinity, particle size and measurement method. Carbon based fillers appear to be excellent as they have high thermal conductivity and have low density. In case of fibers, they are highly anisotropic and show large difference in fiber direction and perpendicular. Metallic fillers like powders of silver, copper, nickel and aluminum can be used to increase thermal conductivity of polymers as well as electrical conductivity; however their higher density and large possibility of oxidation limit their application. Thermal conductivity of metallic fillers depends on particles shape and size, weight fraction and arrangement in polymer matrix. H. S. Tekce et al [77] investigated the copper filled thermoplastic with different shapes. Particles, fibers and plates shaped filler was used. He observed rapid increase in thermal conductivity above 10vol%, however below this concentration rapid increase was not seen due to less interaction. In carbon based fillers synthetic graphite filled composites have large increase in thermal conductivity [78].

2.6.   Magnetic Properties

Induction heating of ferromagnetic and conductive materials is based on magnetic polarization and on induced eddy currents. If magnetic materials are exposed to electromagnetic fields, heat is generated due to hysteresis losses by magnetization and demagnetization cycle. Magnetic materials are classified into two broad categories, i.e. soft and hard magnetic materials. Soft magnetic materials are characterized by large permeabilities and very small coercivities. Hard magnetic materials demonstrate high saturation magnetizations and large coercivities. Soft magnetic materials give less heating due to losses, however due to high permeability they can work at high frequencies. In magnetic materials, losses are attributed to three physical mechanisms. These are hysteresis losses, eddy current losses and losses due to dynamic movements of magnetic domains [79]. Magnetic hysteresis can be determined by a vibrating sample magnetometer (VSM). VSM is used to measure the

magnetic properties of materials as a function of magnetic field, temperature and time. Nickel powder is a typical magnetic filler of high saturation magnetization; however its disadvantage is high density. Permalloy flakes are also being used due to their high magnetic permeability. The magnetic properties of composites depend on particle size their separation at a given filler concentration. Lin Zhu et al. [80] observed the saturation magnetization of nickel fibers and nickel particles 51.7 emu/g and 47.8 emu /g, respectively. Chuncheng Hao et al [81] found saturation magnetization of nickel nanoparticles and magnetic composites of 29.0 emu/g and 6.0 emu/g, respectively, that is smaller than that of bulk nickel (Ms = 54.39 emu/g) [82].

From filler concentration point of view, in magnetic percolation there is no need for point to point contact between the fillers as in electrical percolation. When a particle is under uniform magnetic field, it distorted it in the near vicinity of the particle. If another particle is brought near the first particles and separation gap is larger than 2.7 times the radius of particles [83], they behave like isolated particles. If the separation gap is less than this, they interact with external magnetic field and distorted field of neighbor particle. For particles, electrical percolation can be achieved at 33% filler concentration. In electrical percolation they are touching one and other and are densely packed.

2.7.   Factors that influence induction heating

There are different factors that may affect the induction heating. It takes place due to eddy currents losses and magnetic hysteresis. Former works with fibers and later works with particles, however polymer matrix doesn't have both of these properties. Fillers were incorporated to make polymer matrix either electrically conductive or ferromagnetic for heat generation. Properties of fillers as susceptor materials and testing parameter (i.e. machine parameters) influence on heating.

Machine Parameters:

Coil Current: Coil current gives more power to the system and higher current gives more power therefore fast heating can be achieved [83]

Frequency: For fast heating, usually high frequency is required, however it limits the penetration. For particles filled composites, it depends on size. [29]

Coil Geometry: Magnetic flux density depends on coil geometry [84]

Coupling distance: It's the distance between sample and coil. Less the distance higher will be heating, however sometimes higher distance required for homogeneous heating and overheating can be avoided. [85]

Flux concentrators: If we use flux concentrators for concentrating the magnetic field, it can increase the heating rate. When magnetic field was focused on a limited area, inhomogeneous heating can take place due to high heating. [84]

Materials Parameters:

Electrical Conductivity: In order to obtain a conductive loop, minimum conductivity is necessary. In case of fibers or fabrics, a higher electrical conductivity promotes dielectric heating [45]

Thermal Conductivity: A high thermal conductivity helps to achieve homogeneous heat distribution [86] [87]

Heat Capacity: For faster heating, the heat capacity should be minimized [86] [87].

Magnetic Permeability: A higher magnetic permeability results in higher losses which promotes heat generation especially in case of particles [88]

Density: Lower the density, helps for fast heating [87]

Size of particles/ fibers: No general statement possible since complex aspect and dependent on other material and machine related parameters [49] [83] [89]

Surface morphology: Possible shielding effects by surface contamination can lead to poorer heating [90] [91]

Curie temperature: This is considered to be a limiting factor for heating. It is mainly observed where hysteresis is a dominating heating mechanism [92].

3. Experimental

3.1. Materials

3.1.1. Polymer Matrix

Polypropylene (PP) was used as a thermoplastic as model system due to its cost and ease of processing. PP is widely used in automobiles, household appliances, and the construction industry because of its balanced mechanical properties and due to its high performance to cost ratio. Moplen HP400R is a homopolymer from LyondellBasell. It has a density of 0.90 g/cm^3 and a melt flow index of 25 g/ 10min. It has a softening temperature of 154°C and a tensile modulus of 135 MPa. Although PP is extensively used in many fields of applications, its utilization has been limited in structural materials because of its relatively low service temperature

3.1.2. Fillers

Different fillers with different properties were investigated. These fillers were nickel coated short carbon fibers (NiCSCF), nickel coated graphite particles (NiCGP), multiwall carbon nanotubes (MWNTs) and permalloy flakes. The metal coating of fibers will not only increase the conductivity but also reduce weight in comparison to pure metals. Carbon fibers are prepared by different methods, however poly-acrylic-nitrile (PAN) based production method is widely used. Carbon fibers have specific electric conductivity of $6,25x10^4$ S/m [93]. To increase the electrical conductivity of carbon fiber, metal coating can be applied. Nickel coated fibers were used because the coating increases the electrical conductivity and leads to good adhesion properties. There are different methods for metal coating. Electroless nickel plating is a widely used technique for metal coating. In this process, a nickel-phosphorous alloy without the use of an electrical current is deposited.

Nickel coated short carbon fibers (NiCSCF)

The Nickel coated short carbon fibers (NiCSCF) were purchased from Toho Tenax Co. Ltd. (type: Tenax®-J HT C903). This is a high performance carbon fiber made from poly-acrylic-nitrile (PAN). They were 6 mm in length, 7.5 µm in diameter and exhibit a density of 2.70 g/cm^3. The nickel coating thickness was 0.25µm and the NiCSCF had a tensile strength of 2750MPa, a tensile modulus of 215 GPa, and a specific electrical resistance of 7.5×10^{-5}Ωcm. In figure 17(a), pure fibers can be seen. In figure 17(b), SEM images can be seen.
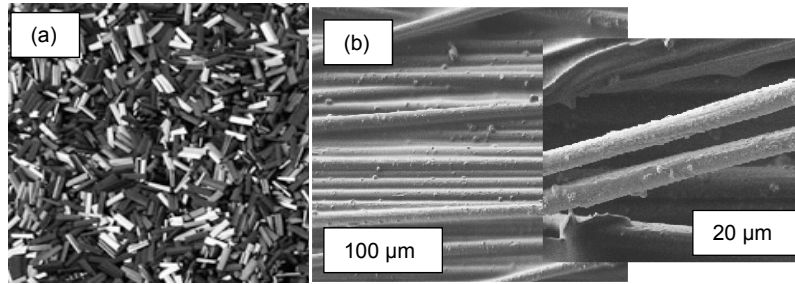
Figure 17: Nickel coated carbon fibers (NiCSCF) (a) pure and (b) SEM image

Nickel coated graphite particles (NiCGP)

Nickel coated graphite particles (NiCGP) were supplied from Novamet Speciality Products. NiCGP were having average particle size of 90 µm in diameter, having a density 3.8- 4.0 g/cm^3 and nickel coating was 60%w by weight. These coated graphite particles provide low density and good electrical conductivity. In figure 18, SEM images of particles can be seen. It is very clear from figure that nickel coating was very good.
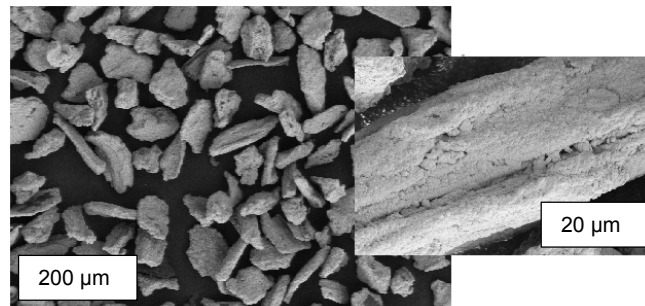
Figure 18: SEM image of nickel coated graphite particles

Multiwall carbon nanotubes (MWNTs)

Multiwall carbon nanotubes (MWNTs) are considered to be promising filler due to high electrical conductivity, thermal conductivity, and high mechanical performance [94] [95] [96]. Due to high intrinsic electrical conductivity and high aspect ratio, conductivity can be achieved at very low filler contents [97]. Noll et al [98] observed the percolation threshold below 0.77vol% during electrical conductivity measurement prepared via double screw extruder.
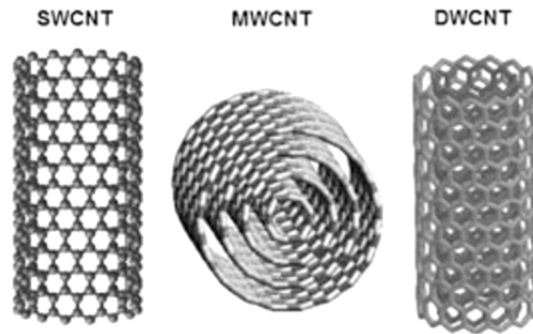
Figure 19: Different types of CNTs [99]

MWNTs are available in different forms like single-wall carbon nanotubes (SWCNTs), double-wall carbon nanotubes (DWCNTs) and multi-wall carbon nanotubes (MWCNTs). The images of different CNTs can be seen in figure 19. They are available in different commercial grades and also available in master batches with thermoplastics matrix. MWNTs were prepared by catalytic chemical vapor deposition method. A master batch of MWNT / PP (Nanocyl-PLASTICYL™ PP2001) was purchased from Nanocyl (Sambreville, Belgium). Master batch consists of 20wt% MWNTs, having density of 0.97 g/cm^3, MWNTs' diameter 9-11 nm, average length 1.2 µm.

Permalloy flakes

Permalloy is the highly magnetic alloy having magnetic permeability of around 100000, compared to nickel and steel. It is alloy of nickel, iron and molybdenum with 82% nickel, 16% iron and 2% molybdenum. It has a density of 8.72 g /cm^3 and in the form flakes with 0.4 micron thickness.
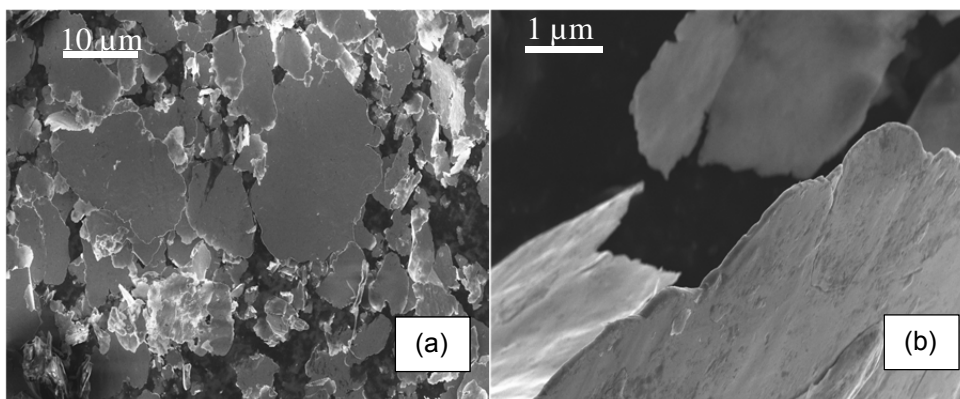
Figure 20: SEM images of Permalloy flakes

In figure 20, SEM images of pure permalloy flakes can be seen. In figure 20(b) shape and thickness of flakes can be seen.

3.2.   **Manufacturing Method**

Selection of manufacturing process is a critical aspect and needed that it is applicable at industrial scale. Thin sheet of composite were prepared by melt mixing of nickel coated short carbon fibers (NiCSCF) & nickel coated graphite particles (NiCGP) together with the Polypropylene matrix using double Screw Extruder (ZE25A X 44 D, Krauss-Maffei Berstorff GmbH). It has outer diameter of 25 mm and a processing length of 1100 mm. Calandering process was adopted for approximately 500μm thick sheets on a calandering machine for optical films (Dr. Collins GmbH). Different compositions of NiCSCF and NiCGP were prepared. The main parameters were the processing temperature 220°C, the screw rotation speed of 300 rpm, and the throughput of 9 kg/h. The above mentioned processing parameter and feeding pumps were all computer controlled. All manufacturing parameters were kept constant for all composites sheets. Feeding of PP granules was into the main feeder; NiCSCF and NiCGP were added by a side feeder with a gravimetric controlled dosing system. Vacuum was applied at end of the polymer melt to avoid porosity. The NiCSCF/ PP and NiCGP/ PP melt came out directly on the calandering rollers for thin sheet forming and rolling at the end of calandering machine.
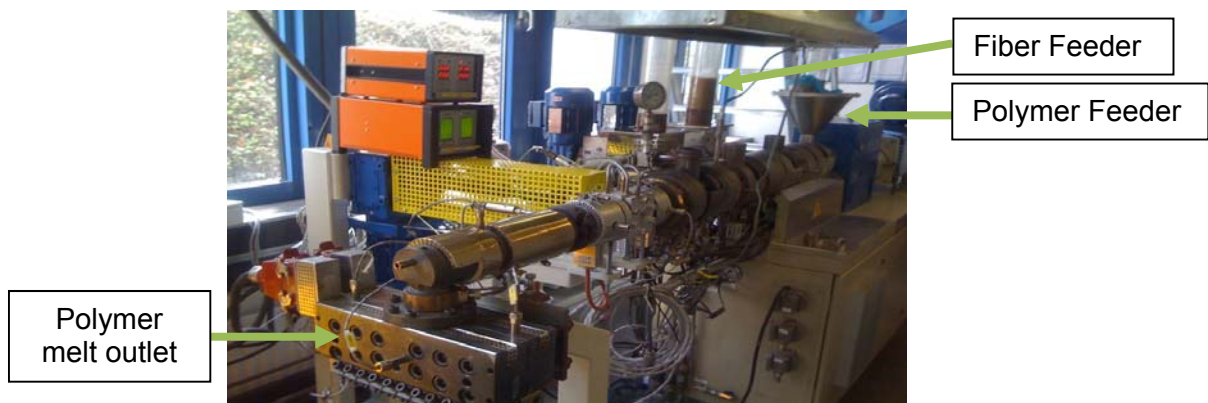
Figure 21: Double screw extruder

Figure 22: Calendering Machine (Dr. Collins, GmbH)

At small scale, Brabender lab extruder was used to prepare samples. For small scale, main parameters for processing were temperature 230°C, screw rotation speed was 80 RPM and mixing time was 15 minutes. Later on, samples for induction heating were prepared by compression molding by hot press. NiCSCF/ PP, MWNTs / NiCSCF/ PP, Permalloy/ PP and Permalloy/ NiCSCF / PP were at small scale.

Figure 23: Brabender lab-scale extruder

Table 3-1. Nickel coated short carbon fibers, coated graphite particles and their combinations.

Materials	NiCSCF (wt%)	NiCGP (wt%)
NiCSCF/ PP	8	-
NiCSCF/ PP	10	-
NiCSCF/ PP	12	-
NiCSCF/ PP	13	-
NiCSCF/ PP	15	-
NiCSCF/ PP	16	-
NiCSCF/ PP	18	-
NiCSCF/ PP	20	-
NiCSCF/ PP	22	-
NiCGP/ PP	-	8
NiCGP/ PP	-	10
NiCGP/ PP	-	12
NiCGP/ PP	-	13
NiCGP/ PP	-	15
NiCGP/ PP	-	16
NiCGP/ PP	-	18
NiCGP/ PP	-	20
NiCSCF/ NiCGP/ PP	8	6
NiCSCF/ NiCGP/ PP	10	6
NiCSCF/ NiCGP/ PP	12	6

NiCSCF/ NiCGP/ PP	13	6
NiCSCF/ NiCGP/ PP	14	6
NiCSCF/ NiCGP/ PP	16	6
NiCSCF/ NiCGP/ PP	18	6

Materials	Notations	NiCSCF (wt%)	NiCGP (wt%)
NiCSCF/ NiCGP/ PP	8-6	8	6
NiCSCF/ NiCGP/ PP	10-6	10	6
NiCSCF/ NiCGP/ PP	12-6	12	6
NiCSCF/ NiCGP/ PP	13-6	13	6
NiCSCF/ NiCGP/ PP	14-6	14	6
NiCSCF/ NiCGP/ PP	16-6	16	6
NiCSCF/ NiCGP/ PP	18-6	18	6

Table 3-2. MWNTs, coated fibers plus MWNTs, coated graphite particles plus MWNTs combinations

Materials	NiCSCF (wt%)	MWNTs (wt%)	NiCGP (wt%)
NiCSCF/ MWNTs/ PP	0	2	0
NiCSCF/ MWNTs/ PP	0	4	0
NiCSCF/ MWNTs/ PP	6	2	0
NiCSCF/ MWNTs/ PP	6	3	0
NiCSCF/ MWNTs/ PP	10	2	0
NiCSCF/ MWNTs/ PP	10	3	0
NiCSCF/ MWNTs/ PP	15	2	0
NiCSCF/ MWNTs/ PP	15	3	0
NiCGP/ MWNTs/ PP	6	0	2
NiCGP/ MWNTs/ PP	6	0	3
NiCGP/ MWNTs/ PP	10	0	4
NiCGP/ MWNTs/ PP	10	0	5

Table 3-3. Permalloy, coated fibers plus permalloy and coated fibers plus graphite particles combinations

Materials	NiCSCF (wt%)	Permalloy (wt%)	NiCGP (wt%)
NiCSCF/ Permalloy/ PP	0	2	0
NiCSCF/ Permalloy/ PP	0	4	0
NiCSCF/ Permalloy/ PP	0	6	0
NiCSCF/ Permalloy/ PP	6	3	0
NiCSCF/ Permalloy/ PP	8	3	0
NiCSCF/ Permalloy/ PP	10	3	0
NiCSCF/ NiCG/ PP	6	0	3
NiCSCF/ NiCG/ PP	8	0	3
NiCSCF/ NiCG/ PP	10	0	3

3.3.   **Characterization**

3.3.1. **Electrical Properties (DC Conductivity)**

Electrical conductivity of NiCSCF/ PP & NiCSCF/ NiCGP/ PP composites was determined according to DIN EN ISO 3915 (1999) [100]. A four-point measuring method was used with Keithley 2601A electrometer. In figure 24, the testing method is illustrated. Measurements were performed in fibers direction. In the four-point test setup, two electrodes were used for power supply and two for measuring the potential difference. Five samples were tested for each filler concentration. The specimens were prepared by stacking several sheets of composite films and subsequent hot pressing to obtain a final thickness of 4 mm. Later on 30 x 10 x 4 mm^3 small rectangular samples were prepared by cutting the specimen with a band saw. The polymer rich surface was removed by grinding and polishing. To reduce the contact resistance, the surfaces were covered with a silver paste (G3692 Acheson Silver DAG 141). Electrodes were thin pins and were spring loaded.
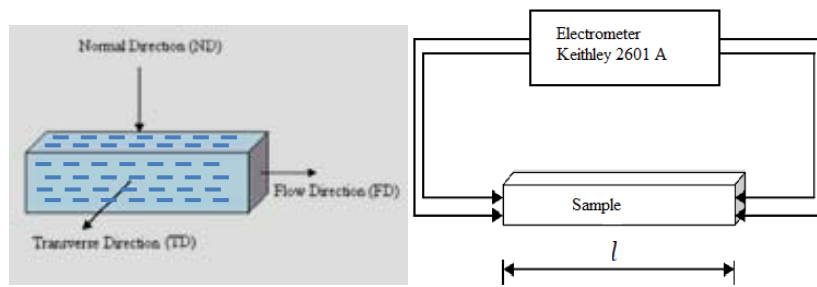
Figure 24: Four-point measurement principle

The resistivity of the sample was measured and the volume specific conductivity was calculated by

$$\sigma = 1 / \rho = \frac{L}{A\,R} \qquad\qquad (3\text{-}1)$$

where, ρ = volume resistivity (Ω-mm), R = measured resistance (Ω), L= distance between electrodes (mm), A = cross-sectional area (mm^2) and σ = volume conductivity (Ω^{-1}-mm^{-1}). Five samples were tested and average value of the resistivity in parallel direction (i.e. longitudinal, sheet processing direction from calandering) obtained. Later on conductivity was calculated from equation (3-1).

3.3.2. AC Conductivity (Impedance)

AC Electrical conductivity (Impedance)analysis was performed by means of a high resolution dielectric/impedance analyzer ALPHA-S from Novocontrol in the frequency range of $1e^{-3}$ - $1e^{7}$ Hz. A parallel plate capacitor of about 30 mm diameter and 0.1 mm thickness is formed with the sample by using two gold-plated electrodes. Circular disc shaped samples were cut-off from sample sheet by using manual punch. In figure 25, testing equipment as well as measuring cell can be seen.

Figure 25: Impedance measurement test setup (L) cell (R)

Electrical conductivity was also measured under applied pressure in materials testing machine. Circular disc specimens of 25 mm diameter with 2 mm thickness were used. Test set-up and sample holder can be seen in the figure 24. At first two plastic sheets were used to avoid any connects with materials testing machine fixtures. Later on copper sheet was used to avoid contact resistance. Before using copper sheet, its oxide layer was removed using sand paper and cleaning with iso-propanol. Pressure was applied and hold for three minutes for stability. Later on Keithley built-in program was run to record the data.
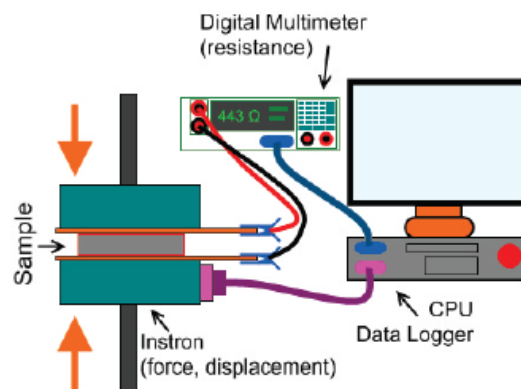
Figure 26: Electrical conductivity measurement under applied pressure[101].

3.3.3. Thermal Properties

Thermal conductivity measurements were performed with a measuring cell built in-house at the Center for Composite Materials at the University of Delaware according to ASTM E 1225 – 04[102]allowing measurements of circular samples with a diameter of 50 mm at thicknesses from 3-5 mm. In figure 27, cross-sectional view of measuring cell for thermal conductive measurement is shown. Numbers were marked for various parts on the equipment, 1-guard heater; 2-upper guidance ring; 3-top meter bar heater; 4-meter bar insulation; 5-thermistor positions 1 and 2;6-lower guidance ring; 7-thermistor positions 3 and 4; 8-sample; 9-lower meter bar;10-guard pipe insulation; 11-bottom plate.
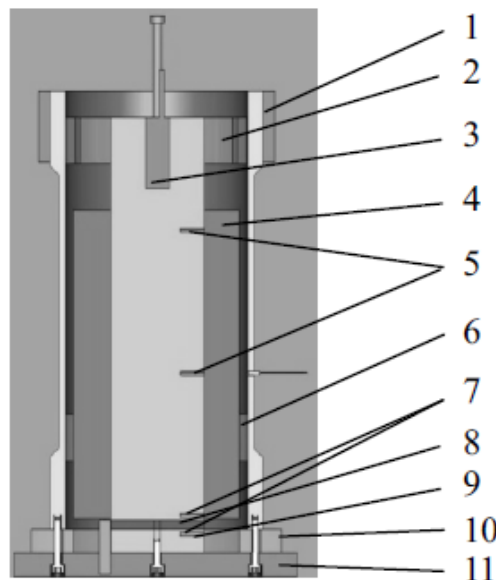
Figure 27: Thermal conductivity measuring cell (cross-section)

A heat flux, approximately 2000 W/m^2, was introduced by a cartridge heater. Three thermistors in the top meter bar were used to measure heat flux which is assumed to be constant while traveling through the sample into the lower meter bar where a fourth thermistor recorded temperature. The top meter bar was insulated with foam and additionally shielded by a guard heater to prevent radial heat loss. Conductivity paste (OT-201 from Omega with K = 2.3 W/m K) was used in order to facilitate coupling and to reduce interfacial thermal resistance between meter bars and samples. The bottom meter bar contacted a cool plate to provide a heat sink with a constant temperature beneath the bottom plate. All of the thermistor information was evaluated by a LabVIEW-based program.

3.3.4. Magnetic Properties

Magnetic properties were performed on vibratory sample magnetometer (VSM). Testing was performed in perpendicular direction to fibers and at a frequency of 40 Hz. All the testings' were performed at room temperature. In VSM, sample is placed in the center of sensing coils and it goes to sinusoidal motion by mechanical vibrations. In figure 28 VSM and its internal sketch can be seen.
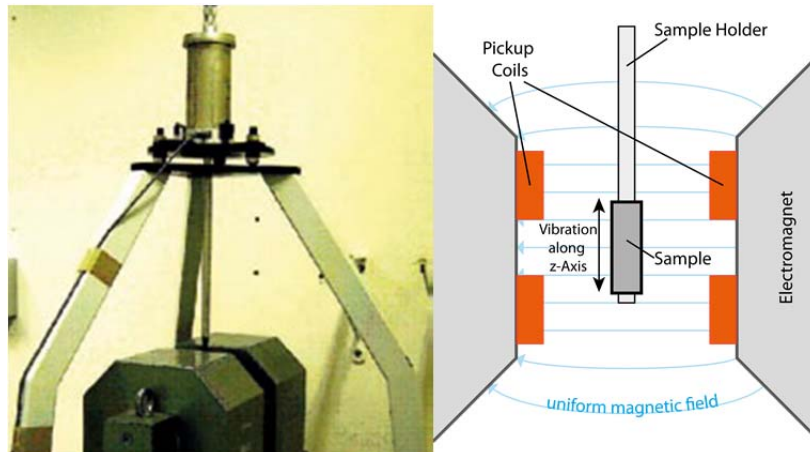
Figure 28: Vibratory sample magnetometer (left) and sketch (right)

Sample is mounted in the center of coils. Uniform magnetic field was applied and colored lines showing the field towards the sample. It works on the Faraday's law of induction. It states that an alternating magnetic field produces a measurable electrical field. Magnetic properties such as saturation polarization, coercive force and remanence were obtained.

3.3.5. Induction Heating Properties

To study the heating behavior, induction heating experiments were performed in a static mode. Testing setup was consists of generator, coil and capacitor box. Heating test was performed using generator TruHeat HF 5010, Trumpf Hüttinger (Germany). Generator maximum current was 35A that transformed to a coil circuit current of 280A[103]. Coil used in this testing was five turn circular pancake coil, having diameter of 100mm, thickness
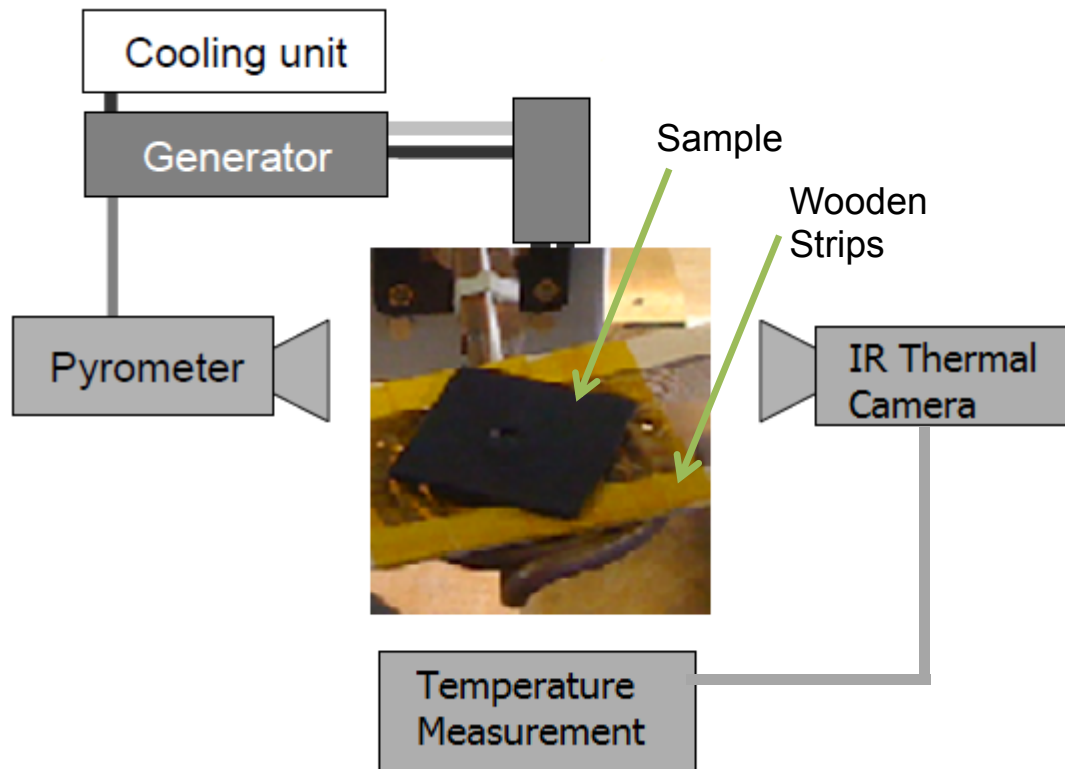
Figure 29:Induction heating test set-up

of 6mm, with internal water cooling to reduce a self-heating of the coil. In order to avoid overheating, pyrometer was used to limit the heating.

Samples for induction heating tests were prepared from thin sheets of 100 x 100 mm^2 for fibers filled and 60 x 60 mm^2 for particles filled by cutting from sheets obtained by Calandering process (thickness = 0,5mm) and compression molded sheets (thickness = 1mm). Sheets were exposed to alternating magnetic field at a coupling distance of 2 mm. To keep the distance between sample and coil constant, wooden strips were used. Tests were performed at different frequencies and generator current. The shape of the magnetic field distribution follows a dome with the highest magnetic field strength located to the center of the coil. Due to the maximum effect at the center of the coil, samples were also aligned with the coil center. Large samples were stick by polyamide tape on wooden test block and small samples were stick on wooden strips. Temperature measurements were performed by infrared (IR) thermal camera imaging system. It consists of camera (Infratech), data processing software (IRBIS-3 professional) and a computer. The distance between sample and camera was kept 0,50m. Software was used for recording the images and temperature vs time graph. IR camera system is a real time non-contacting measurement system of two dimensional surface measurements.

3.3.6. Morphological Properties

X-ray computed micro tomography scans (micro CT) were performed using a commercial micro CT (nanotom by Phoenix x-ray systems, Germany) for visualization of the three-dimensional distribution of fibers and particles in the composite. Light microscopic analyses (Diaplan, Leitz, Germany) were carried out to observe macroscopically the fiber orientation and fiber length distribution of NiCSCF & NiCSCF / NiCGP, using digital images and analysis software (AnalySYS FIVE, Olympus GmbH, Germany). Scanning electron microscopy (SEM, Zeiss Supra VP40, Carl Zeiss SMT AG, Germany) was performed to obtain further morphological information. Before SEM analysis samples were coated with platinum-gold layer in a sputtering device (Oerlikon Balzers, Liechtenstein).

4. Results and Discussion

4.1.   Electrical Properties

4.1.1. DC Conductivity Results

Figure 30, depicts the specific electrical conductivity of NiCSCF/ PP and NiCSCF/ NiCGP/PP composites. Conductivity was measured in processing direction i.e. fiber direction. At lower filler concentrations the conductivity increases slightly, while at 13wt% filler concentration substantial increases in conductivity was observed, however at 15wt% filler concentration sharp rise was observed. The major source of conductivity enhancement is intrinsic conductivity of fibers due to this nickel coating. Other factors are semi-conductive carbon fibers, high aspect ratio and the formation of a fiber network due to electrical contacts and aspect ratio of fibers. At lower concentrations, few fiber contacts were available and few were close to each other so that electric current may flow by means of hopping or tunneling. At higher filler concentrations, the number of interconnecting networks increased, supporting the conduction of electrons. Fiber were aligned in processing direction, therefore fibers were connected in head to tail sequence and head to body. Fibers were slightly angled that made better connections between different layers of fibers, hence whole sheet was interconnected and huge nest of connections were present that caused high conductivity values. Thermoplastic PP matrix impurities may have minor additional effects on conductivity. Pure metals have excellent conductivity however their coating also gives better results in comparison to uncoated fibers.
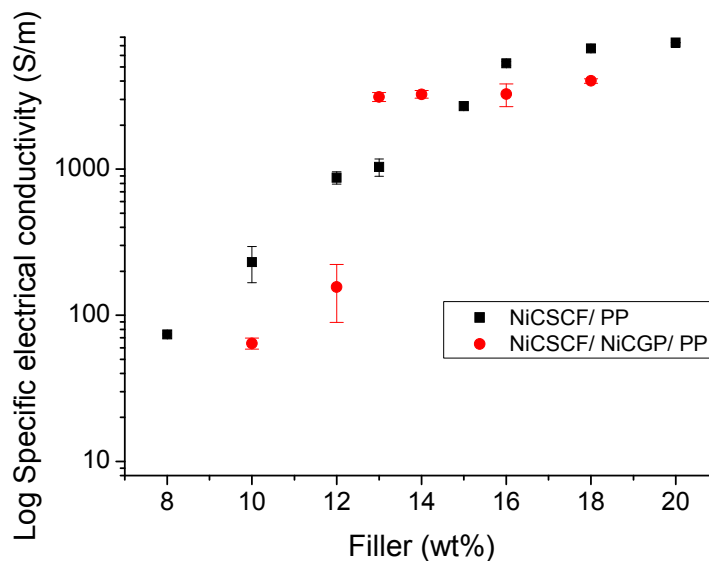
Figure 30:Log specific electrical conductivity vs filler concentration of NiCSCF/ PP and NiCSCF/ NiCGP/ PP composite

Above percolation threshold, the increase in conductivity was value limited, however a further rise can be seen. Usually it has been observed by various researchers that above percolation, conductivity tends to be constant. It was not useful to use higher filler concentration as there is no much improvement in the conductivity. During extrusion process, reduction in fiber length was observed. The initial length of fibers was 6mm, however after processing the fiber length was in the range of 250-300 microns. Due to the reduction of fiber length, fibers were unable to form a conductive network. Therefore the slight reduction in conductivity due to fiber reduction may be one of the reasons.

In figure 30, log specific electrical conductivity of fibers plus particles hybrid filled thermoplastic composites was also shown. Fibers (NiCSCF) concentration was increasing (i.e. 8wt%, 10wt%, 12wt%....) while particles (NiCGP) concentration was constant (i.e. 6wt%) therefore properties of fibers will be dominating. At lower filler concentrations from (8-6)% to (12-6)%, there was slight increase in conductivity observed. At higher filler concentration at (13-6)%, there was sharp rise observed. It was noticed that the addition of particles helped to increase the network formation, however there was a reduction in conductivity in comparison to only fibers. Particles somehow increased the junction formation between fibers and percolation threshold was decreased from 15wt% fiber to (13-6)%hybrid fillers. Increase in conductivity is due to the good network of fibers and particles as well as intrinsic properties of the fillers. Addition of particles made connections between top and bottom layers of fibers, however decrease in conductivity was observed by adding nickel particles. Mironov et al. [104]studied the conductivity of short carbon fiber with nickel powder and observed that resistivity increase by adding nickel powder due to contact resistance. Similar decreasing trend by addition of NiCGP particles on conductivity can be seen.
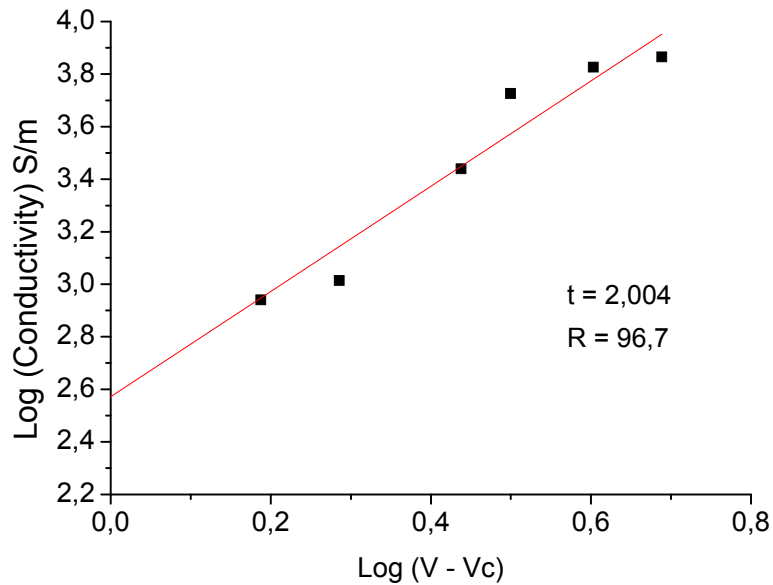
Figure 31: Ln specific electrical conductivity vs filler concentration of NiCSCF/ PP Composites

In figure 31, the logarithmic specific electric conductivity versus log volume filler concentration is plotted. The volume filler concentrations were calculated with the help of densities (PP = 0,9 g/cm^3 and NiCSCF = 2.7 g/cm^3). The constants 't' and 'A' were mentioned in equation 2.7, the critical exponent 't' value of 2.00 obtained, which is in good agreement of published work [93] [105].The values of critical exponent do not depend of percolation character however on the space dimensionality. Theoretically the values of constant A should approach the conductivity of NiCSCF. The intrinsic conductivity of carbon fibers was reported 252 S/m, however we observed the conductivity of 375 S/m for nickel coated fibers.

4.1.2. AC Conductivity (Impedance) Results

Usually when AC currents pass through a conductive material four mechanisms can takes place i.e. electronic polarization, ionic polarization, orientation polarization and interface or space charge polarization. The response of electric field can be understood from impedance with frequency [106].

In figure 32, the measured impedance versus frequency of various filler concentrations of fibers were plotted. Generally, impedance decreases continuously with frequency in polymeric materials [107].It can be seen that at lower filler concentrations and at low frequencies the value of impedance is very high. The reason behind the high impedance at lower frequencies is space charge polarization in the polymer ma-

trix. There can be potential barriers at interface that may delay the pole rotation which increases the impedance. However at higher filler concentrations and at low frequencies the values of impedance are very low due to less potential barriers and enhanced effect of orientation polarization. These space charges are the source of potential barriers that increase the impedance [108].
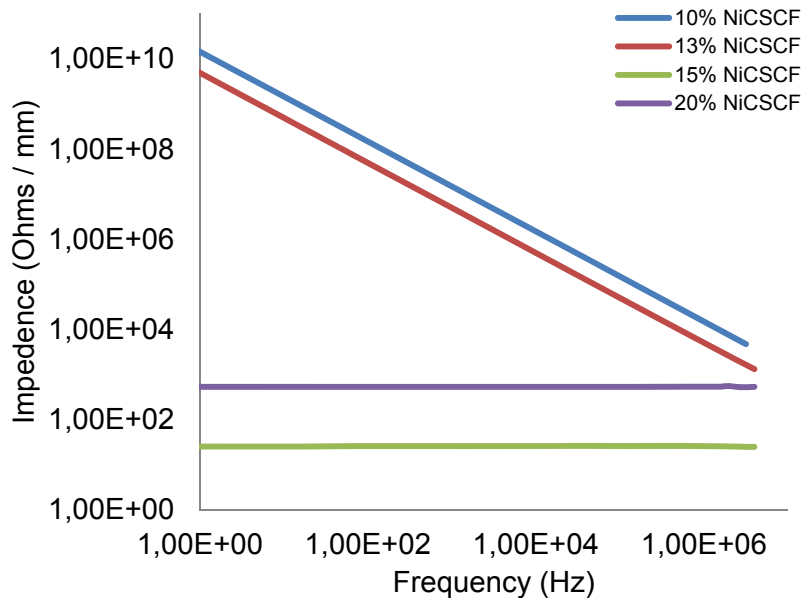
Figure 32:Impedance of NiCSCF/ PP composites as a function of frequency.

In figure 33, impedance versus frequency of different hybrid filler concentrations were plotted. At low filler concentrations i.e. (10-6)% and (12-6)%, reduction in impedance with increasing frequency can be seen. As the filler concentration increases, addition of polarization due to interfaces increases. From the filler point of view, interfaces increases with the filler concentration. Therefore the charges form due to polarization of interfaces. At higher filler concentration, impedance became independent to filler concentration.

The dielectric properties are represented by dielectric constant and dielectric loss. The former is a function of its capacitance, which is proportional to the quantity of charge stored. When electric field is applied, the quantity of charge will increase due to polarization of the fiber-polymer interface. Therefore, by increasing the filler concentration, dielectric constant will increase as the interfaces increases.
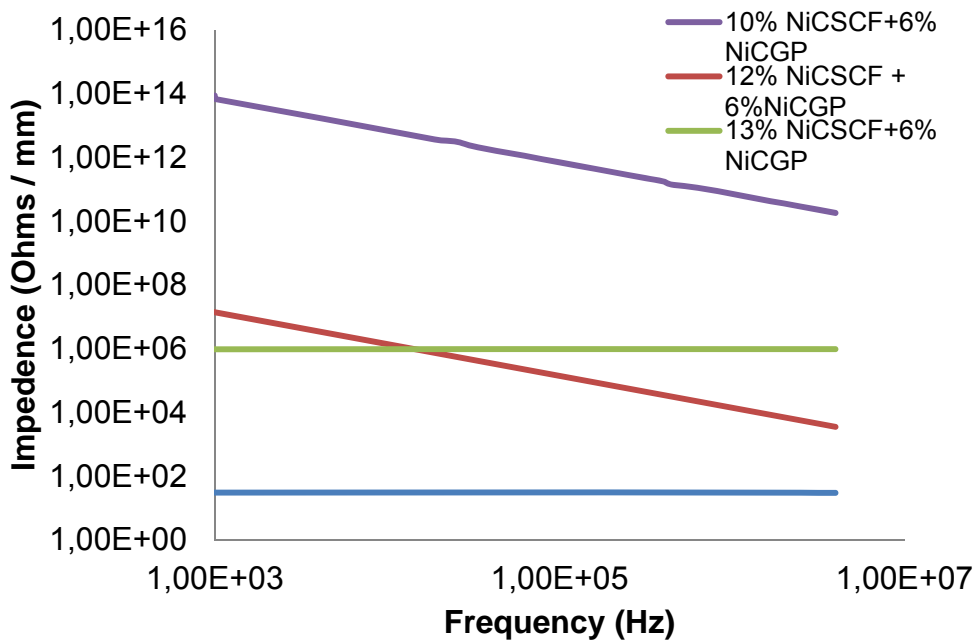
Figure 33: Impedance versus frequency of NiCSCF/ NiCGP/ PP hybrid composites

4.1.3. Electrical Conductivity results under applied pressure

In figure 34, electrical conductivity versus filler concentration of NiCSCF/ PP composites is shown. Conductivity was measured under applied pressure of 50 MPa, in test-setup shown in figure 26. Circular disc samples were used for conductivity measurement and measurement was performed perpendicular to fiber direction. It can be seen that with increasing the filler concentration, also conductivity was increased under applied pressure. At lower concentrations of 6wt%, 8wt% and 10wt%, large increase in conductivity was observed. Further increasing the concentration, the conductivity remains stable, however at 18wt% slight increase was observed.
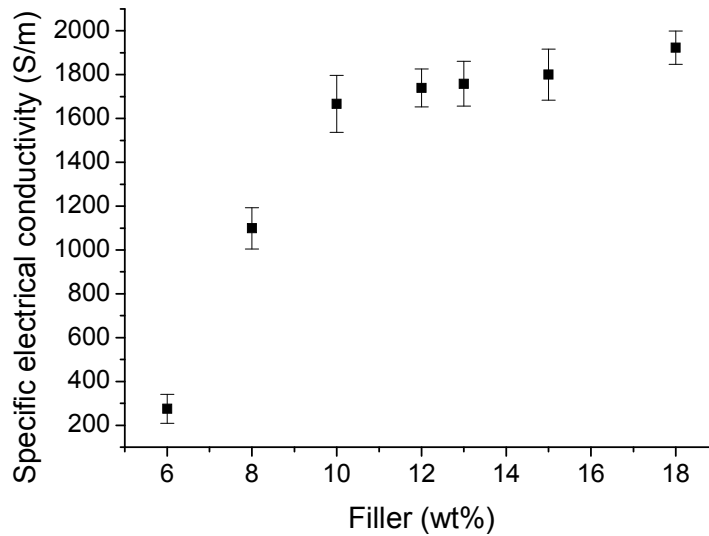
Figure 34: Specific electrical conductivity vs filler concentration of NiCSCF/ PP @ 50 MPa

Thermoplastic PP polymer chains and fibers were inter-linked; however fibers were aligned in processing direction. Applied pressure causes movement of the polymer chains, which affects the conductive fiber network. The change in conductivity measured under applied pressure can be explained by considering two phenomena that occur in the system: formation of additional conductive networks and breakdown of few existing conductive networks. The formation of this continuous conducting path occurs not only by direct contact between electrically conductive fibers dispersed in the PP matrix, but also when the inter-fiber distance reduces up to few nanometers therefore electrons can easily jump across the gap [109].

In figure 35, the specific electrical conductivity versus hybrid filler concentration is shown. In the hybrid system, fibers and particles were combined in these measurements. Fiber concentration was increasing while particle concentration was constant. Measurements were performed perpendicular to the fibers direction. It can be seen that at lower filler concentrations there is slight increase in conductivity under applied pressure of 50 MPa. However at high filler concentrations rise in conductivity can be seen. Percolation threshold lays around (13-6)% of fibers plus particles. Adverse effect of particles addition was observed. It was supposed that the addition of nickel coated graphite particles will enhance the conductivity, however due to contact resistance adverse effect was observed. Theoretically, fibers will be in the form of layers and particles will enhance the network formation under applied pressure. In these measurements, when pressure is applied the separation gap between fibers will reduce and fibers which were misaligned will tend to align and there was a possibility

that gap may generate during alignment. Addition of particles will be make bridging effect. N.C. Das et al [110] observed in increase in resistance due to breakage of conductive network under applied pressure in short carbon fiber filled composite.
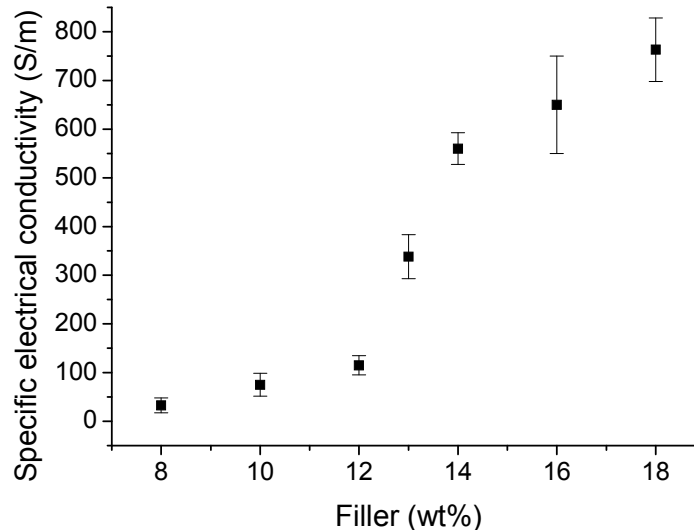
Figure 35: Specific electrical conductivity vs filler concentration of NiCSCF/ NiCGP/ PP @ 50 MPa (Fiber 8%, 10%, 12%...particles 6% constant)

4.2.   Thermal Conductivity Results

In induction heating or welding, thermal conductivity is an important factor. High thermal conductivity increases heating homogeneity, however, due to difference between eddy current losses and magnetic hysteresis losses, the thermal conductivity may have different effects. In figure 36, thermal conductivity values were plotted against filler concentration of fibers. Samples were prepared by stacking circular pieces and finally discs of 5 mm thickness were produced and measured perpendicular to fibers. Therefore the possibility of a thin layer of polymer separating the fibers cannot be neglected along with contact resistance of fibers. When filler concentration increases the thermal conductivity also increase however there was a small reduction observed lower filler concentrations. At higher concentrations above 18% of fibers, the values remain stable. At lower filler concentration (10 vol%), filler were scattered without interaction [77]. We also observed similar trend as the filler concentrations were also in the same range. Therefore, it can be concluded that up to 22wt% filler content variation may be due to less interaction of fillers to be effective for high thermal conductivity. Excluding two results, it can be mentioned that increasing the filler concentration also increases. No substantial increase was observed. Contact resistances decrease the thermal conductivity and we observed in few samples the

thickness variation. Samples were prepared by stacking thin sheets and compression molded, therefore the possibility of included air bubbles cannot be neglected. SEM images of cross-section were also taken and no evidence found. This may be the reason for large variations. A. Demain et al. [63] measured the thermal conductivity of carbon fibers in perpendicular direction and also observed the large variation in results, however he observed linear increase at higher filler concentrations.
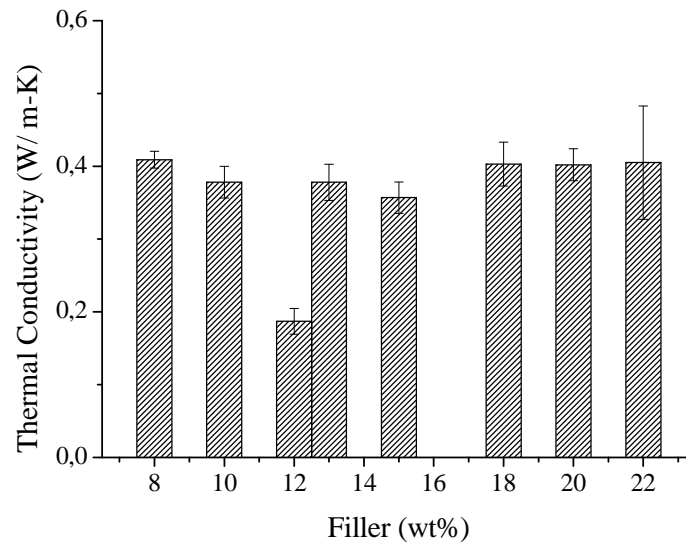
Figure 36: Thermal conductivity vs filler concentration of NiCSCF/ PP @ RT

If we look through the gradual increase in fibers, at low concentration fibers were well aligned however were not close to one another. As the concentration increases the inter fiber distance reduced and several channel developed for thermal conduction. Therefore at lower filler concentrations conductivity values were non-linear. Electrical percolation was observed around 15% of fiber filler concentration that thermal conductivity also got increment at 13% and at higher concentrations slight increase was observed. It shows that various inter-fiber connections were developed for heat conduction.

Thermoplastics have very low thermal conductivity values and lies in range from 0,10 – 0,22 W/ m-K [111]. Most frequently used fillers are metallic particles (aluminum, nickel, copper) or carbon based fillers (carbon particles, short carbon fibers, CNTs). Intrinsic thermal conductivity, aspect ratio as well as polymer-filler interface has great influence on thermal conductivity. H.S Teckce et al. [77]used copper in different forms (spheres, plates, fibers) and observed that spheres need higher filler concentrations, while plates in lower quantity than spheres and finally fibers more less than plates. Hybrid fillers also have good impact as the packing density improves [112].
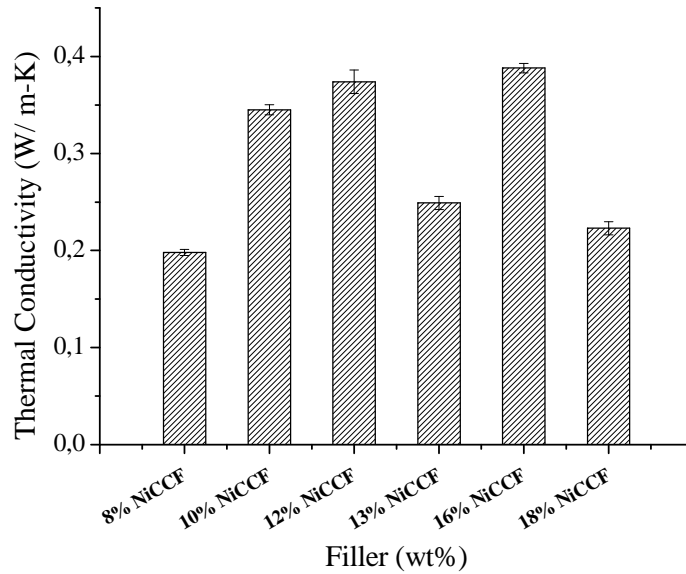
Figure 37: Thermal conductivity versus filler concentration of NiCSCF/ NiCGP/ PP @ RTNiCGP with 6% constant filler concentration

In figure 37, thermal conductivity versus filler concentration of hybrid filler (fibers plus particles) were plotted. At lower filler concentration, rise in thermal conductivity can be seen. At higher filler concentrations large variation was observed that show some problem in samples. As the samples were prepared by staking sheets and compression molded, there might be dislocation of fibers and particles or air trapped in samples. Very small pore was observed during polishing near top and bottom surface; however no air bubble observed air cross-sectional view of sample. Packing density of the fillers plays an important role during heating conduction. As it was observed that small filler concentrations of fibers have higher thermal conductivity however the hybrid filler has less thermal conductivity. From electrical conductivity results, it was concluded that nickel particles have adverse effect on electrical conductivity due to contact resistance.

4.3.   Magnetic Properties

Metal polymer composites can combine properties of both metal and polymers, however, due to their higher density, metal coated particles and fibers can be ideal solution. Nickel is chemically stable and is preferred over ferrous materials, aluminum and copper [113]. It is well known that sub-micron size metal powders can improve the magnetic and electrical properties as well as mechanical properties of polymer composites[114] [115] [116] [117]. Fillers can be particles or fibers. In ferromagnetic materials, magnetic hysteresis loss is due to polarization and depolarization and frictional heat is obtained. The hysteresis loop enclosed area describes the energy ob-

tained by hysteresis loss, therefore the larger the area of the hysteresis the higher will be the thermal energy [118]

Göktürk et al [56] investigated the magnetic properties of nickel coated graphite fibers and observed that magnetic permeability values increase linearly with increasing the nickel concentration. Relative magnetic permeability of nickel powder composites (67vol%) and nickel coated graphite fibers composites (20vol%) have been reported 5,80 & 1,38 respectively at 1 kHz]. The magnetic permeability values at 10 Hz to 100 kHz remained steady. Yamashita et al. [57]measured the susceptibility value as ratio of parallel to normal aligned fibers and got higher values in aligned fibers. The low penetration depth at high frequencies confines the heat energy to the surface regions of the part.

In the present work, magnetic properties were determined by using vibratory sample magnetometer (VSM) and magnetic permeability was taken from hysteresis loop from Physical Properties Measuring System (PPMS). In VSM, samples were tested in perpendicular direction to the fibers. Different filler concentrations of fibers, particles and hybrid system were analyzed.

4.3.1. NiCSCF/ PP Composite sheets

In figure 38, a plot of polarization (J) versus magnetic flux density (μ.H) shows the hysteresis loop of the magnetization of NiCSCF/ PP composite of selected filler concentrations. Fibers were nickel coated and the amount of nickel can significantly affect the magnetic properties. It was found that as the filler concentration increased, saturation polarization also increased. Under an applied external magnetic field, each fiber/ particle generates its own field. When the filler concentration increased, the response from fibers or particles also changes, depending on the distance in the range of radius (radial distance). At low concentrations fibers/ particles behave similar like an isolated particle, however at higher concentrations the electrical conductivity increases due to the interaction of fibers/ particles. At low filler concentrations magnetic properties increases linearly and at higher concentrations, properties change with higher rate.
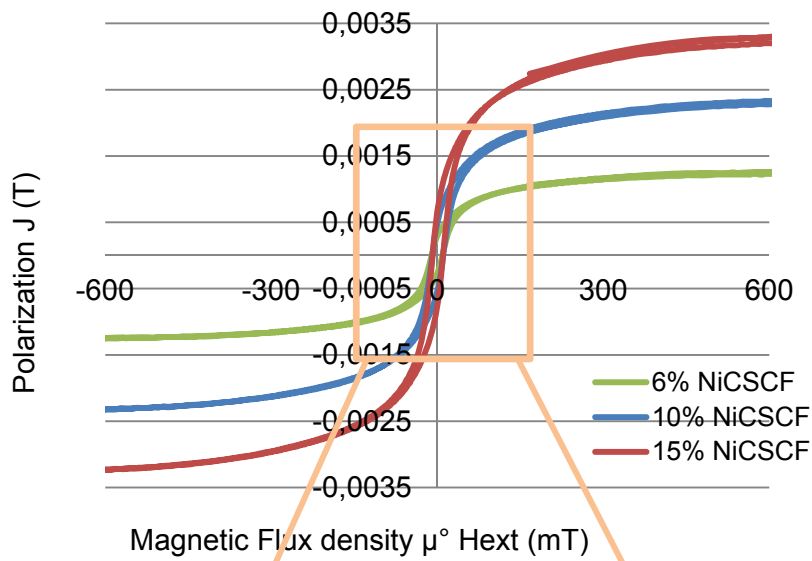
Figure 38: Hysteresis loop of NiCSCF/ PP composites with different wt%.
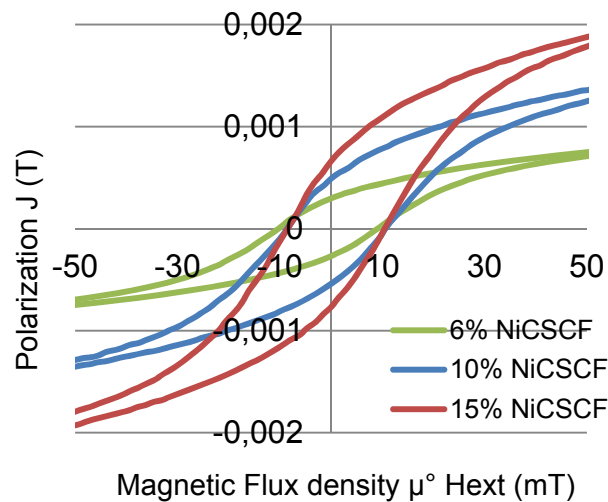
Figure 39: Extended hysteresis loop of NiCSCF/ PP composites with different wt%.

The hysteresis loop of nickel coated graphite particles were also investigated, particles had 90μm diameter. To achieve percolation threshold, their concentration must exceed 48wt% [119]. Therefore, for lower as well as for higher concentrations, the rise in magnetic properties was linear. The hysteresis loop of fibers plus particles hybrid filled thermoplastic with different filler concentration were also investigated. In this hybrid filler system, fibers concentration was increasing and particles remain constant. Saturation polarization of (8-6)% and (10-6)% hybrid system is slightly different, however at (13-6)% hybrid filler large increase can be seen. There may be two reasons for large change in (13-6)% and (10-6)%. Increasing the filler concentra-

tion also increases the polarization and second is that the distance between the fibers was narrow and interaction between the neighboring fibers was also higher. This inter fiber interaction enhance the electrical conductivity. In figure 30, electrical percolation can be seen that was also obtained at (13-6)% hybrid filler.

4.3.2. Comparison

Magnetic hysteresis loops of fibers, particles and hybrid filler were compared and analyzed. In figure 40, selected filler concentration of fibers (NiCSCF), particles (NiCGP) and fiber plus particles (NiCSCF/ NiCGP) were plotted. We have observed the electrical percolation in NiCSCF/PP around 15% and in hybrid filler around (13-6)%, therefore these were selected for comparative analysis. Saturation polarization of these three is in the order of increasing trend. Magnetization of fibers is less than the particles and particles are less than hybrid. At 15% only fibers filler concentration of particles and fibers, particles has more thick coating of nickel in comparison to fibers, therefore magnetization is high, however inter fiber distance is less.

If we go through the remanence and coercivity of fiber and particles, coercivity is almost close with 10% and 15% filler concentration, however remanence has slight difference at 10% and 15%. This may be due to higher nickel coating at particles than fibers.

Table 4-1: Coercivity and remanence of fibers and particles with different filler concentrations

Filler (wt%)	NiCSCF / PP		NiCGP/ PP	
	Hc (mT)	Remanence (T)	Hc (mT)	Remanence (T)
6	10,4	0,0003	*	*
10	8,5	0,0005	8,4	0,0004
15	8,5	0,00065	8,5	0,0008
20	*	*	8,5	0,0012

Similarly, fiber and hybrid filler magnetic properties were compared in table 4-2. coercivity as well as remanence of hybrid filler at 10% filler concentration is higher than fibers.

Table 4-2: Coercivity and remanence of fibers and hybrid filler with different concentrations.

Filler (wt%)	NiCSCF / PP		NiCSCF/ NiCGP/ PP	
	Hc (mT)	Remanence (T)	Hc (mT)	Remanence (T)
6	10,4	0,0003	*	*
8	*	*	8	0,00069
10	8,5	0,0005	9,5	0,00085
13	*	*	10	0,0012
15	8,5	0,00065	*	*
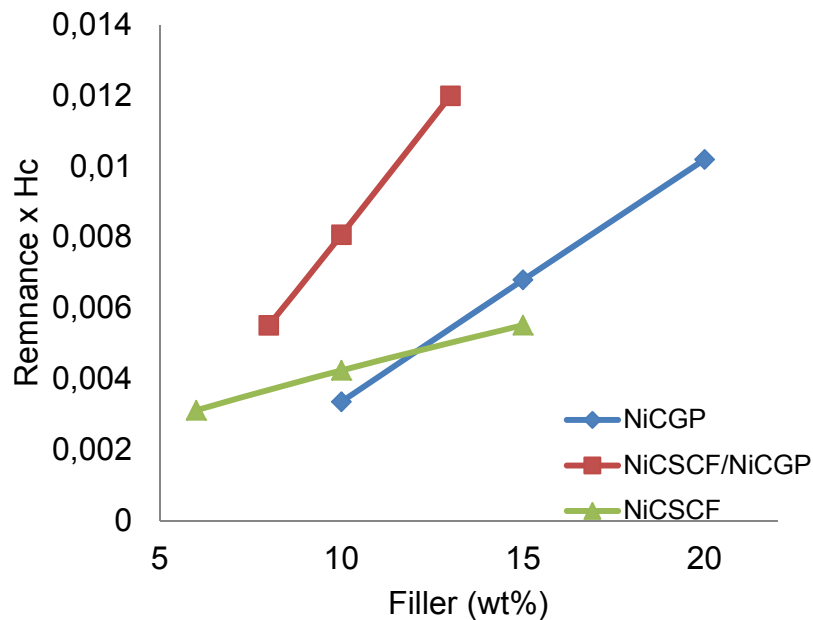
Figure 40: filler versus Hc x remnance

In figure 40, filler concentration versus remnance time's coercivity was plotted. Remnance and coercivity explains about the hysteresis loop area and it shows about the losses. The increase in the filler concentrations we have observed increase in losses, however, particles has higher losses due to thick coating on particles. Fibers had fewer losses as compared to particles. Similar trend was observed hybrid fillers. Maximum losses were obtained by hybrid fillers.

4.4.   Heat Capacity

Heat capacity was measured by DSC (Mettler Toledo) at constant pressure. Reference material was sapphire. PP was semi-crystalline therefore heat capacity goes through a large change around the melting point. For induction heating applications, heat capacity should be minimized for faster heating[87]. It is related with material's ability to retain heat and the rate at which it will heat up or cool down.
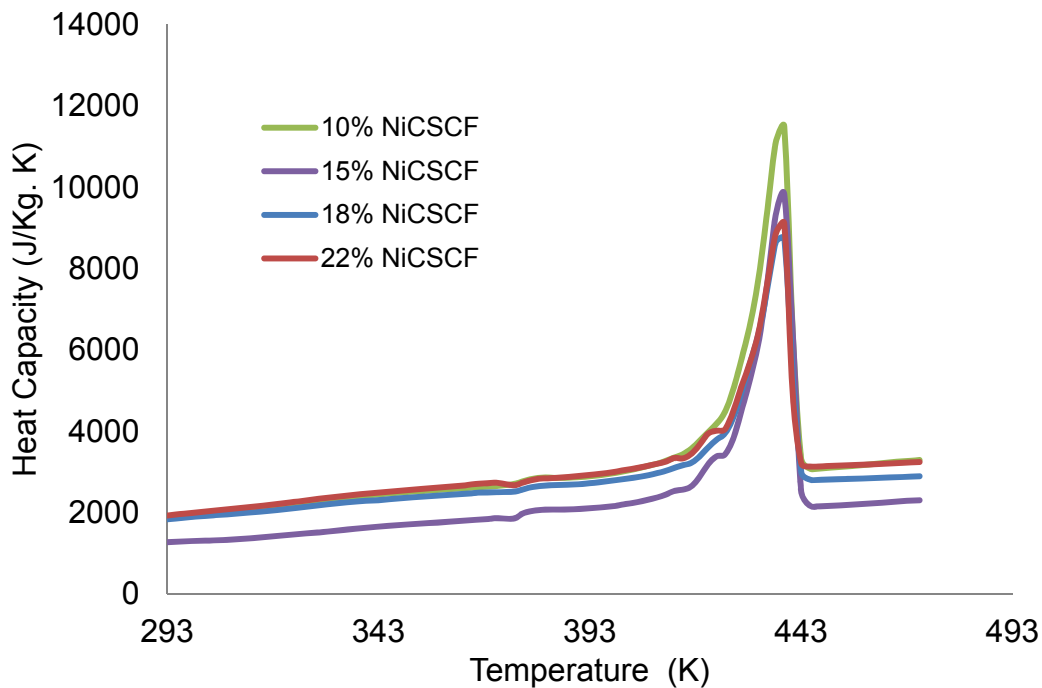
Figure 41: Heat capacity versus temperature of fibers at different filler concentrations

In figure 41, heat capacity versus temperature graph of different filler concentrations of fibers were plotted. When filler concentration increase the reduction in heat capacity can be seen. Large difference can be seen between 10% and 15% filler concentration, may be due to percolation near 15% filler concentration. However at higher filler concentrations close difference was observed.

4.5. Induction Heating Results

4.5.1. Effect of Fillers

Induction heating results of the fibers (NiCSCF/ PP), particles (NiCGP/ PP) and hybrid filler (NiCSCF/ NiCGP/ PP) systems with different fillers concentrations were analyzed. Induction heating effects of the fillers as well as influence of different microstructures of the samples were studied. Fibers (NiCSCF) and particles (NiCGP) were two fillers used in this study. PP thermoplastic was used as matrix. Fibers were 6mm long and 7,5 μm diameter therefore have high aspect ratio and particles were in 90μm diameter however the shape was irregular, and the particles have a low aspect ratio. Different concentrations of these fillers were prepared separately. During induction testing, time temperature graphs were obtained and recorded by IR thermal camera. These graphs with different fillers concentrations were compared and analyzed.

In figure 42, the time-temperature graphs of three filler (NiCSCF) concentrations are shown. IR thermal camera recording was started before starting the generator. After 5 seconds, generator was switched-on. After 60-70 seconds, generator was switched-off and cooling took place.
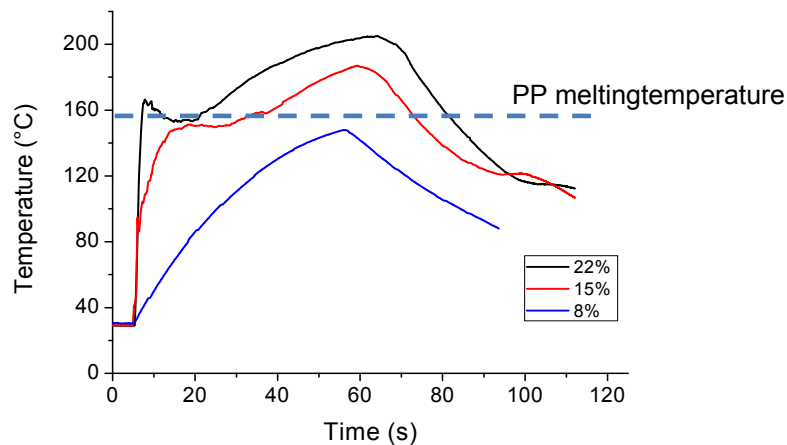
Figure 42: Time-temperature graph of different wt% NiCSCF/ PP composites tested @ 30A & 456 kHz, sample thickness 500μm

Increase in heating rate with increase in filler concentration can be seen. At 8wt% filler concentration, heating was slow, however a sharp rise can be seen at higher concentrations i.e. 15wt%. This sudden rise in heating is due to the change in electrical conductivity as electrical percolation was observed at this filler concentration. A

significant rise in electrical conductivity around 15wt% filler loading was observed and can be seen figure 30. A good network of fibers at higher filler concentrations was developed that leads to a sharp rise in electrical conductivity and heating rate due to eddy current losses and junction losses (i.e. dielectric heating and contact resistance), this is in line with observations published in [120]. Overall heating is the combined effect of joule losses and magnetic hysteresis. Fibers were nickel coated and have high conductivity as compared to carbon fibers without coating. Heating contribution was also from magnetic hysteresis due to the presence of nickel. The magnetic hysteresis heating was confirmed from IR thermal images (figure 81). Miller et al. [121]and Fink [122] investigated the carbon fiber reinforced thermoplastic heating by induction. Miller [121]observed that heating is due to joule losses in fibers; however, a closed conductive loop is required. Fink [122], observed that heat generation is due to dielectric losses, as fibers were not in direct contact due to thin separating layers of polymer. As we used short fibers, they were interconnected within the layers. Heating may consist of fiber heating and contact resistance, however thin layer of polymer may be present between different fibers, and the possibility of dielectric heating cannot be neglected.

At lower concentration, it is difficult to reach melting temperature within 60s, however at higher concentrations melting was achieved within less than 10s. The time-temperature graph of 15wt%, shows the behavior of heating, due to small thickness, during induction heating, the coupling distance was increased and later on reduced. After switched off the generator, cooling started. It can be seen that around 60 seconds, the temperature declines due to cooling and crystallization in polymer takes place after approx. 100 seconds.

In figure 43, filler versus temperature and electrical conductivity graph was plotted. Induction heating tests were performed at 30A and at 456 kHz frequency, temperature was taken during first 10 seconds. This time interval was selected due to the heating trend of sheets. Sample sheet was placed on wooden frame and glued, however due to large area the sheet makes oval shape. Therefore it changed their distance between coil and sample during heating hence time-temperature graph shows reduction in heating at higher filler concentrations. Temperature versus filler concentration and conductivity versus filler concentration follow a similar trend. Both of these properties increase as the filler concentration increase. It can be seen that at low concentrations, the temperature achieved was low in this time-interval. Further increasing the concentration, lead to a gradual rise of temperature with concentration until a maximum is reached at around 18wt%. However at higher filler concentrations

the temperature decreased again. This may be due to a limited penetration of the electromagnetic field into the sample. Fibers were well aligned in processing direction and at lower concentrations, inter fiber distance was large, however at higher concentrations this distance further reduced. Due to high concentration of aligned fibers, it behaves like unidirectional fibers [123]. Increasing the filler concentration also increases the nickel concentration and increased magnetic permeability. This may limit the penetration of electromagnetic waves; however thickness of these sheets were around 500 microns that will not affect too much.

Figure 43: Filler versus conductivity and time of NiCSCF/ PP composites graph, EC tested @ room temperature, induction heating @ 30A & 456 kHz, sample thickness 500µm

In figure 44, time versus temperature graph of NiCGP/ PP sheets of lowest, middle and highest concentrations were plotted. Induction heating testing parameters and procedure was kept constant. As there was no conductive network was present, 60 x 60 mm^2 samples of NiCGP/ PP sheets were selected for testing. In circular pancake coil, electromagnetic field has its maximum strength at the center therefore sample melts from the center. At lower concentration, heating was very slow. Increasing the filler concentration, heating also increased and at further increasing the filler concentration up to 22wt% further rise in heating was observed. Heating obtained is only due to magnetic hysteresis i.e. polarization and depolarization of ferromagnetic materials, therefore within the materials magnetic dipoles gives heat due to friction of these dipole movements [124]. In ferromagnetic materials, hysteresis losses occur and the amount of energy obtained is proportional to the area of the hysteresis curve as well as frequency of alternating electromagnetic field. Due to low aspect ratio of particles, highest filler concentration was below the percolation threshold [120]. The only heating mechanism was magnetic hysteresis [49]. This mechanism gives off

heat as long as Curie temperature or point is not reached, where it stops heating[83]
[125].
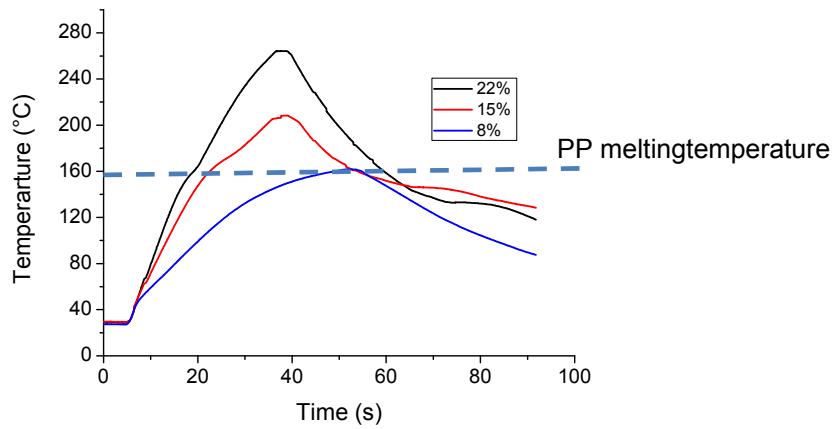
Figure 44: Time-temperature graph of different wt% of NiCGP/ PPcom @ 30A & 456 kHz,
sample thickness 500µm

At higher concentration, temperature graph around 160°C bends slightly. At this point
samples having 15wt% NiCGP/ PP, were started to melt and therefore the coupling
distance reduce. Further rise in temperature was due to reduction in coupling dis-
tance; however initial heating rate is faster than lower concentrations. Similar obser-
vation can be seen in 22wt% filler concentrations. Cooling starts after switching off
the generator. It can be seen that in higher concentrations around 40 seconds, tem-
perature declines due to cooling and crystallization in polymer takes place around 75
seconds.
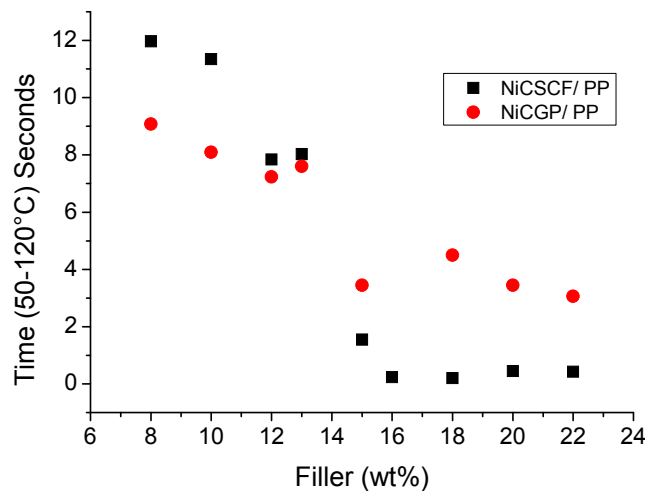
Figure 45: Time vs filler concentration graph of NiCSCF/ PP & NiCGP/ PP composites @
30A & 456 kHz, sample thickness 500µm

In figure 45, time versus filler concentration graph of fibers (NiCSCF/ PP) and parti-
cles (NiCGP/ PP) was plotted. Time was taken from 50- 120°C temperature for vari-
ous concentrations of both the fillers. Time was taken in temperature interval, was
selected for comparison. During heating tests, gradual rise in time-temperature graph
in particles filled sheets was observed therefore this temperature interval was select-
ed for comparison. Heating in increasing the filler concentrations, a reduction in time
to cover temperature interval can be seen. Particles took less time at lower concen-
trations. At higher concentrations sharp decline in time in fibers can be seen, at this
point electrical percolation was achieved and heating was the combination of hyste-
resis and joule losses. Due to nickel coating, high electrical conductivity as well as
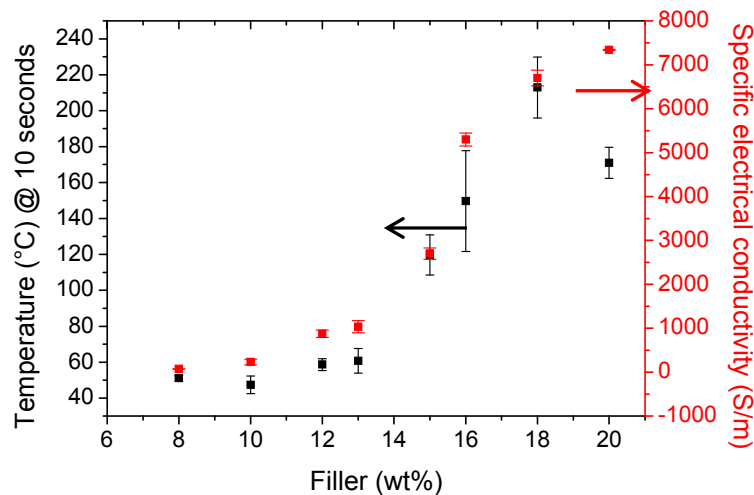susceptibility of nickel, contribute for quick heating.
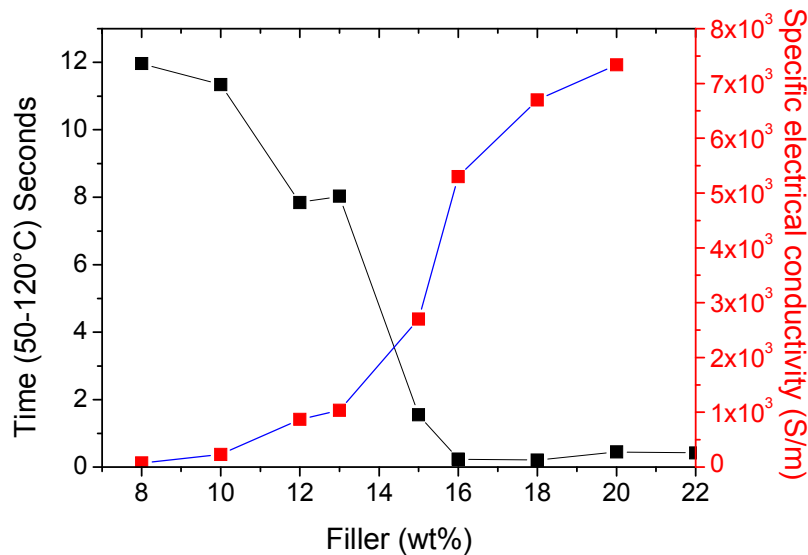
Figure 46: Filler versus conductivity and time of NiCSCF/ PP composites graph, EC tested @
room temperature, induction heating @ 30A & 456 kHz, sample thickness 500μm

In figure 46, filler concentration versus electrical conductivity and filler concentration
versus time was plotted in the same graph. In figure 46, time was taken for tempera-
ture interval due to sudden rise in heating and remains stable. During this interval
heating graph remains persistent. It can be seen that at lower filler concentration,
electrical conductivity was low and it took more heating time. As the filler concentra-
tion increased, electrical conductivity was also increased and time was reduced i.e.
fast heating achieved. Increasing the heating rate by increasing filler concentration is
not only from joule losses but also from hysteresis effect. However heating from
magnetic hysteresis increase gradually while heating by joule losses sharp increase
can be seen due to electrical percolation.

4.5.2. Hybrid Filler Effect (NiCSCF/ NiCGP/ PP)

Induction heating experiments were performed on hybrid fillers sheets. In hybrid filler, particles and fibers were compounded together. Filler concentration of particles was kept constant while fibers were increasing. Heating tests were performed using same testing parameters on Hüttinger generator at 30A with pancake coil at a frequency of 456 kHz. In figure 47, selected filler concentrations were taken for time-temperature graph. One is well below and one is above electrical percolation. It can be seen that both the concentrations were similar with regard to the heating gradient, however, (14-6)% was higher. Lower concentration (10-6)% takes more time to reach melting while (14-6)% takes less time. Similar trend in cooling can be seen.
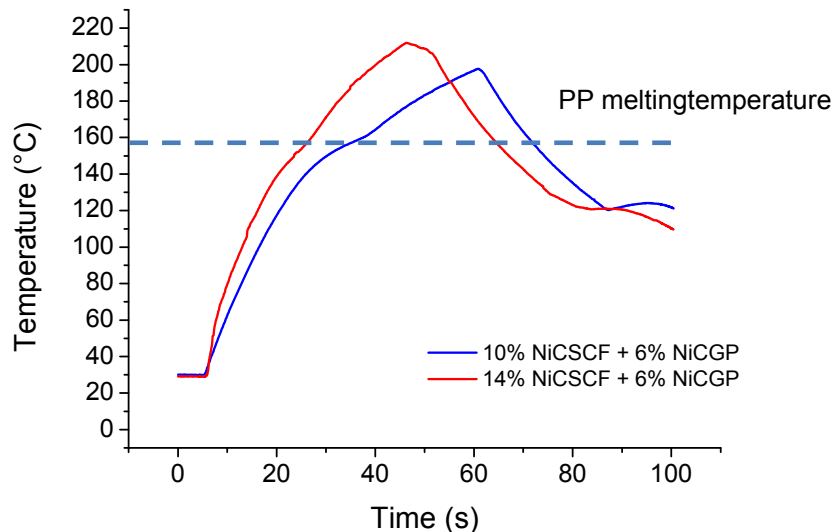
Figure 47: Time versus temperature graph of hybrid filler (NiCSCF/ NiCGP/ PP) composites tested @ 30A and 456 kHz, sample thickness 500µm

In figure 48, filler versus temperature graph for fiber and hybrid filler were plotted. The time temperature graph was obtained from IR thermal camera, initial 10 seconds were selected to calculate the average temperature obtained in this time interval. Testing was performed at 30A and 273 kHz frequency. Increasing the filler concentration increases the average temperature during selected time internal in both the filler system. At low concentrations, hybrid filler is ahead in heating while fibers were below in heating. This high temperature gain may be due to different factors. Addition of NiCGP particles contributed more heating from magnetic hysteresis effect and formation of additional contacts with the help of particles and junctions that generated heat due to contact resistance. At higher concentrations, fibers are ahead in heating while hybrid filler is well below. In both the filler systems, electrical conductivity of the

fibers was higher than hybrid fillers. As it was more resistance from hybrid fillers, higher heating was achieved. From electrical conductivity results, it can be seen that percolation threshold of fibers lies around 15wt%, however for hybrid filler it lays around (13-6)%.

Figure 48: Effect of filler concentration on heating NiCSCF / PP and NiCSCF / NiCGP / PP, tested @30A & 273 kHz, sample thickness 500µm

In figure 49, filler concentration of both the fillers versus temperature graph was plotted. Fiber (NiCSCF/ PP) and hybrid filler (NiCSCF/ NiCGP/ PP) samples were tested at 30A and at a frequency of 456 kHz. Temperature is taken after first 10 seconds of induction heating. Both the fillers were compared at different concentrations. Gradual increase in heating of fibers and hybrid filler composite sheet at lower concentrations can been seen, however hybrid filler is more efficient than on fibers filled sheets. In hybrid filler, sharp rise can be seen at (13-6)%. This may be the effect from electrical percolation. We observed the electrical percolation of hybrid filler at (13-6)%, as it can be seen in figure30. In fibers, we observed the electrical percolation around 15% and sharp increase in heating was observed. At higher concentrations in both the filler systems further rise was observed, however fibers were ahead from hybrid system at higher concentrations. At higher frequency, heating is faster than lower frequency at same filler concentrations.
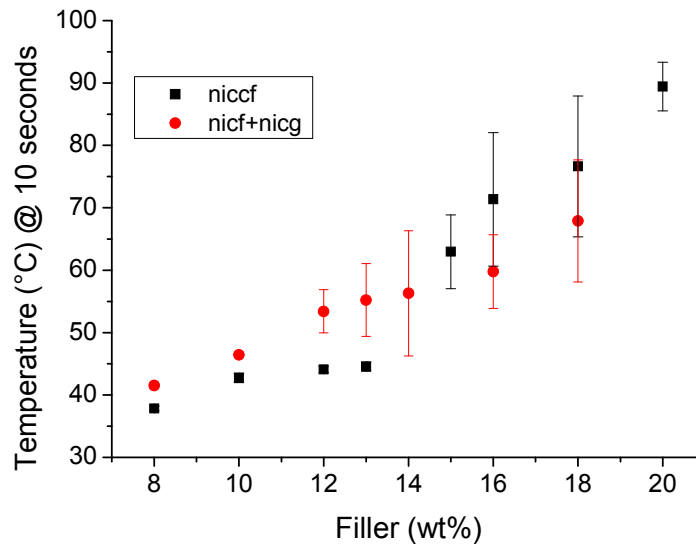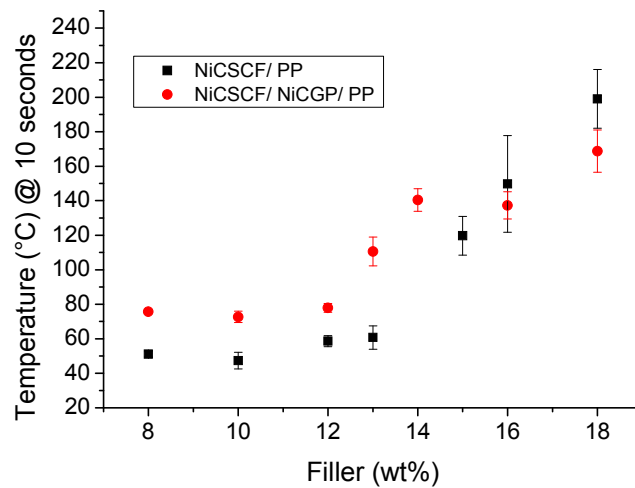
Figure 49: Effect of filler concentration on heating NiCSCF/ PP and NiCSCF/ NiCGP/ PP, tested @30A & 456 kHz, sample thickness 500µm

In figure 50, hybrid filler concentrations versus electrical conductivity and induction heating temperature were plotted. In the hybrid filler system, the fiber concentration was increasing (8%, 10%, 12% …) and particles were at fixed concentration (6%). Similar increase in heating pattern as well as conductivity results were observed that were seen in fiber filled sheets. Increasing the filler concentration, temperature and electrical conductivity were also increased. At lower concentrations, low rise was observed, however at electrical percolation sharp rise was also observed in induction heating. However heating is combined effect of magnetic hysteresis and joule losses. Electrical conductivity heating is faster than magnetic hysteresis therefore heating follow the same trend.
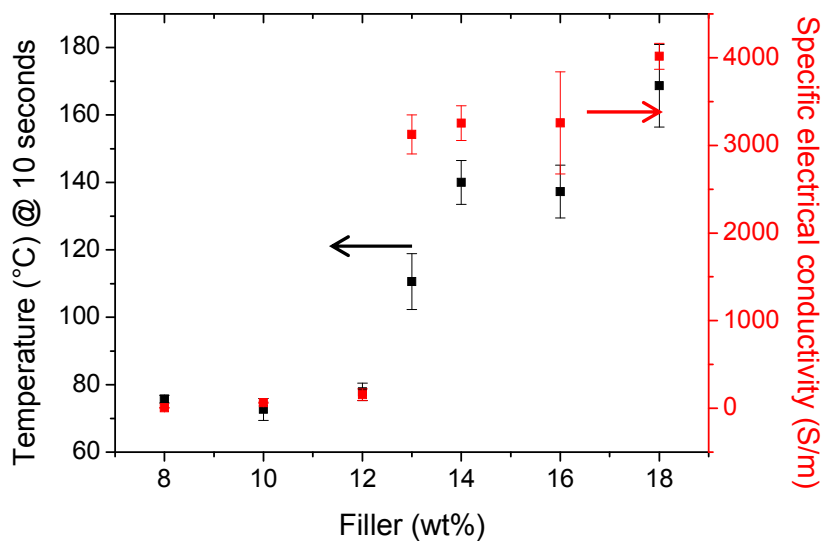
Figure 50: Filler versus conductivity and temperature of hybrid composites graph, EC tested @ room temperature, induction heating @ 30A & 456 kHz, sample thickness 500µm

If we summarize the effect of fillers (fibers, particles and hybrid) on induction heating, fibers have high electrical conductivity and electrical percolation was obtained at 15% filler concentration, where sharp rise in heating was observed. Short fibers were uni-directional aligned, well connected with other and good inter layer connections observed that caused high heating due to joule losses, junction losses and magnetic hysteresis. However, particles were well dispersed in polymer matrix and below percolation and heating were only due to magnetic hysteresis. Finally, the combination of fibers and particles has good heating; however, a sharp rise was not seen. Electrical conductivity was less as compared to only fibers and additional filler concentration of particles made extra heating due to magnetic hysteresis. Heating was combination of joule losses and junction heating along with magnetic hysteresis. DC electrical conductivity and impedance values also reflect that in fibers and hybrid filler, percolation also correlate with heating.

4.5.3. Effect of Frequency

Induction heating test was performed at different frequencies. This can be obtained by using different capacitors in the external circuit of the generator. Frequency is a product of test setup of oscillating circuit. It consists of coil, capacitors and generator as well as sample. Test setup like coil and generator were same therefore frequencies can be changed by changing the capacitors.

Table 4.3 Frequencies with different capacitors obtained by pancake coil

Matchbox ca-pacitors(µF)	100	170	270	330	430	500	670
Frequency (kHz)	744	565	453	408	360	334	289

By increasing the frequency higher power can be supplied to the materials in testing. Theoretically by increasing the frequency, the heating rates of conductive materials[46] [126] also increase, however it decreases due to many factors e.g. charged inductor impedance, losses in mountings and other related negative factors. Frequency is a parameter that is related with generator-capacitor system.

Another problem associated with high frequencies is skin depth effect. High frequencies have smaller penetration depth in comparison to low frequencies. For carbon fiber reinforced composites high frequencies are used [55].

In figure 51, frequency dependence on induction heating at different filler concentrations of NiCSCF/ PP composites were evaluated from time-temperature graph. Temperatures were taken after initial 10 seconds of experiment and average temperature calculated by different concentrations at various frequencies, generator power was kept constant during testing.
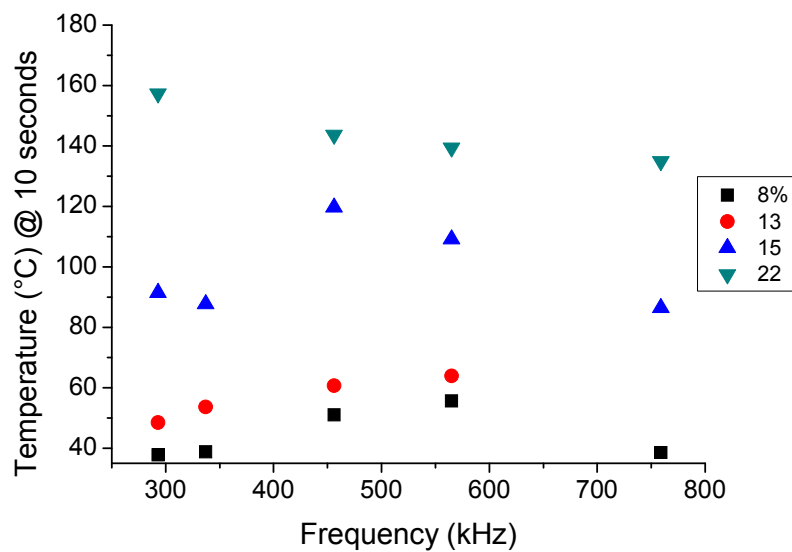
Figure 51: Temperature versus frequency graph of various filler concentration of NiCSCF/ PP composites tested @ 30A (759 kHz @ 15A), sample thickness 500µm

Increasing the frequency increased the heating effect and attained higher temperature after a 10 seconds testing interval. Average temperature was calculated in the mentioned time interval. This time interval was selected as the graph remains stable in this range. This credited to high intrinsic electrical conductivity of NiCSCF and finally the overall conductivity of the composite. At lower frequency and lower filler concentrations, heating was slow. When filler concentrations increase, heating also increased. It can be seen that heating increases gradually as filler concentration increases. Increasing the frequency, gradual rise in heating was also observed. At 456 kHz frequency, highest heating was observed. At higher filler concentrations, effect of frequency was higher as compared to lower filler concentrations. Heating by resistive losses due to eddy currents increase quadratically and hysteresis heating depends linearly on applied frequency.

At higher frequency near electrical percolation, heating further increased, however formation of straight burning lines were observed that may be due to restricted formation of eddy currents.

In figure 52, hybrid filler sheets were tested at different frequencies. Temperature was calculated during first 10 seconds. At low frequency, heating temperature increases with increasing concentration. It was observed in electrical conductivity results, percolation threshold was around (13-6)%. During induction heating, similar results can be observed in low frequencies as well as higher frequencies. However, at higher frequencies, there was no distinct difference in temperature observed by changing the frequencies. At different frequencies, increase in heating was observed. We also observed in magnetic properties data (table 4-2) that at lower concentrations saturation polarization was very close and a large difference was observed above electrical percolation. At (8-6)% and (12-6)%, heating difference can be seen. Particles concentration was constant in all the hybrid sheets, the heating trend should be followed at lower concentrations with fibers. As the fibers concentration increases the rise in temperature was observed at all the frequencies; however temperature difference was very close at higher frequencies.
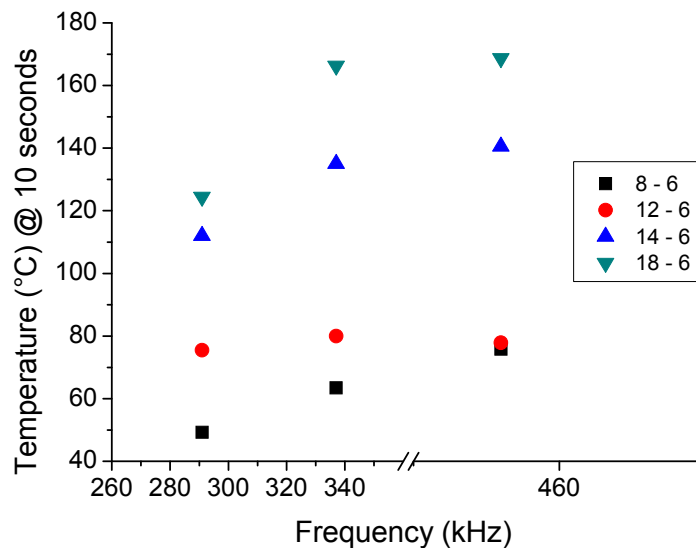
Figure 52: Effect of filler concentration vs frequency on heating @ NiCSCF/ NiCGP/ PP @ 30A, sample thickness 500µm

In figure 53, particles (NiCGP) filled sheets were tested at different frequencies. Time was calculated from 50°C to 120°C temperature interval as there was gradual increase in heating with respect to time. Frequency 456 kHz was found suitable frequency where maximum heating was obtained in fiber based sheet testing. However,

in case of particles, at higher frequency of 565 kHz, less time it took i.e. fast heating was observed. Further increasing the frequency, decline in heating was observed.
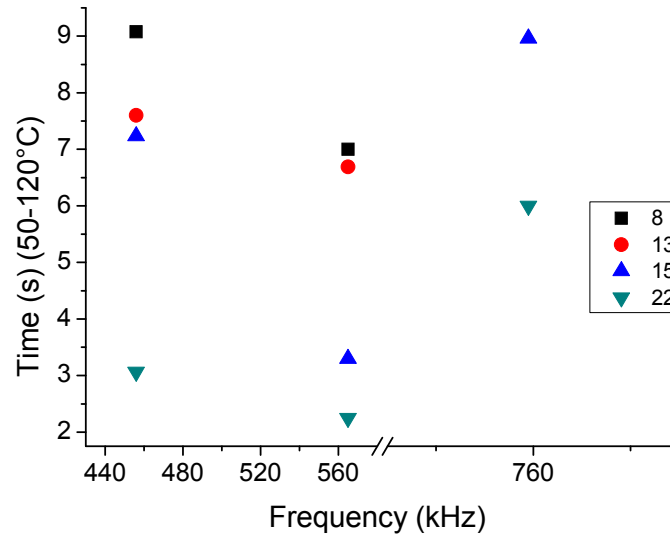
Figure 53: Effect of filler concentration vs frequency of Induction Heating of NiCGP/ PP @ 30A (*759 @ 15A), sample thickness 500µm

Magnetic testing data showed that particles filled sheets were higher in saturation polarization. Therefore for high frequency applications high saturation polarization is important[127].At 565 kHz frequency heating was faster than 456 kHz, however less than 759 kHz.

If we extract the conclusion from the frequency effect on fibers, particles and hybrid filled PP matrix, high heating can be obtained with increasing the frequency. In fibers, good heating was achieved at 456 kHz frequency, while in particles 565 kHz and hybrid has also good heating at 456 kHz, however at different filler concentrations, heating behavior was different. Higher frequency gives higher heating, however due to impedance of inductor and may be skin depth effect decrease the heating efficiency. Due to high magnetic polarization of particles, high frequency increased the heating.

4.5.4. Generator Power

The generator power level was not a part of this investigation as the target was to achieve the melting point temperature of the samples in reduced time; the generator power was kept at 30A in all of the experiments. Generator power can be changed by shifting the generator current. At its optimum level, the generator delivered 30 A.
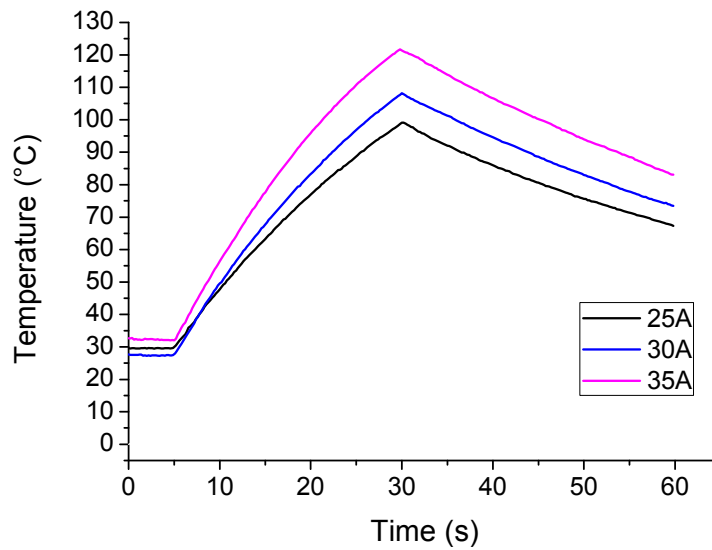
Figure 54: Induction heating of 10% NiCSCF/ PP at 456 kHz frequency, sample thickness 500µm

4.5.5. Coupling Distance

The separation gap or distance between the sample and the coil is known as coupling distance. It play very important role as the gap increases the magnetic field strength decreases and reduction in heating rate due to increasing the gap. In figure 55, time versus temperature graph was plotted. Two filler concentrations were selected and separation gap of 2 mm and 4 mm were used to observe their effect. In the below mentioned results it takes more time to reach the same temperature by increasing the separation gap. Therefore reduction in heating rate was observed.
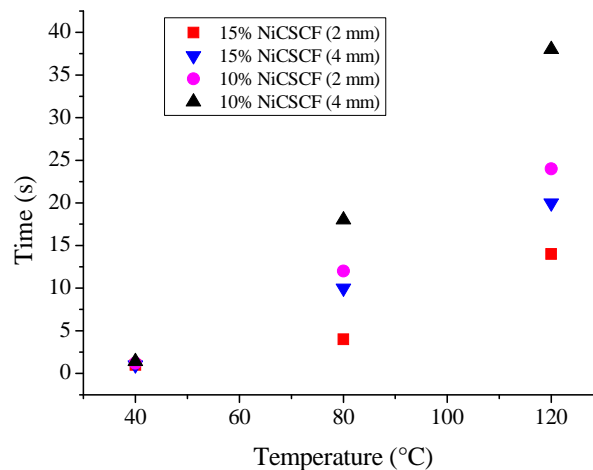
Figure 55: Effect of coupling distance on the heating time of different filler concentration, sample thickness 500µm

By increasing the coupling distance, magnetic potential function was considered for heat reduction. The function represents the energy distribution with respect to a single point in space. It was generally expressed that reduction in energy from its actual point in a reciprocal way[128]. However, we observed that it also depends on filler concentration.
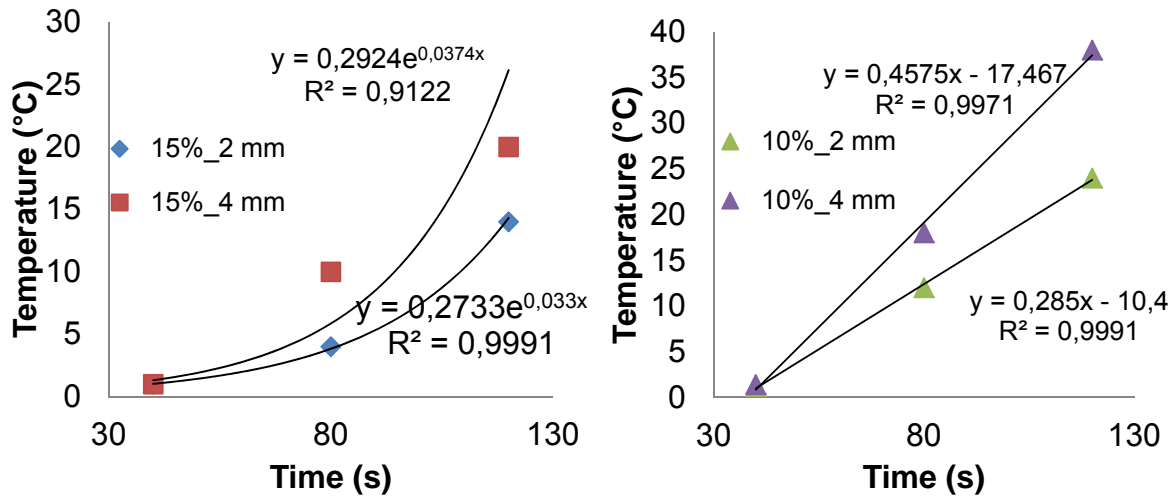
Figure 56: Calculation for coupling distance.

When there is a large gap between sample and coil, field strength reduces and heating rate also reduced. Two different filler concentrations were selected for comparison. In figure 56, exponential and linear functions were applied. Below electrical percolation, heating rate was inversely linear. However, above percolation, heating rate was reduced quadratically.

4.5.6. Perforated Sheets

Metal mesh susceptor was investigated by Yarlagadda et al[129] to melt thermoplastic, however non-homogeneous heating was observed. This was due to un-even heating from coil and difference in thermal expansion of metal and composite materials. Later on they did specific pattern for eddy current by cutting at different points to generate uniform heating. However adhesion was not good due to mesh coarseness[124]. Induction heating experiments were also performed in this study on perforated sheets to observe the heating in mesh format and further it can elaborate between joule loss and hysteresis loss. Perforations were generated manually with different sizes. Large holes of 25 mm diameter and small holes of 8 mm were made by manual punch die. Induction heating was analyzed by different filler concentrations of fibers (NiCSCF) and hybrid fillers (NiCSCF/ NiCGP) concentrations.

We observed in NiCSCF/ PP sheets without perforations that increasing the filler concentrations heating rate increases and at 15wt% NiCSCF/ PP sheets fast heating effect. A good interconnected fiber network was developed due to high aspect ratio. During mixing in double screw extruder fibers dispersion was very good, however substantial reduction in length was observed.
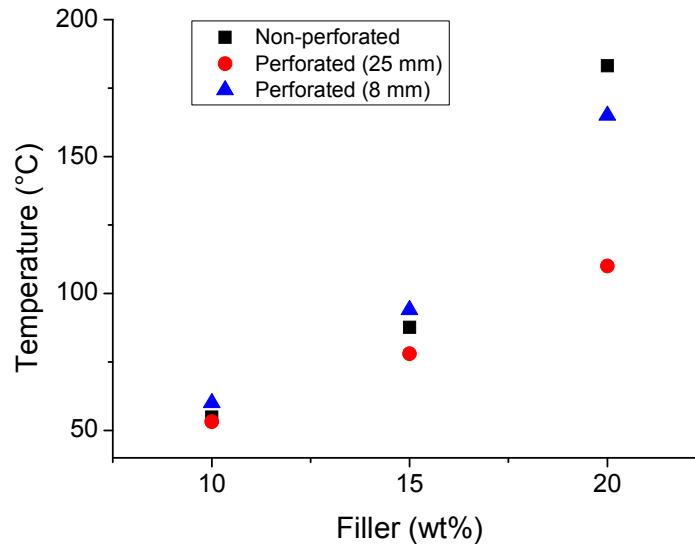
Figure 57: NiCSCF/ PP composites sheets, tested at 30A and 337 kHz, sample thickness 500μm

In figure 57, Temperature versus filler contents graph was plotted. Non-perforated and perforated sheets with similar concentrations were selected for comparison. In non-perforated sheets as well as in perforated sheets, temperature increases as the filler concentration increases, however non-perorated sheets were faster than perforated sheets of 25 mm diameter. If we compared the perforated sheets of 8 mm and 25 mm diameter, smaller hole sheets performed better than larger holes. Difference in heating may be caused by less available networks. Paths for eddy current travelling were less in larger holes as compared to smaller holes. Therefore eddy currents were better spread on small hole sheets and due to inherent resistance gives more heating. Slow heating rate was observed at lower filler concentrations, however a sharp rise was observed at 20wt% filler concentration. In perforated sheets no sharp rise was observed at higher filler concentrations. Although the electrical conductivity was higher and percolation threshold was around 15wt%.

During non-perforated sheets testing, joule losses, junction losses and magnetic hysteresis showed volumetric heating. In perforated sheets, reduction in heating may attribute due to less amount of fibers, fiber junctions and magnetic hysteresis, how-

ever due to formation of channels, resistivity increases and overall heating attribute due to different networks. These networks have limited paths for eddy currents.
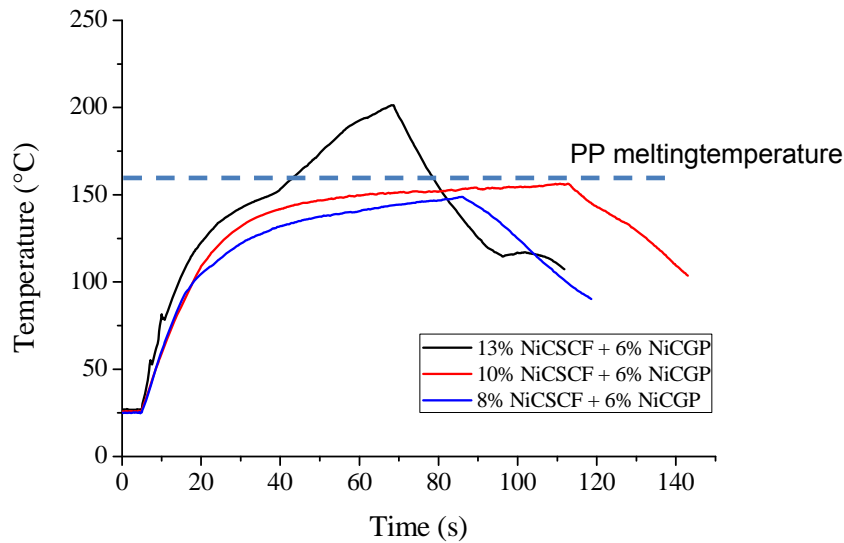

Figure 58: Time-temperature graph of NiCSCF/ NiCGP/ PP composites perforated sheet of 8mm diameter, tested @ 30A and 337 kHz, sample thickness 500µm

In figure 58, time-temperature graph of hybrid fillers were obtained during induction heating at generator current 30A and frequency 337 kHz. Fibers filler concentration develops the conductive network and particles provide an additional network formation support. Although the addition of nickel particles have adverse effect on electrical conductivity however has better effect on induction heating. Heating effect of hybrid system was slightly different as compared to fibers i.e. NiCSCF / PP sheets. Lower concentrations as well as higher concentrations were performed similar heating rate during initial stages, however at later stages large difference in temperature was observed. In hybrid system we found percolation threshold for electrical conductivity at (13-6)% hybrid filler. Electrical conductivity of hybrid filler sheets were well below than NiCSCF/ PP sheets. This reduction showed huge difference during initial stages of induction heating.

Heating rate at higher filler concentration increases abruptly, this may be due to melting of polymer that creates additional networks or melting reduces the coupling distance, therefore further rise in temperature can be seen. In hybrid perforated sheets higher fillers concentrations may give higher heating rate, however the sheets were brittle enough that got damaged during perforations.

4.5.7. Parallel Sheets (0°/ 0°) (NiCSCF/ PP)

During inducting heating, dielectric hysteresis and contact resistance are the heating mechanisms in fiber filled sheets. In 500µm sheets fibers were separated by thin lay-

ers of polymer and others were in contact and dielectric hysteresis and contact resistance heating obtained. However to increase the heating further, two sheets were compression molded to structure in single sheet. Two sheets of 500μm were stacked up in parallel direction of fibers to form one sheet of 1 mm thickness. This was achieved by compression molding. In induction heating, junction heating gave more heating due to dielectric hysteresis and contact resistance. Infigure59, time-temperature graph of 10% and 12% fibers (NiCSCF) was shown. In both the filler concentrations heating takes sharp rise within short span of time. This sharp rise in temperature was due to formation of unidirectional heating lines or dispersion of fibers in bottom and top layers. When two sheets were hot-pressed in fibers direction, possible dispersion of fibers cannot be neglected. The polymer melts and moves towards different directions due to compression. Micro CT images also revealed that fibers were dispersed in top and bottom side of sheet. However, at center fibers were well aligned. At lower concentration of parallel sheets, combined heating effect was present as it was in single sheet, however at higher filler concentrations, straight heating lines were present.
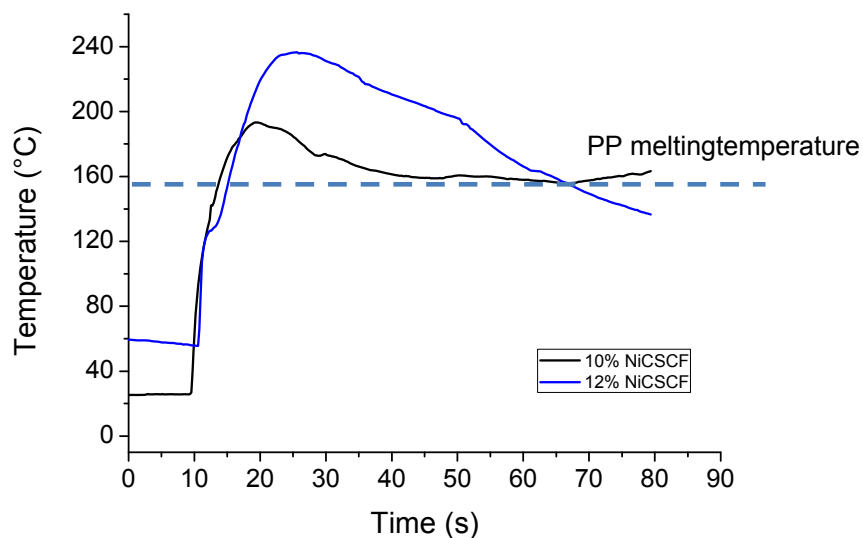
Figure 59: Time-temperature graph of NiCSCF/ PP composites (Parallel sheet), tested @ 30A and 337 kHz, sample thickness 1mm

For further investigation of these heating lines during parallel sheet heating experiments, very low current was provided. Heating lines were originated from middle of the sheet and spread out in the center and coil images was also present. At higher concentrations and higher current, joule losses heating mechanism was present along with these lines. These strong heating lines may be due to accumulation of fibers or due to limited penetrations of the filed.

Skin depth was also calculated on the basis of magnetic permeability of 15% NiCSCF/ PP sheet by using first curve of magnetization. The first curve of magnetization was taken by PPMS. Following were the values selected for μ = 2,95; ρ_{II} = 3,63 x $10^{-4}\Omega$.m; and frequency (f) = 456000 Hz. We obtained the skin depth value of 8.30 mm. Below 15% NiCSCF/ PP, the skin depth will be higher and therefore temperature gradient due to skin effect should not exist.
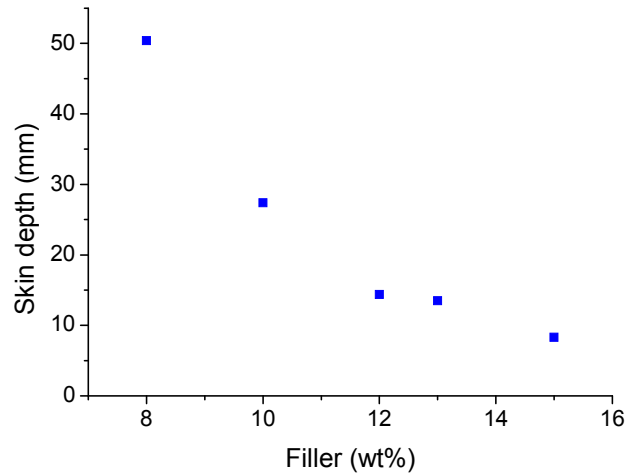
Figure 60: Skin depth versus filler concentration

In figure 60, if we take the value of magnetic permeability of 2,95 as reference and calculate the skin depth at lower concentrations, it reveals that no temperature gradient should exist.

4.5.8. Cross Sheets (0°/ 90°) (NiCSCF/ PP)

Induction heating of carbon fiber fabric filled thermoplastic composites, heating was observed due to large number of cross-over points due to contact resistance [41]. To develop cross-over (junctions) points, two sheets were compression molded by placing 0°/90° direction. In cross (0°/90°) sheet, two thin sheets of 500µm were stacked up in perpendiculardirection to fibers to form one sheet. Final thickness of the sheet was 300-350µm. Thickness of the sheet was reduced therefore fibers may come in contact. At lower filler concentrations heating was not homogeneous. This may be due to different reasons. Thickness was reduced; therefore most of the materials were squeezed out from the mold. Actual directions of the fibers were not perpendic-

ular. In figure 61, time-temperature graph of 10% and 13% fibers (NiCSCF) was shown. In both the filler concentrations heating takes sharp rise as it was in parallel.
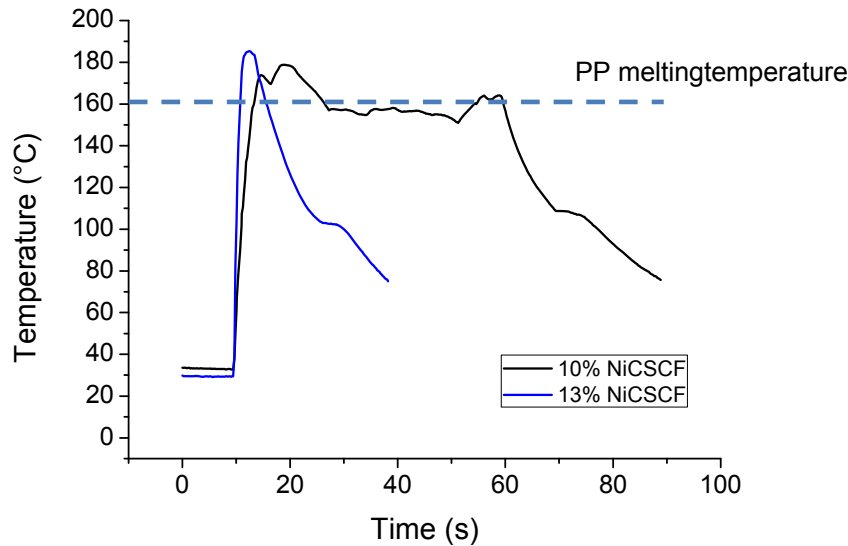
Figure 61: Time-temperature graph of crossed NiCSCF/ PP composites sheet, tested @ 30A and 337 kHz, sample thickness 300-350µm

Heating was not homogeneous this may be due to strong hot spots were developed at few locations. During compression, fiber were squeezed out and accumulated at different locations. This was confirmed by removing the border area of the sample. The large number of contact regions as in carbon fiber fabric need to be developed for further increase in heating. Frequency and magnetic properties limit the penetration depth and heating was more or less similar in thin (300-350µm) and thick (1 mm) samples.

4.5.9. Combined effect of NiCSCF and MWNTs

Induction heating experiments were performed by the addition of MWCNT with different filler concentrations of NiCGP and NiCSCF. Various researchers observed, that addition of MWCNT significantly affect the electrical properties of the composite [98]and have observed the percolation threshold even at a lower loading of 1&2 wt%CNT [66]. The MWCNT carry a good electrical conductivity property and form a conductive network in the matrix. However at this lower concentration, they form very small close circuit loop which is not enough to obtain heating by eddy current losses. Only MWNTs gave very slow heating [86] and similar results were observed, heating may be due to heat conduction by coil. MWNTs were incorporated with different filler

concentrations in combination with fibers (NiCSCF). In figure 62, time-temperature heating graph of fibers with and without MWNTs were plotted. The addition of MWCNT was helpful to add as extra filler with fiber that improved the conductivity network in the composite.

Figure 62: Time versus temperature graph of NiCSCF/ PP sheets with and without MWNTs, tested @ 30A and 337 kHz, sample thickness 1mm

Percolation can be obtained around 1-2wt% in MWNTs; however we obtained good heating at 3wt% MWNTs with fibers. Similarly, different filler concentrations of particles (NiCGP) were used along with MWNTs, however at lower concentrations of MWNTs, heating was very slow. At higher concentrations of MWNTs, heating was increased, however heating pattern was hysteresis. It reveals that lower concentration of MWNTs didn't make conductive network and heating was due to particles. At 5% MWNTs, heating pattern was combination of eddy current losses and hysteresis losses.
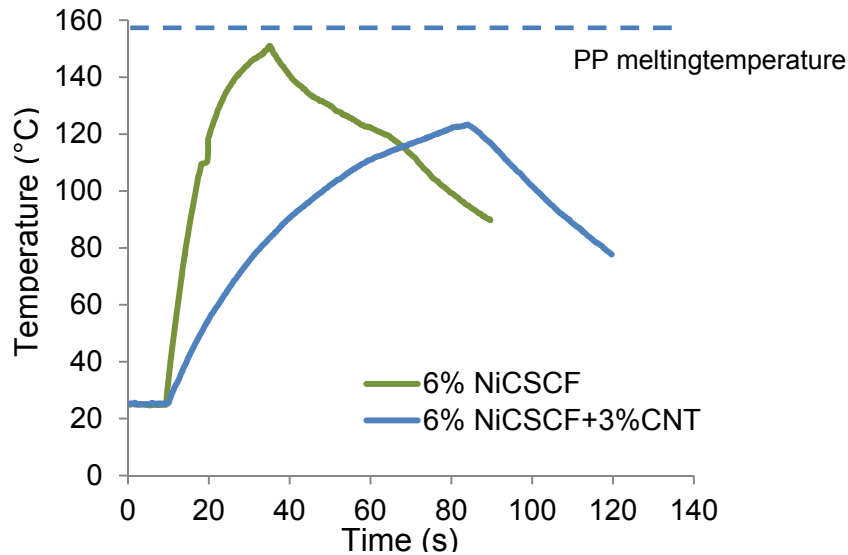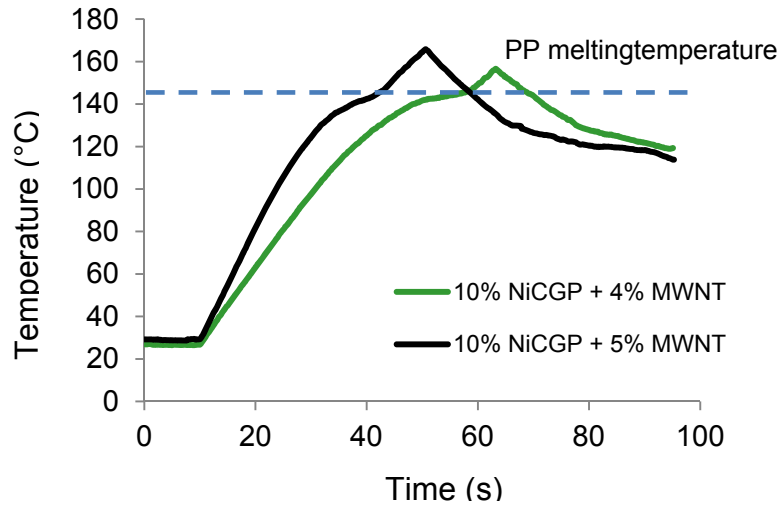
Figure 63:Time versus temperature graph of NiCGP/ PP sheets with MWNTs, tested @ 30A and 337 kHz, sample thickness 1mm

In figure 64, different filler concentrations of fibers were selected with and without MWNTs, however MWNTs were 3% in all the fiber-MWNTs composites.
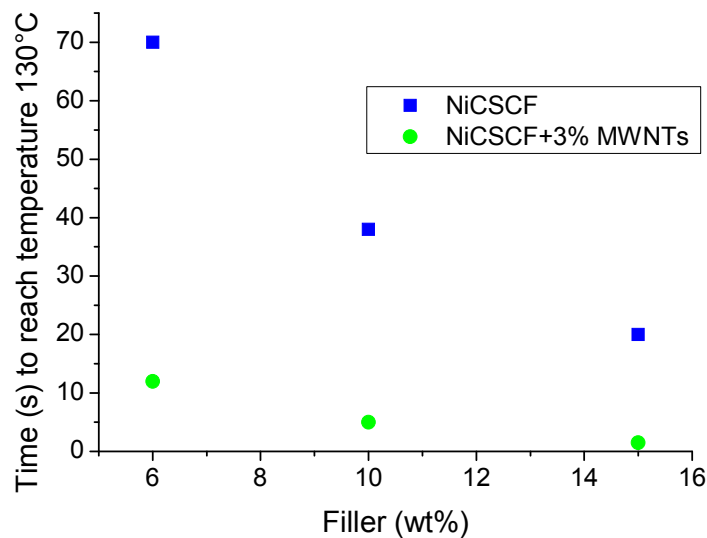
Figure 64: Filler versus Time graph to reach temperature 130°C with and without MWNTs tested @ 30A and 337 kHz, sample thickness 1mm

NiCSCF/ PP with and without MWNTs were compared and time was taken to the reach 130°C temperature. In NiCSCF/ PP sheets (without MWNTs), it can be seen that increasing the fiber filler concentration heating time was reduced. As the filler concentrations increases the conductive network increases, therefore electrical conductivity increases. At higher concentrations of fibers, heating time was reduced. Therefore addition of MWNTs along with fibers reduce the amount of fibers.

4.5.10. **Permalloy and Permalloy/ NiCSCF**

Flake shaped metallic magnetic particles were used with polymers. These materials were high permeability and high loss at high frequency [130A] however their thickness should be less than skin depth. For induction heating by hysteresis, polarization and depolarization generates heat due to friction. Hysteresis loop area quantifies the heat losses and it comes in soft magnetic materials, however magnetic permeability helps to apply high frequency. When particles filled thermoplastic suceptors sheets were tested, there was a large difference between the temperatures i.e. center and outer region. Pancake coils have high electromagnetic field strength at center therefore heating mostly takes place near center region. Permalloy was selected on the basis of high magnetic permeability so it works at high frequency. Permalloy flakes are alloy of nickel and iron. Physically they are in the form of flakes having thickness of 0,4 µm and aspect ratio of 84,7.Different low filler concentrations were selected for initial investigation. At 2% filler concentration, heating was slow, however the advantage that the difference in heating at center and outer region is lesser than other particles. In 35 seconds, permalloy with 2%, 4% and 6% filler concentrations heats up to 55, 70 and 92°C respectively. They were tested at 30A and at a frequency of 291 kHz.
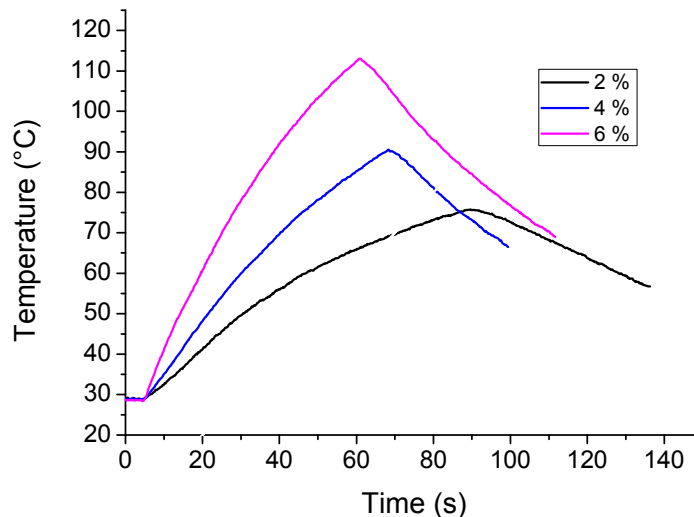
Figure 65:Temperature versus time graph of Permalloy/ PP @ 30A and 291 kHz, sample thickness 1mm

Permalloy flakes filled thermoplastic sheets were tested at high frequency. Heating was enhanced at high frequency. In 35 seconds, permalloy with filler concentration of 2%, 4% and 6% heats up to 67, 88 and 115°C respectively. In figure 66, time versus temperature graph of permalloy thermoplastic sheets were test at 456 kHz frequency.
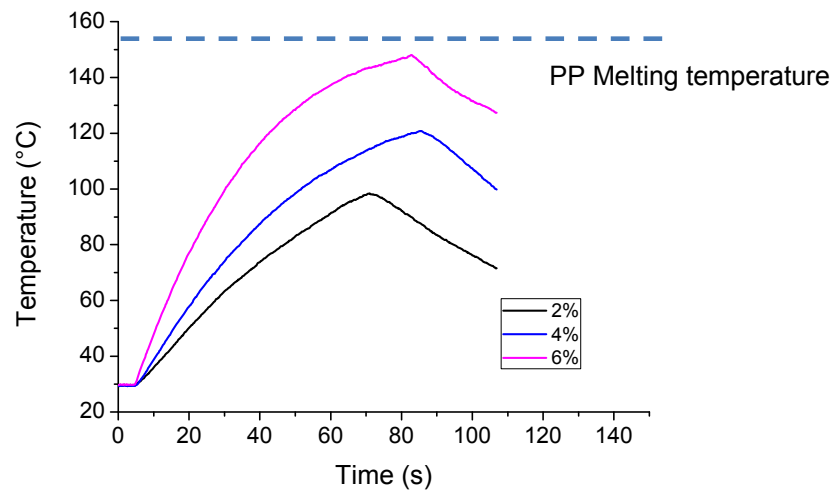
Figure 66: Temperature versus time graph of Permalloy/ PP @ 30A and 456 kHz, sample thickness 1mm

At low frequency, heating was slow however at higher frequency heating was enhanced. Due to the high density of permalloy flakes only very small quantity were used, however for induction welding, also small strips could be used.
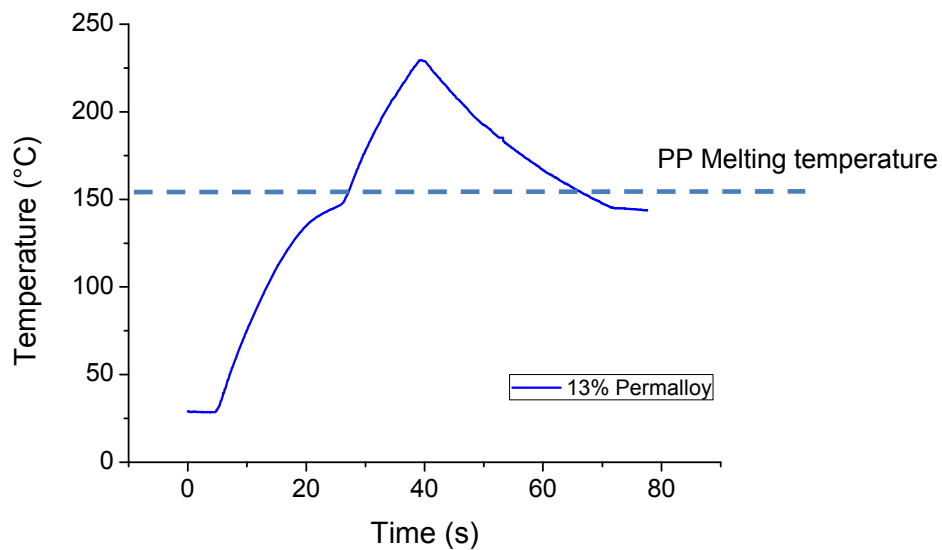
Figure 67: Time versus temperature graph of Permalloy/ PP Tested @ 30A and 565 kHz, sample thickness 1mm

Filler concentration of permalloy was further increased and frequency was also increased from 456 to 565 kHz. Heating rate was increased further by increasing the frequency. In the thermal image (figure 68), it can be seen there is a little difference in temperature at the center of the coil and the outer region.
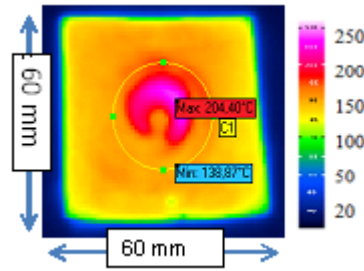
Figure 68: IR thermal image of 13% Permalloy/ PP
(30A, 565 kHz, sample thickness 1mm, time 34s)

Induction heating samples of fibers plus permalloy flakes were prepared at lab scale extruder from Brabender. Experiments were performed at 30A generator current and 565 kHz frequency. Heating of permalloy was due to hysteresis, however due to addition of fibers, joule losses was also present. Fiber were randomly distributed and well interconnected. Permalloy flakes further increased the connection in fibers and enhanced the heating. In figure 69, it can be seen that time-temperature graph starts in a similar way as it was with only fibers. It reflects that electrical conductivity was good enough and sharp increase in heating was observed. Permalloy flakes developed a good network with fibers and their high magnetic permeability further increased in heating due to application of high frequency.
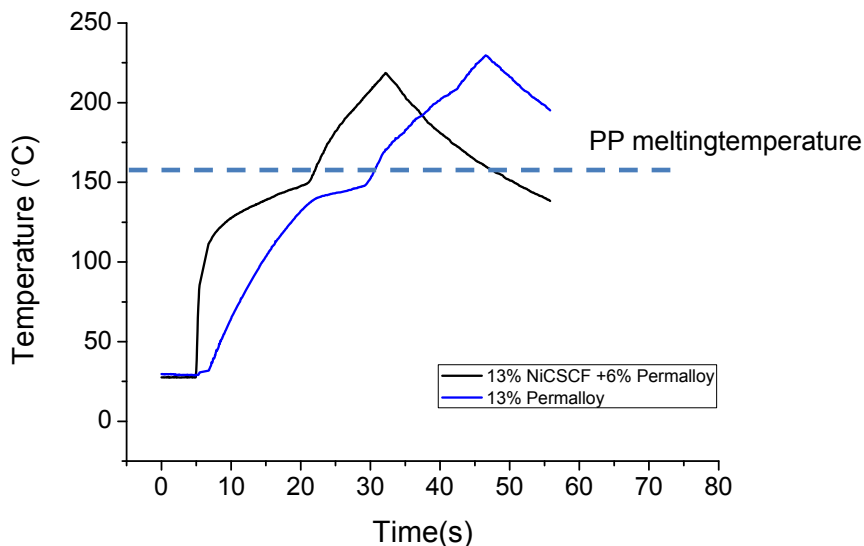
Figure 69: Time versus temperature graph of Permalloy/ PP and Fiber plus permalloy, tested @ 30A and 565 kHz, sample thickness 1mm

Comparative analysis of coated and non-coated samples.

Short carbon fibers (without nickel coating) filled PPS thermoplastic composites were tested to investigate the eddy current losses. The compounding was carried out via melting mixing using double screw extruder and samples were prepared by injection molding. Fibers were well aligned in processing direction. Samples for induction heating were prepared by compression molding. Sample thickness was 1 mm.

Samples with 10% and 20% filler concentration of short carbon fibers filled PPS thermoplastic were selected for comparison. Sample having 10% fibers demonstrated slow heating, while 20% fibers were faster. Heating mechanism was eddy current losses as there was no ferromagnetic materials coating, hence the heating obtained was only eddy current losses.
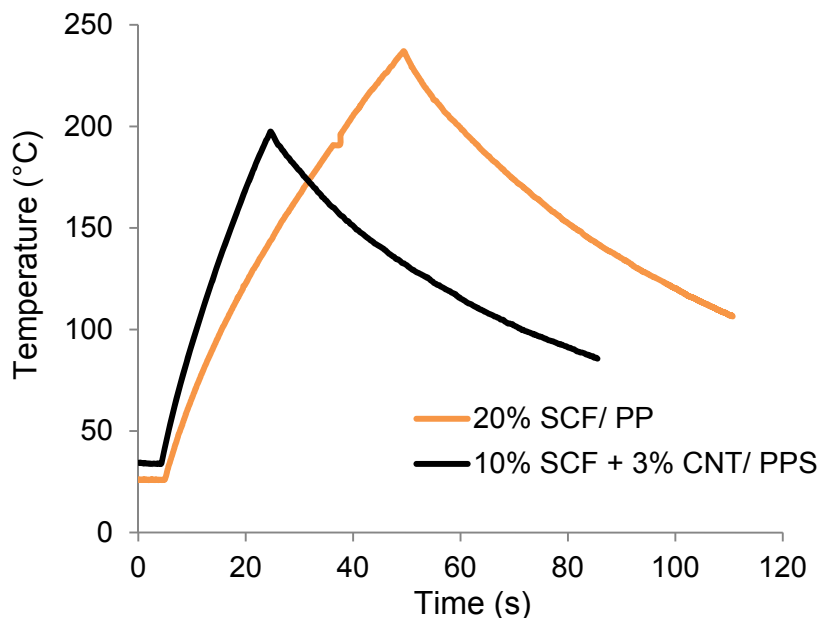
Figure 70: Time versus temperature graph of 10% and 20% short carbon fibers, sample thickness 1mm

In the same graph, fibers (without coating) plus CNTs filled thermoplastic sheet was tested. Heating is faster than 20% SCF/ PPS sheets. CNTs made very good conductive network and high electrical conductivity, therefore addition of small amount of CNTs not only increase the heating rate but also reduces the filler concentration of fibers.
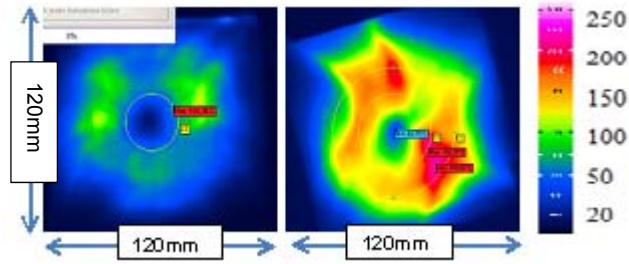
Figure 71: IR thermal images of SCF/ PPS and SCF/CNTs/ PPS (30A, SCF 456kHz, SCF/CNT 337kHz, sample thickness 1mm)

In thermal images, eddy current heating effect can be seen. Short carbon fibers were well above percolation threshold (6,39wt%) and heating is due to joule losses and junction heating. In other thermal image short carbon fibers with CNTs were induction heating tested. Heating pattern is similar like eddy current losses. For induction heating, injection molded sample was compression molded therefore heating effect is slightly different however replicate the eddy current losses.

In figure72, time-temperature graph of short carbon fibers (nickel coated and without nickel coated) with MWNTs were compared. Initial testing time was left to observe the heating trend. After reaching at 200°C temperature, generator was switched-off for cooling. It can be seen that NiCSCF/MWNTs/PP and SCF/MWNTs/ PPS attained the mentioned temperature almost same time. However the generator power was 20A in NiCSCF while in SCF it was 30A.
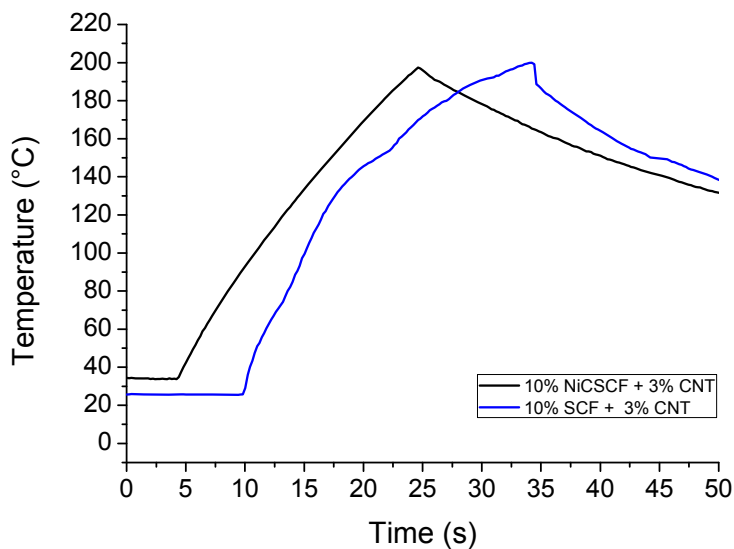
Figure 72: Time-temperature graph of NiCSCF (20A, 337kHz) and SCF (30A, 337kHz) with MWNTs, sample thickness 1mm

4.6.   Morphological Properties

4.6.1. Micro CT Images

NiCSCF/ PP, NiCGP/PP and Hybrid

Figure 73(a) and (b) are micro CT images of NiCSCF/ PP and NiCGP/ PP respectively. It can be seen that the dispersion was very good. The fibers (NiCSCF) were well aligned in processing direction. Only a Few fibers were tilted to small angels at higher concentrations. After extrusion process, fiber length was reduced to approximately 250-300 microns, however in reduced length seems in similar range. In figure 73(b) well dispersed particles (NiCGP) can be seen. In NiCGP/ PP composites, ferromagnetic hysteresis heating was the sole source of heat generation, therefore a good dispersion of the particles in the matrix was required. Proper mixing and uniform dispersion of the particles was achieved due to adequate temperature shear compounding, however possible oxidation of particles cannot be neglected.
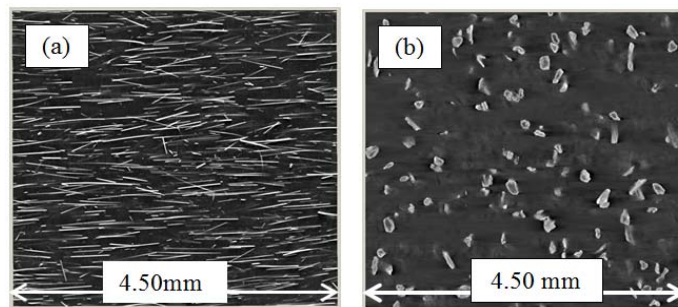
Figure 73: (a) Micro CT image of wt% (a) NiCSCF/ PP (b) wt% NiCGP/ PP

NiCSCF/ PP composite sheets were processed through calandering therefore the fibers were aligned in processing direction. In micro CT imaging in figure 74(a) 3D image of aligned fibers can be seen. The magnified cross-sectional view in figure 74(b) of the same sheet further explains the inside structure. Due to some misaligned fibers a good interconnecting in plane as well as between different layers was achieved. Therefore a good heating effect was obtained in such films. Head-tail connections served as contact junctions also, that adds to the heating further. At higher concentrations fiber made a dense net and formed several paths for electrical conduction.
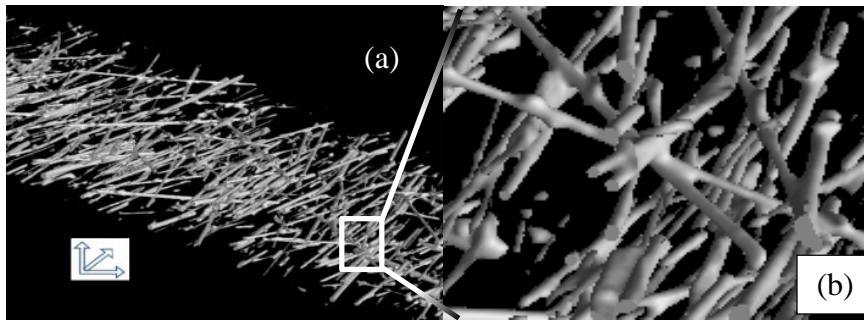
Figure 74: (a) Micro CT image of 15wt% NiCSCF / PP, cross-sectional view (b) close view

Figure 75(a) and (b) are micro CT images of NiCSCF/ PP and NiCCF/ NiCGP/ PP composite samples respectively. In hybrid system figure 75(b), good dispersion of fibers and particles can be seen, however fibers seem to be not well aligned at few locations. Particles provided the extra connections between fibers. Higher heating may be due to three reasons, 1- due to extra filler concentration in hybrid filler,2- misalignment of fibers i.e. random distribution of fibers, 3-more resistance due to contact resistance between fibers and particles. During sheet forming, particles made negative effect as fiber which were in close proximity were not well aligned. Due to particles, friction got increased that resulted further reduction of fiber length and their dispersion. Head-to-tail connection between fiber were not proper than head-to-body connections.
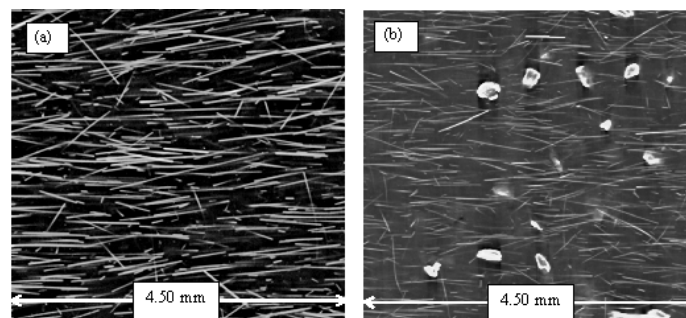
Figure 75: (a) 13% NiCSCF/ PP & (b) (13-6)% NiCSCF/ NiCGP/ PP

In figure 76(a) and (b), micro CT images of NiCSCF/ PP were taken before and after induction heating experiments for comparison. Before induction heating experiments aligned fibers can be seen. After heating experiment, melting regions can be seen as fibers got misaligned.
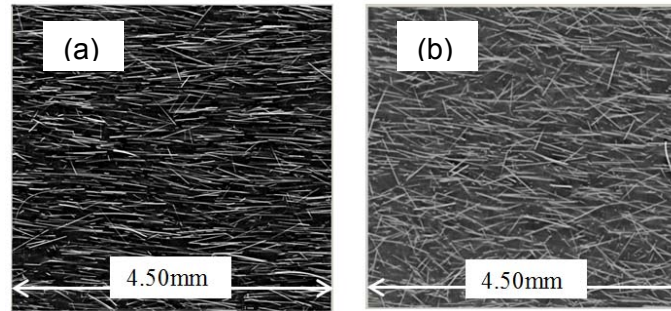
Figure 76: Micro CT images of NiCSCF/ PP, (a) before melting (b) after melting

Parallel (0°/0°) NiCSCF/ PP sheets

In parallel sheet, two sheets were stacked up in parallel direction to form one sheet of 1 mm thickness. This was achieved by compression molding. During molding, matrix squeezed out from the square shaped mold. Possible misalignment of fibers cannot be neglected. In figure 77, micro CT images that were taken from bottom, center, and top dispersion of fibers can been seen. Top and bottom side shows large dispersion of fibers, while center part was well aligned fibers can be seen.
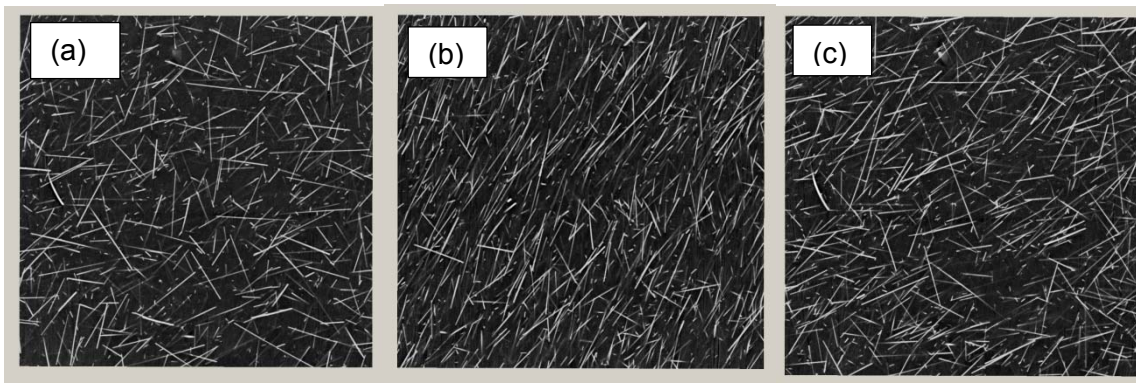
Figure 77: Micro CT image of 10wt% NiCSCF/ PP (Parallel) (a) bottom (b) center (c) top side

Small scale extruded samples (Lab scale samples)

At lab scale, small extruder from Brabender was used for compounding fiber and particles. Counter rotating screw direction was used. After compounding, sheet of 1 mm thickness was prepared by compression molding and a piece was selected for micro CT image. Fibers were well dispersed in polymer matrix. Reduction of fiber length was also observed however large variation can be seen. During compression molding, as polymer moves to different direction, accumulation of fibers at few locations cannot be neglected.
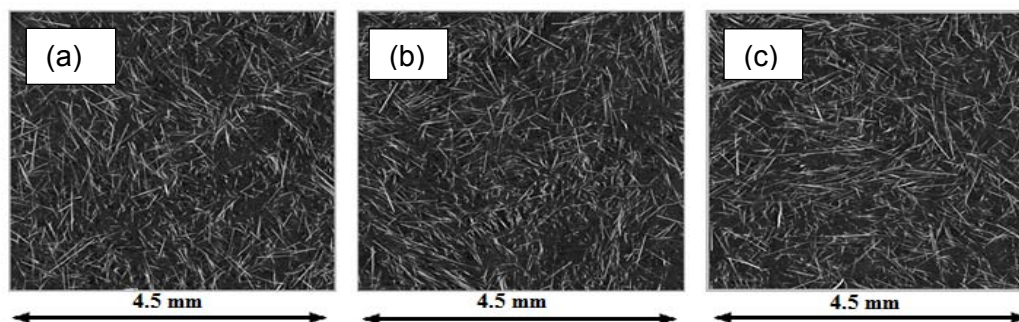
Figure 78: Micro CT image of 13% NiCSCF/ PP (a) bottom (b) center (c) top view

Similarly, at lab scale compounding of fiber and particles was carried out using same counter rotating mode. In figure 79, micro CT images of lab scale samples can be seen. They were well and homogeneously dispersed in polymer matrix. The mixing timing and temperature was constant for both the materials. The reduction in fiber length was not the same. This may be due to added friction from particles.
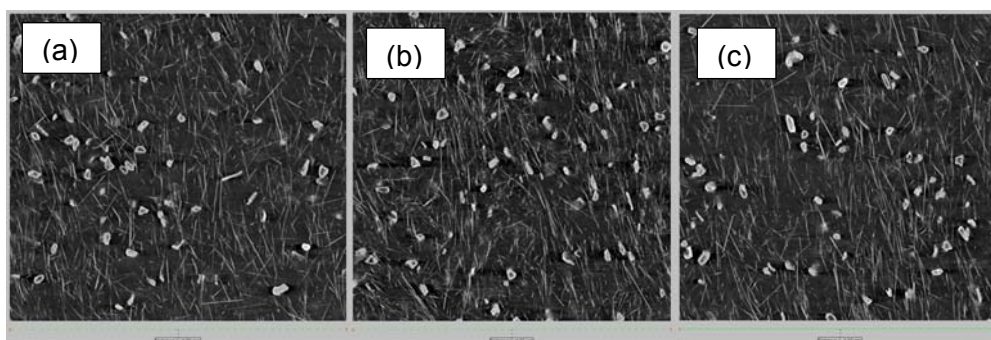
Figure 79: Micro CT image, (12-6)% NiCSCF/ NiCGP/ PP (a) bottom (b) center (c) top view

4.6.2. IR Thermal Imaging

NiCSCF/ PP, NiCGP/ PP & Hybrid

Infrared thermal imaging is a non-contact temperature measurement technology and it is being used for real time measurement of two dimensional surface temperature fields. Infrared thermography usually consists of a camera, data processing software and a computer. Time-temperature measurements were performed by thermal imaging. Through this imaging system, heating mechanisms can also be distinguished, whether it's eddy current losses or magnetic hysteresis losses. When there is a heating at the center of the sample, this is due to magnetic hysteresis. When there is a heating in outer region other than center, this is due to joule losses. Usually ferromagnetic particles filled samples losses heat due to magnetic hysteresis. Pancake

coil has maximum field strength at the center and eddy currents travels in outer region.
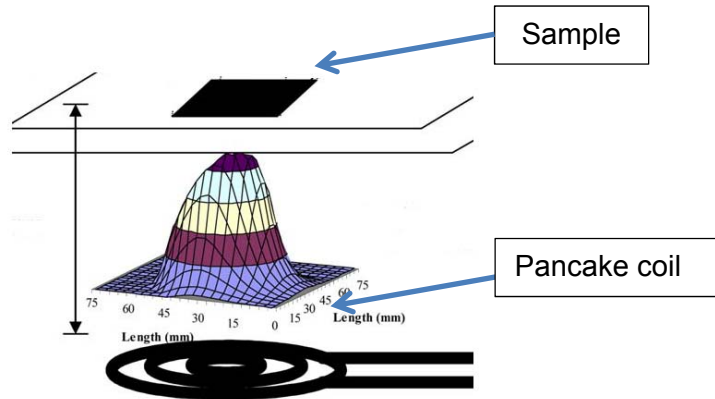
Figure 80: Heating Pattern in pancake coil

In figure 81, IR thermal images were taken during induction heating experiments. In figure 81(a) heating pattern shows a characteristic typical for the magnetic hysteresis effect due to heating spot at the center and out region is also giving heat due to eddy current loss. As the fiber was nickel coated, the magnetic hysteresis effect was dominating the eddy current loss. Although NiCSCF's conductivity was around 230 S/m heating contribution is also due to eddy current losses. At higher concentrations, heating was fast enough nevertheless heating patterns were similar with slightly oval shape. This might be due to the aligned fibers.

In figure 81(b), thermal image of NiCGP/ PP sheet was taken during heating experiment. Perfect magnetic hysteresis was obtained during NiCGP heating, the same pattern was observed in low and high filler concentrations. The difference was slow and fast heating. In particles small sample was selected for testing, therefore hot spot in both the mechanism is not the same.
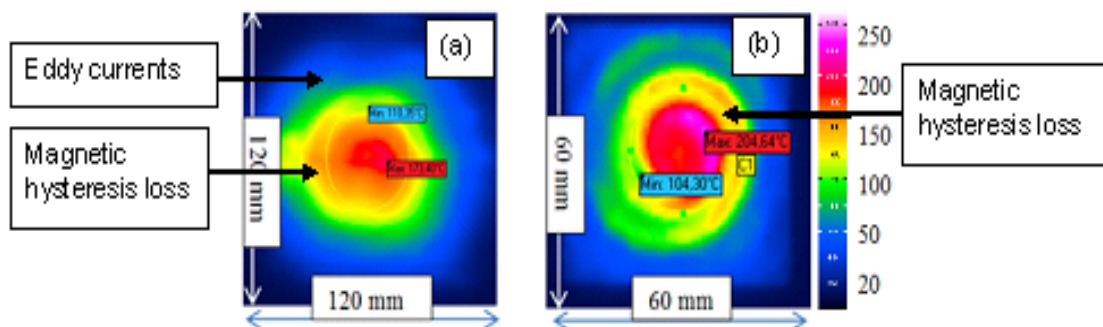
Figure 81: (a) 13wt% NiCSCF/ PP (b) 15wt% NiCG/ PP
(30A, 456 kHz, sample thickness 500 μm,)

In figure 82, thermal images of carbon fiber and nickel coated carbon fiber were compared. For the comparison purpose carbon fibers filled Polyphenylene sulfide (PPS) with 20wt% filler concentration was selected with same testing parameters. In figure 82(a), it can be easily distinguished that eddy current losses has no hot spot while heating takes places at outer region. In figure 82(b), nickel coated carbon fiber showing combined effect of eddy current losses and magnetic hysteresis.
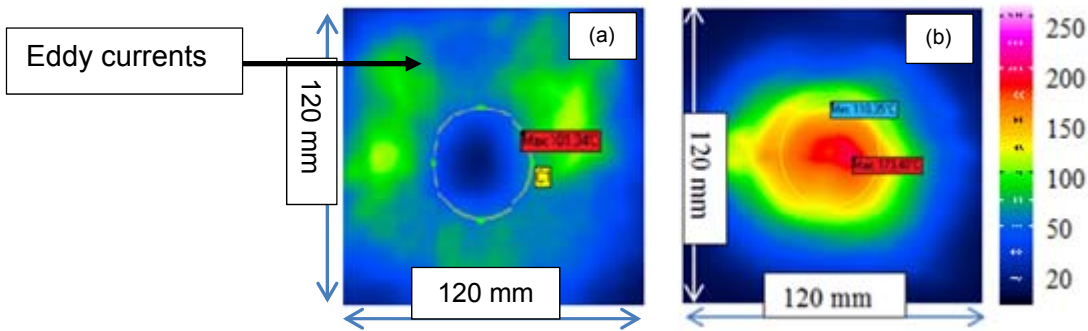
Figure 82: IR thermal images (a) 20% SCF/ PPS (b) 13% NiCSCF/ PP
(30A, 456 kHz, sample thickness 500 µm)

In figure 83, hybrid filled and only particles filled sheets was compared. In figure 83-(a) hybrid sheets showed combined effect of eddy currents and magnetic hysteresis, however hot spot is rather circular. In figure 83(b) NiCGP/ PP only magnetic hysteresis effect is present.
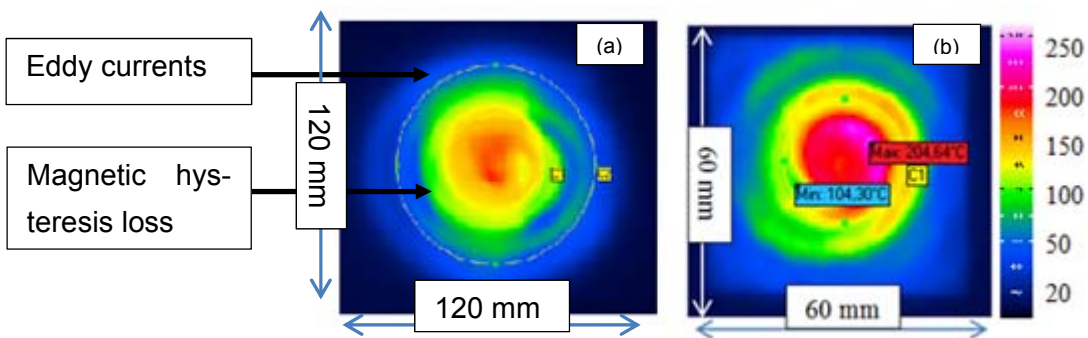
Figure 83: IR thermal images (a) (13-6)% NiCSCF/ NiCGP/ PP (30A, 456 kHz, Time)
(b) 15% NiCGP/ PP(30A, 565 kHz, Time 34s) sample thickness 500 µm

In figure 84, thermal images of fibers (NiCSCF/ PP) and hybrid (NiCSCF/ NiCGP/ PP) sheet samples were compared. In both the figures (a) and (b) shows combined effect of eddy currents and magnetic hysteresis. In both the cases dominant heating effect of magnetic hysteresis, however in figure 84(a), hysteresis effect is more prom-

inent than figure 84(b). This may be due to two reasons. First one is that addition of particles increases the nickel concentration and second is due to reduced electrical conductivity. This can also be compared with hysteresis loop of both the fillers. In figure 4-17, it can be seen that the saturation magnetization of hybrid filled system is higher than only fibers.
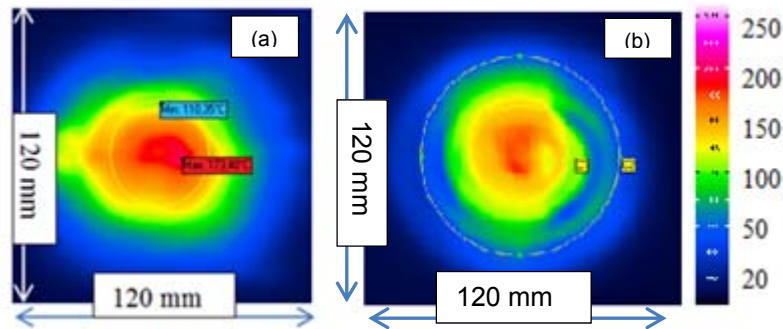
Figure 84: IR thermal images (a) 13% NiCSCF/ PP (time 67s) (b) (13-6)% NiCSCF/ NiCGP/ PP(30A, 456 kHz, sample thickness 500 µm)

In figure 85, comparative analysis of heating patterns can be seen. In figure (a) and (c), fibers and hybrid filler have same heating pattern however the effect is different as the electrical conductivity of these filler were different. Fibers have very high electrical conductivity and sharp rise was observed in heating. In hybrid filler, electrical conductivity was low, therefore no sharp rise was observed however higher temperature was attained in reasonable time.
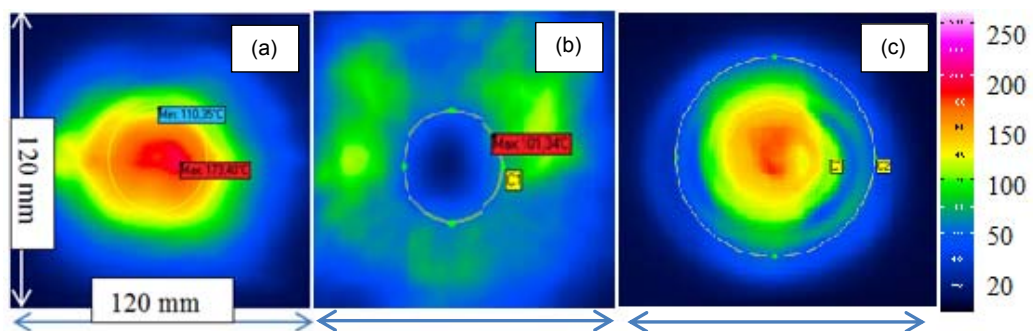
Figure 85: (a) 13% NiCSCF/ PP (time 67s) (b) 20% SCF/ PPS (time 24s) (c) (13-6)% NiCSCF/ NiCGP/ PP(30A, 456 kHz, sample thickness 500 µm)

Perforated Sheets

In figure 86, IR images of perforated sheets having large and small holes diameters were taken during heating experiments. In these images, coil reflections can be seen in a big circular loop, as observed by Xiao et al [131]. During heating, sample starts

to heat similar like coil heating therefore coil reflection can be seen in samples. In figure 5-25(a), heating pattern describes the heating regions due to magnetic hysteresis as coil has highest field strength at the center; however heating regions are spread over the coil. In figure 86(b), heating pattern is very much similar, except the temperature increase makes them different.
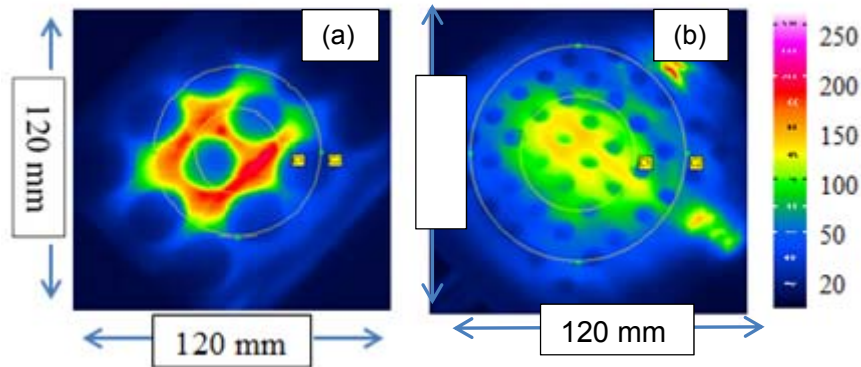
Figure 86: (a) 20% NiCSCF/ PP (25 mm diameter) (b) 15% NiCSCF/ PP (8 mm diameter)tested @ 30A & 337 kHz, sample thickness 500μm

In figure 87, IR images of perforated sheets having small holes diameters were taken during heating experiments. Figure (a) is hybrid filler and (b) is only fibers filled sheets. Hybrid filler perforated susceptor sheet has higher temperature as compared to fibers (NiCSCF/ PP) sheet. Similar effect can be seen in non-perforated sheets in figure 5-26.
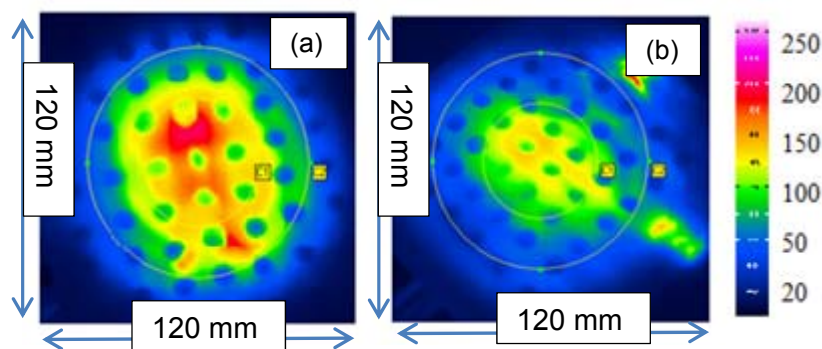
Figure 87: (a) (13-6)% NiCSCF/ NiCGP/ PP (b) 15% NiCSCF/ PP(perforations 8 mm diameter) tested @ 30A & 337 kHz, sample thickness 500μm

In figure 88, IR thermal images of standard size sheets (non-perforated) can be seen. Both of these images showing magnetic hysteresis effect is the dominant heating effect, however due to high electrical conductivity the heating effect is the combined form of joule losses and magnetic hysteresis. Figure 88(a) is a hybrid filler susceptor

sheet that has higher nickel concentration and addition of nickel has adverse effect on electrical conductivity therefore higher heating is due to resistive losses.
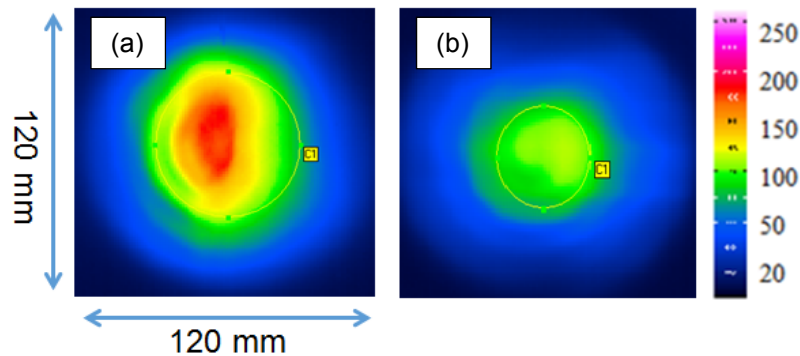
Figure 88: (10-6)% NiCSCF/ NiCGP / PP (b) 10% NiCSCF/ PP tested @ 30A & 337 kHz, sample thickness 500µm

Parallel (0°/0°) NiCSCF/ PP and Hybrid sheets

Induction heating experiments were also performed on 1 mm thick parallel (0°/0°) sheets to investigate the effect of increasing the thickness and effect of dielectric hysteresis. There sheets were prepared by stacking two 500 micron sheets together and pressed in hot press. Compression molding parameters were kept similar as mentioned section small sample preparation. Parallel sheets were 140 x 140 mm in dimension and later on 10 mm strips were removed from every edge to avoid accumulation of fibers.
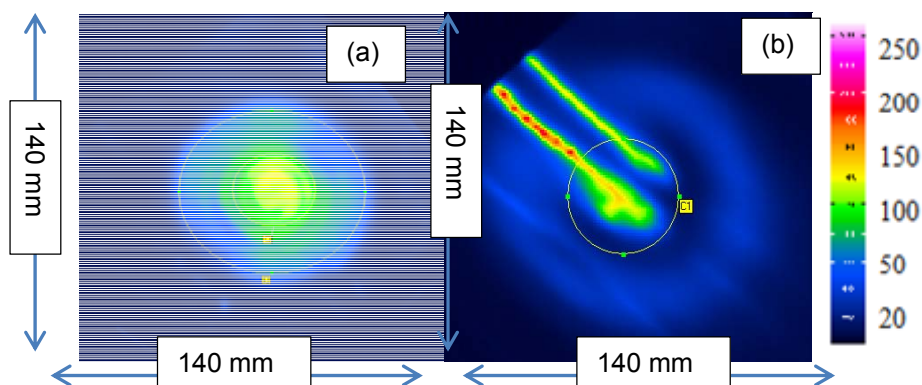
Figure 89: (a) 8% NiCSCF/ PP, (b)15% NiCSCF/ PP (Parallel) @5A & 337 kHz, sample thickness 1mm

In figure 89, IR thermal images of 8wt% NiCSCF/ PP & 15wt% NiCSCF/ PP sheet after stacking two sheet parallel to fibers direction by compression molding and of 1 mm thickness tested at 30A generator current and 337 kHz frequency with 2 mm

coupling distance. In figure 89(a), it can be seen the mirror image of coil was present that shows heating is combined effect of joule losses and magnetic hysteresis. At higher filler concentrations, figure 89(b), parallel sheet showed very different heating pattern. Although outer image of coil can be seen, however heating lines were present and sample was melting on these lines. At higher filler concentrations, when two sheets were stacked together in parallel direction, fibers were accumulated and formed lines of unidirectional fibers. This accumulation of fibers that developed fibers rows prohibits the formation of eddy currents within the sheet.
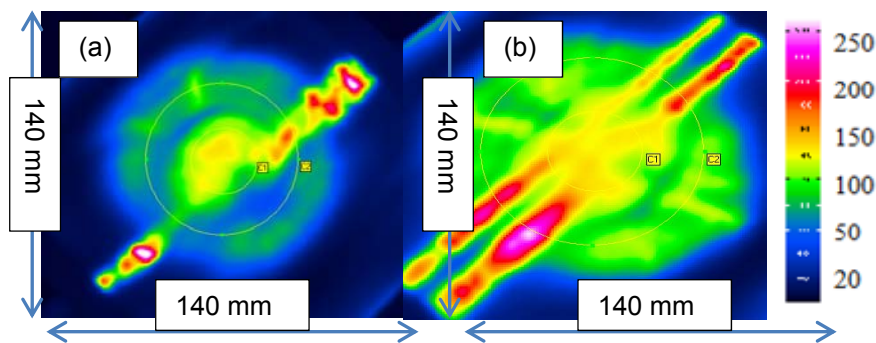
Figure 90: 10% NiCSCF/ PP (Parallel) & 18% NiCSCF/ PP (Parallel) at 30A & 335kHzsample thickness 1mm

In figure 90, IR thermal images of parallel sheets of different filler concentration were taken during heating experiments. This time generator current was kept at 30 amperes. Heating pattern was the combination of magnetic hysteresis and joule losses. Strong straight heating lines can be seen. These lines may be due to formation of straight fibers that were connected together.

Parallel sheets of hybrid filler systems were also prepared and induction heating tested. In figure 91, thermal image of (8-6)% hybrid filler was taken during heating. Magnetic hysteresis was present as heating took place at center, however outer region heating can also be seen. Hence, heating effect was combination of both effects, however faster than single sheet. As two sheets were compression molded, therefore possibility of dielectric hysteresis was increased.
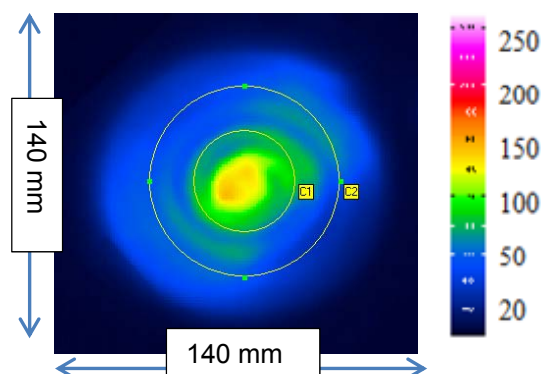
Figure 91: (8-6)% NiCSCF/ NiCGP/ PP (Parallel) tested @ 20A & 347 kHz,

sample thickness 1mm

MWNTs and MWNTs/ NiCSCF filled Sheets

In figure 92, IR thermal images of fibers with and without MWNTs thermoplastic composite sheets were taken during induction heating experiments with 1 mm thickness, prepared at brabender extruder. In figure 92(a) NiCSCF/ PP sheets with filler concentration of 6wt% were tested, heating pattern shows that magnetic hysteresis effect is dominant as heating is concentrating in the center; however coil image can be seen that heating is also taking place due to joule losses. Y. K. Lee et al [127] reported the increase in electrical conductivity of NiCSCF with addition of MWNTs.
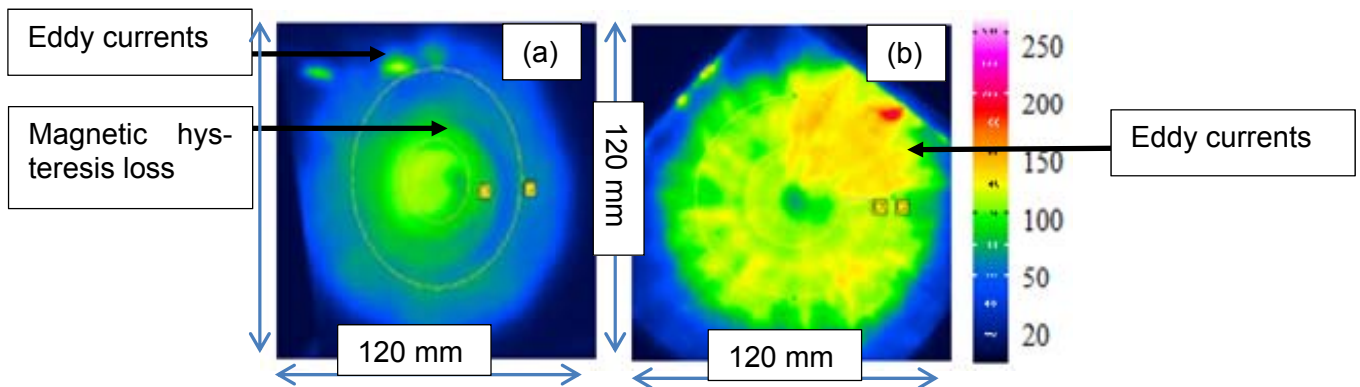
Figure 92: (a) 6% NiCSCF/ PP (b) 6% NiCSCF + 3% MWNT/ PP, tested @ 30A and 337 kHz, sample thickness 1mm

In figure 92(b), 3wt% MWNTs with similar amount of NiCSCF fibers were added and heating pattern was recorded. Dominating heating pattern switched from magnetic hysteresis to joule losses. As the fibers were nickel coated and heating effect of magnetic hysteresis was dominating without MWNTs, however addition of MWNTs forms a broad conductive network. Although MWNTs has higher electrical conductivity, however network is not much efficient. This may be due to resistance i.e. inter tubes resistance and tunneling resistance. In contact resistance, tubes were in physical contact and depend on contact regions; however conduction can take place by means of electrons diffusion.
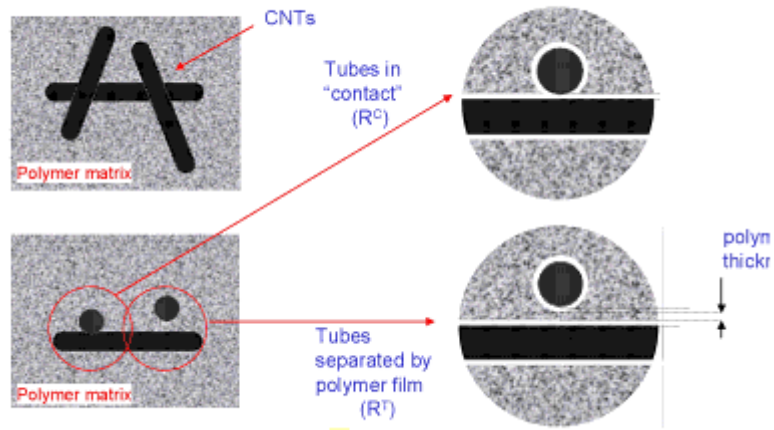
Figure 93: Possible Heating effect by MWNTs for contact and dielectric hysteresis

MWNTs alone cannot heat due to small closed electrical loops. Heating took place in MWNTs with fiber filler system may be due to contact resistance and dielectric hysteresis.
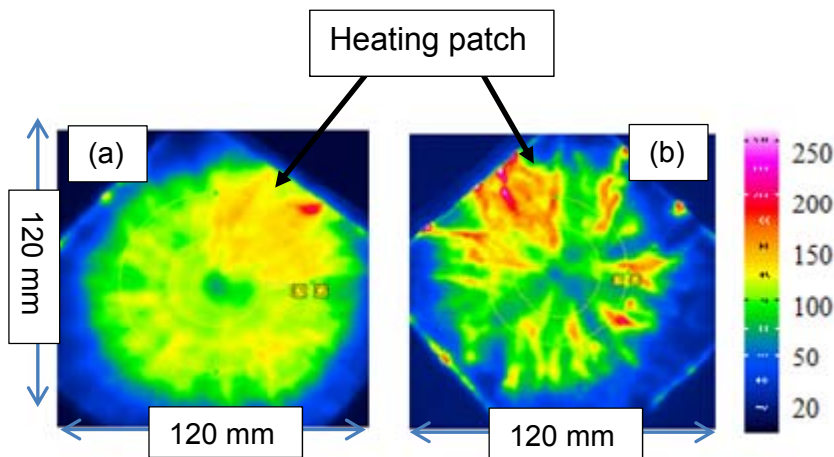
Figure 94: (a) 6% NiCSCF + 3% MWNT/ PP (b) 10% NiCSCF+3% MWNT/ PP tested @ 30A, 337 kHz and sample thickness 1mm

In figure 94(b), fibers concentration was increased while MWNTs remained constant. Heating pattern was joule losses, while overall heating is combined effect. Addition of MWNTs makes additional networks and helps to connect the fibers; therefore heating is due to joule losses and contact resistance, however different heating points were generated; this may be due to accumulation of MWNTs at different location. Large heat patch was due to pending of sheet and less coupling distance therefore high heating can be seen.

Permalloy and Permalloy/ NiCSCF filled Sheets

Permalloy flakes were compounded in PP thermoplastic by melt mixing in lab scale extruder from Brabender. It has very high magnetic permeability however it has a high density and was in flakes forms. Different filler concentrations of permalloy were prepared and tested. Heating was due to magnetic hysteresis. In figure 79, 13% permalloy was compared with NiCGP.
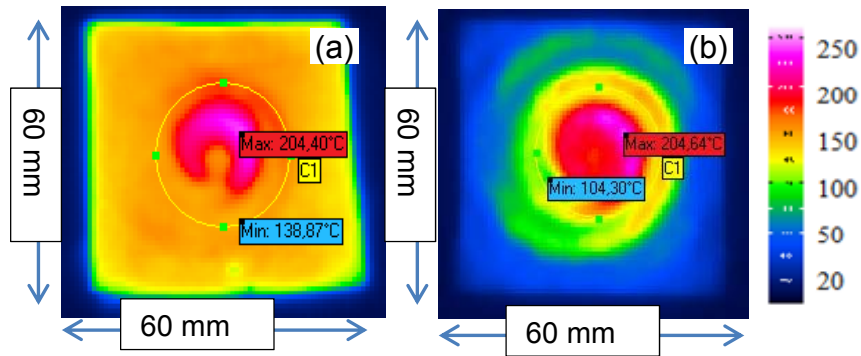
Figure 95: (a) 13% Permalloy/ PP (sample thickness 1mm)@ 30A and 565 kHz
(b) 15% NiCGP/ PP tested (sample thickness 500µm) @ 30A and 565 kHz

In permalloy flakes filled thermoplastic susceptor sheet, only magnetic hysteresis heating was available. Although it has high heating, however magnetic heating is slower than eddy current losses. Therefore, fibers were added along with permalloy flakes to improve the heating rate. Different filler concentrations of fibers were compounded on lab scale extruder. In figure 91, thermal image of 6% fibers and 3% permalloy flakes were taken during induction heating.
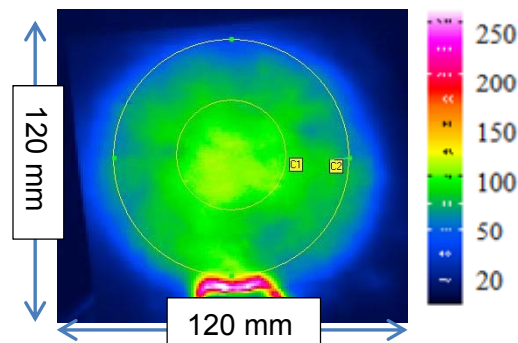
Figure 96: IR thermal image of 6% NiCSCF/ 3% Permalloy/ PP
(30A, 267 kHz and sample thickness 1mm)

It can be seen that heating was homogenous and was fast enough to melt the PP polymer. Due to magnetic hysteresis heating, the center region heating as well as outer region heating can be seen. This may be due to permalloy that has high magnetic permeability or conductive network that developed by fiber plus permalloy. Heating graph of higher filler loading showed that sharp rise in heating is due to joule losses and further rise in temperature is due to magnetic hysteresis. Structure of

permalloy was in flakes that has less thickness and it has developed several paths by joining different fibers at a time and finally made good conductive path.

4.6.3. Correlation of IR thermal images and Micro CT images

During processing of fiber filled thermoplastic composite sheets, fibers were well aligned and well distributed. When the filler concentration increases, alignment further improves. If we compare the micro CT images with IR thermal images, we can correlate these images. At lower filler concentration, fiber alignment as well as inter fiber distance was less than for the higher filler concentration. Therefore heating was enhanced as the filler concentrations increased. But it was also observed that as the filler concentration increased, fibers were well interconnected with head-tail connections and form straight long fiber rope. In IR thermal images, heating shape at 10% filler concentration showed circular cum oval, however at higher concentration oval shape was more highlighted.

10wt% NiCSCF/ PP

120 x 120 mm
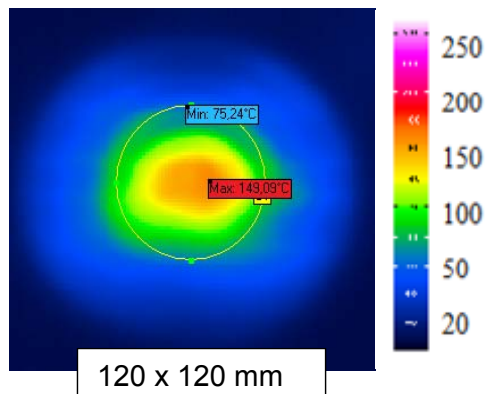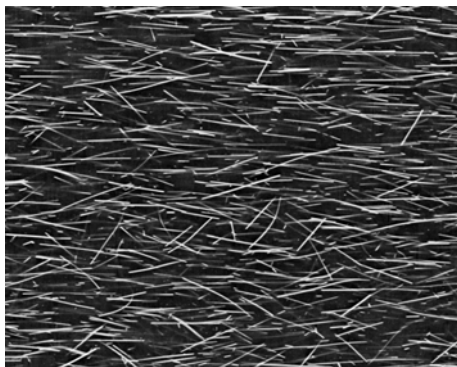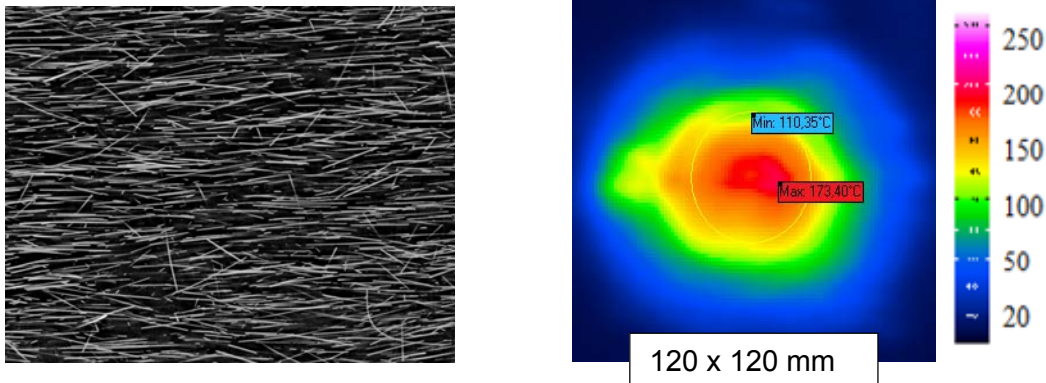
13wt% NiCSCF/ PP

15wt% NiCSCF/ PP
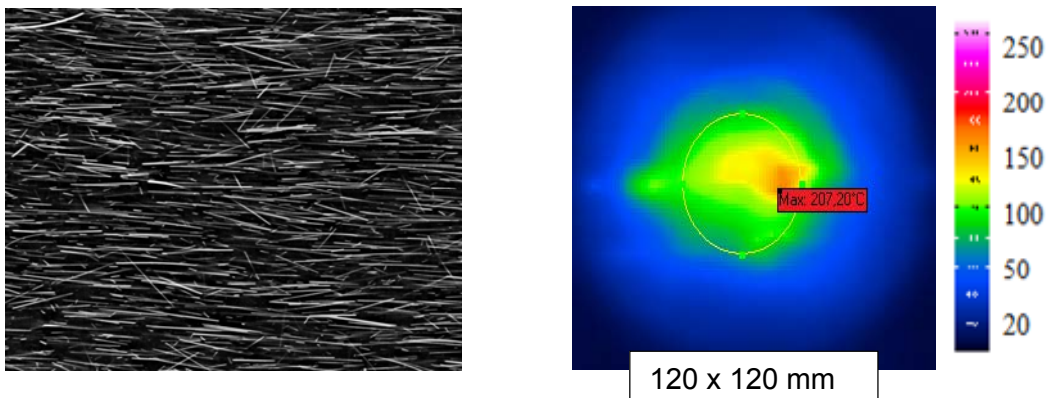
Figure 97: Micro CT images and IR thermal images of different filler (NiCSCF) concentrations

In hybrid filled thermoplastic susceptor sheet, micro CT images and thermal images also reveals the similar. In micro CT image, fibers were not well aligned as it was observed in only fibers susceptor sheet. Addition of particles provides hindrance during Calandering process. Misalignment was large in small concentrations; however at higher concentrations it was improved. During compounding in hybrid filled susceptor sheet, more friction was there due to particles and fibers length reduction was larger than in only fibers susceptor sheet. Therefore small size fibers and particles both have adverse effect in aligning fibers. Heating in thermal images also revealed that shape of image also changes from circular to oval at higher filler concentration.

(10-6)% NiCSCF/ NiCGP
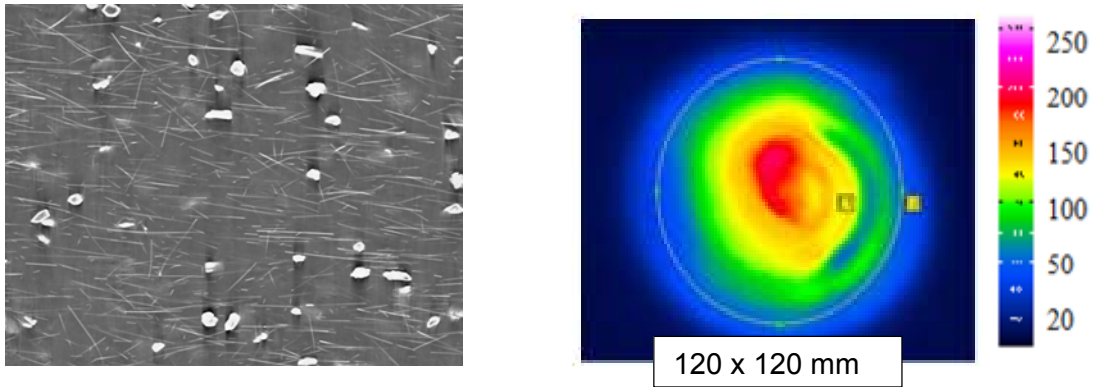
(13-6)% NiCSCF/ NiCGP
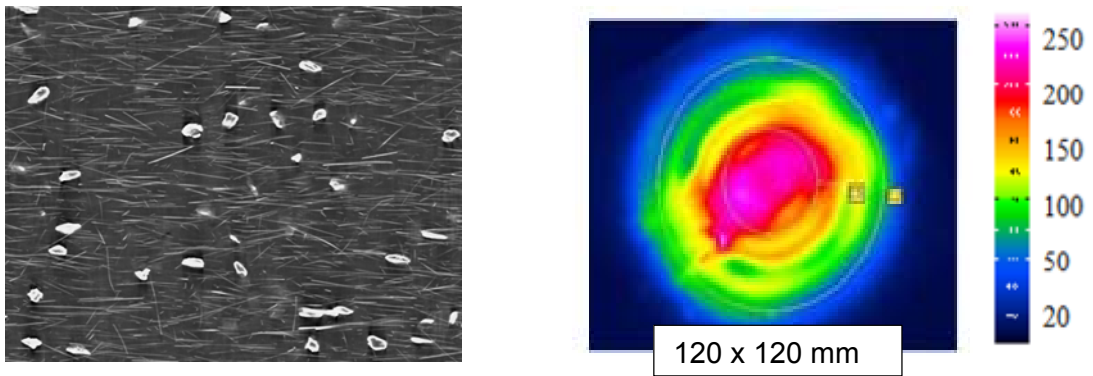
(18-6)% NiCSCF/ NiCGP
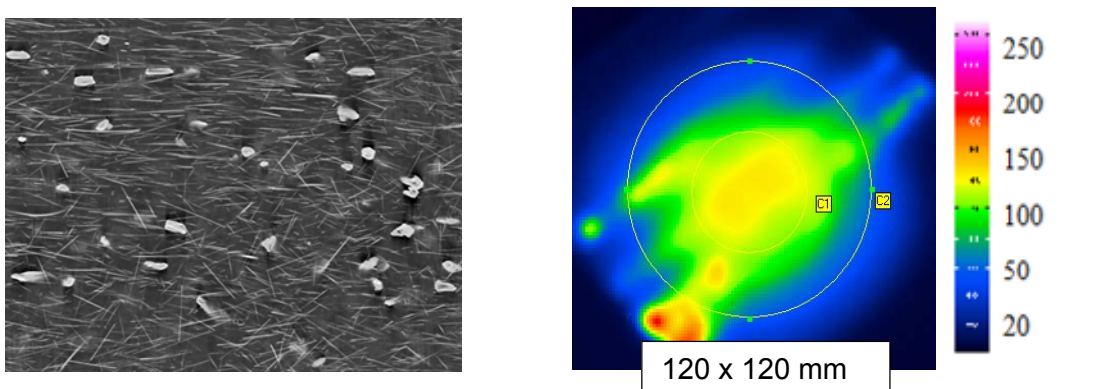
Figure 98: Micro CT images and IR thermal images of different hybrid filler concentrations

4.6.4. SEM Images

Scanning electron microscopy (Ziss GmbH) was applied to characterize the dispersion of fillers i.e. fibers and MWNTs in PP matrix. The specimens were prepared by polishing and sputter coating. Samples selected for SEM analysis were prepared on small extruder. Among these samples, dispersion of 6% NiCSCF and 15% NiCSCF with 3% of MWNT were observed using SEM at different magnifications. In figure 99, distribution of fibers can be seen. Fibers were random distributed in polymer matrix. Due to the 6% concentration, fibers were distributed and separated as isolated. However few were making conductive path. Therefore due to limited conductive path eddy current circulate in within these paths and less heat generate due to less resistance.
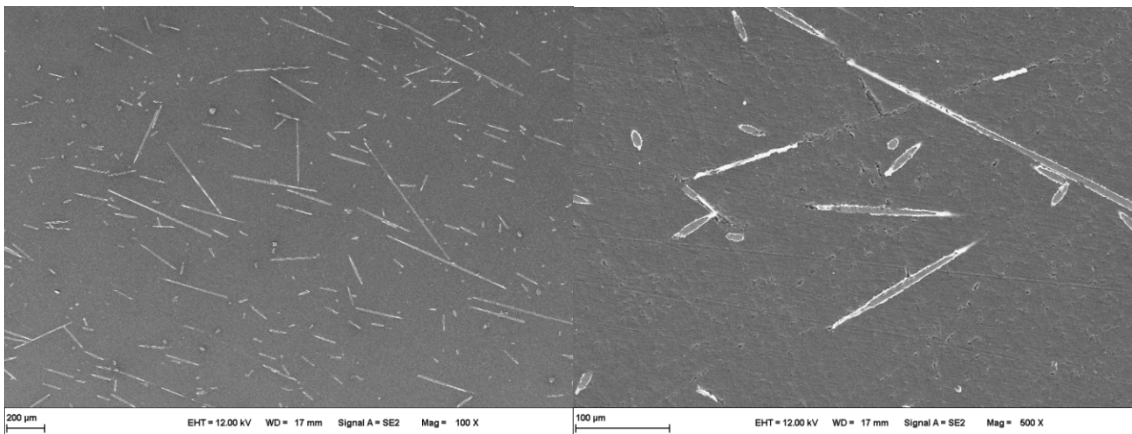
Figure 99: SEM micrograph, 6% NCSCF + 3% MWCNT/ PP

In figure 100, SEM micrographs of the fractured surfaces of the composites are shown. MWCNT can be identified as white, sprouts like particles in cross-section of the PP matrix. Fiber were in layer form and well separated.
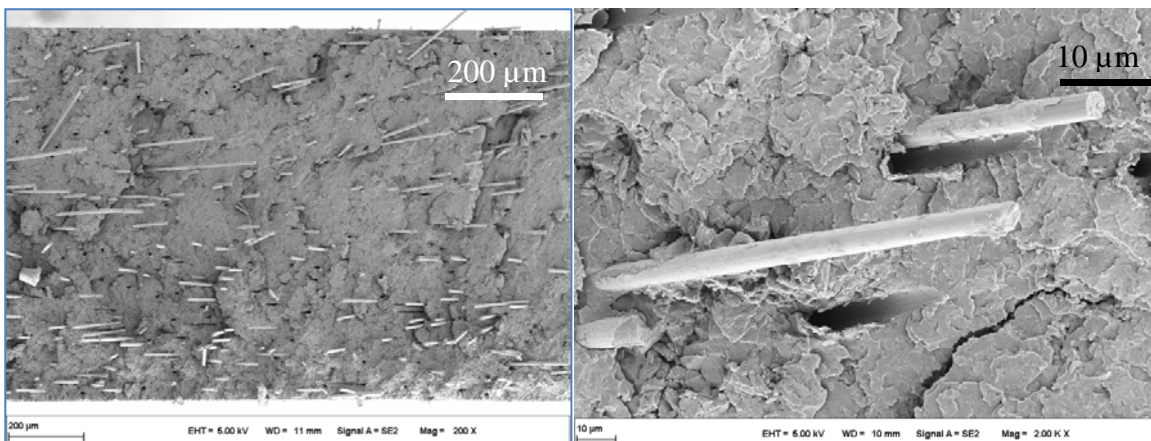
Figure 100: SEM micrograph of fractured surface of 6% NiCSCF+3% MWCNT

MWCNT createda bridge between the fibers and also made more paths within different direction and finally made conductive network with several paths.

Figure 101, dispersion of MWCNT in the PP matrix can be seen, however cluster of CNTs has developed. Since with addition of MWCT to the composite, the electrical pathways produced by the NCSCF were improved to obtain higher conductivity. It was observed that, the hybrid combination of NCSCF and MWCNT fillers increased the overall conductivity of the polymer composite which makes the composite suitable for heating by means of joule losses.
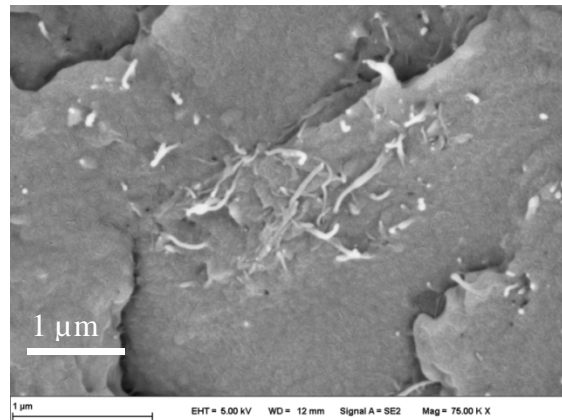
Figure 101: SEM micrograph, 6% NCSCF + 3% MWCNT show the MWCNT dispersion

In figure 102, SEM images of 15% NiCSCF/ + 3% MWNTs were shown with two different magnifications. Fibers were well distributed and fiber length is well within certain range and few large fibers can also be seen. Due to fixed mixing time and temperature, it was assumed that fibers will remain within certain range. The breakage of fibers was well controlled due to fixed mixing time and temperature. However due to increase on filler concentration, shear rate increased and fiber length was reduced.
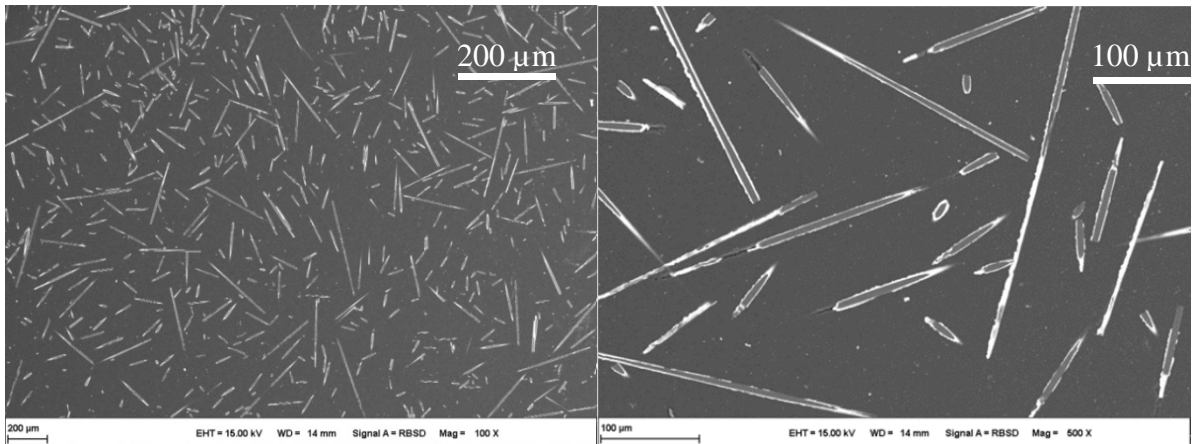
Figure 102: SEM micrograph, of 15% NiCSCF with 3% MWCNT
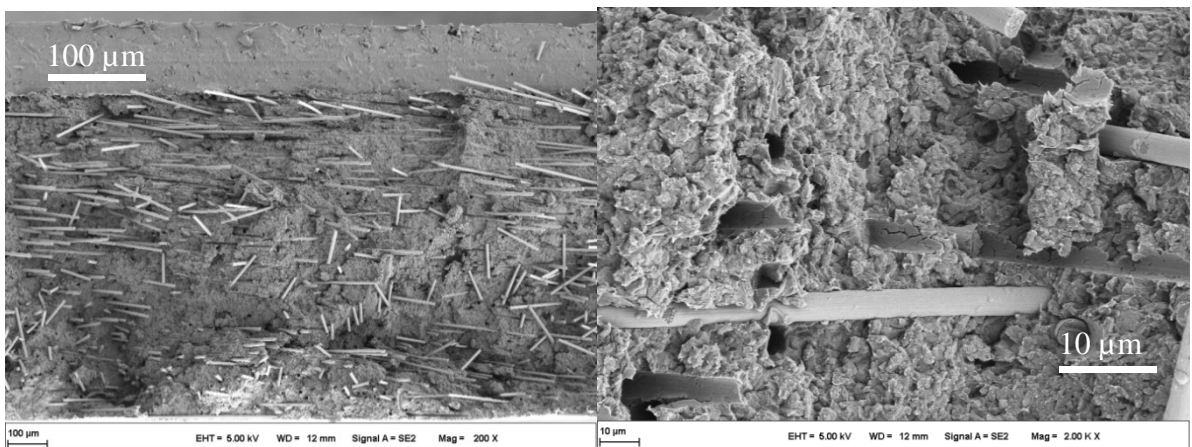
Figure 103: SEM micrograph of fractured surface of 15% NiCSCF+3% MWCNT

Figure 104 shows the dispersed 3% MWNTs in the polymer structure. Since with addition of MWCT to the composite, the electrical pathways produced by the NCSCF were improved to obtain higher conductivity. It was observed that, the hybrid combination of NCSCF and MWCNT fillers increased the overall conductivity of the polymer composite which makes the composite suitable for heating by means of induction.
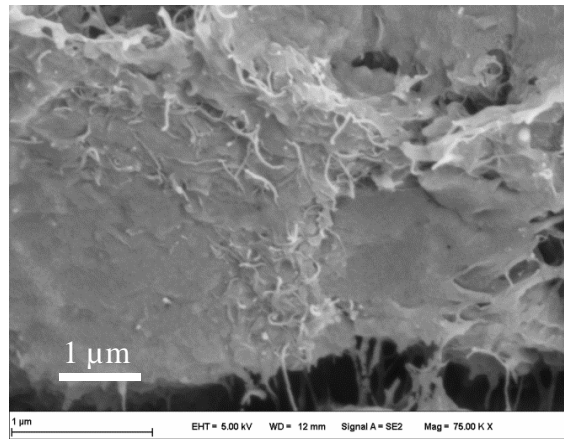
Figure 104: SEM micrograph of fractured surface of 15% NiCSCF+3% MWCNT

In figure 105, SEM image of permalloy along with fibers can be seen. Fiber and permalloy flakes were homogeneously dispersed in the matrix. Permalloy flakes were 0,4 micron thick, and can be seen in silver pieces, while fibers were randomly distributed with different fiber length.
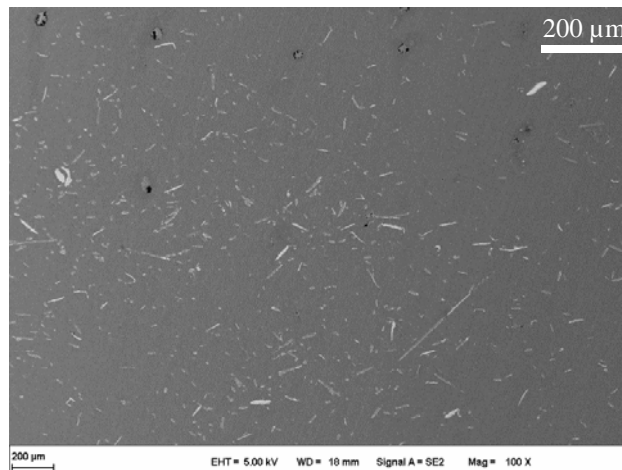
Figure 105: SEM micrograph, 6% NiCSCF+ 3% Permalloy

4.6.5. Light Microscopy

Orientation angel was measures by using transmitted light microscope at magnification of 20x to measure the orientation angle of the nickel coated carbon fibers. A camera was mounted on top of the microscope for taking image using software for analysis.

In figure 106, orientation parameter was calculated from images taken from light microscopy analysis system attached with Digital camera and calculation was performed by software analysis of image taken. Bay et al. observed that weight average gives more accurate orientation results. NiCSCF orientation produced by the image

analysis system, it is plotted against orientation angel and fiber content. It can be seen that fibers were mainly aligned from 0-18° and 162-180°, however at 8% filler concentration; fibers were also aligned at 144-162° angel.
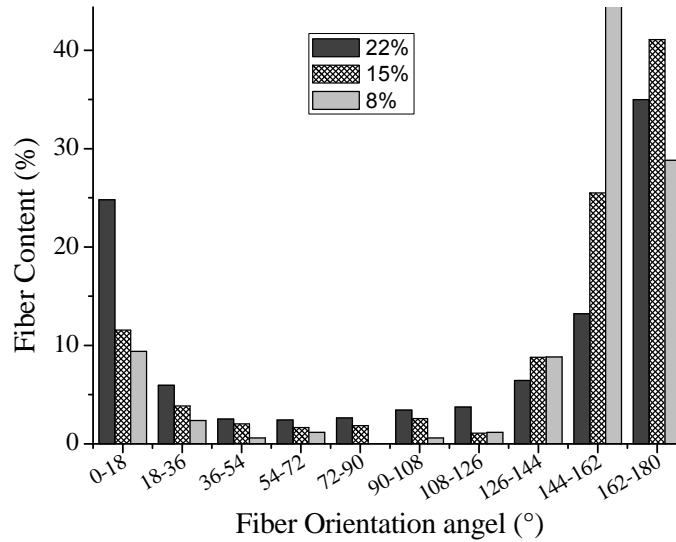
Figure 106: Fiber Orientation angel vs fiber content of different NiCSCF/ PP composite thin sheets

5. Conclusions

A susceptor sheet for induction heating technique was developed that can generate homogeneous and fast heating. It can be applied with non-conducting and non-magnetic materials for joining with induction heating due to contact-less heating.

In this study, investigations were carried out both from a materials point of view (i.e. filler and its concentration) and from a process parameters point of view (i.e. coil current, frequency and coupling distance). Fast and homogeneous heating with a 40°C/ sec heating rate was achieved with nickel coated short carbon fibers (15wt.-%) and multi-walled carbon nanotubes (3wt.-%). Testing was performed at 30A and a frequency of 337 kHz. For 15wt.-% nickel coated short carbon fibers, the heating rate was 24°C/ sec. Testing was performed at 30A and a frequency of 456 kHz. Addition of multi-walled carbon nanotubes enhanced the heating by making an effective conductive network. Nickel coated graphite particles were slow in heating if compared with nickel coated short carbon fibers. Hybrid filler system of fibers and particles was also developed and tested.

Filler concentration (wt.-%)	Heating rate (°C)	Sheet Thickness (mm)
15% NiCSCF/ PP	24	0.5
14% NiCSCF/ 6% NiCGP/ PP	9	0.5
15% NiCSCF/ 3% MWNTs/ PP	40	1.0

Nickel coated short carbon fiber was faster in heating when compared to nickel coated graphite particles. Hybrid filler was faster than nickel coated short carbon fibers at lower filler concentrations; however, above electrical percolation nickel coated short carbon fibers were fast enough (i.e. 24°C/ sec).

The electrical conductivity of nickel coated short carbon fiber was higher than hybrid filler. At 20wt.-% of nickel coated short carbon fibers, electrical conductivity was 7340 S/m. While electrical conductivity of hybrid filler (18-6wt.-% concentration) was 4009 S/m. The higher heating of nickel coated short carbon fiber may be due to the higher electrical conductivity. Thermal conductivity of nickel coated short carbon fiber was not consistent at lower filler concentrations; however, at 18wt.-% nickel coated short carbon fiber an almost 100% increase was observed.

Magnetic properties testing were also performed to establish the relationship of filler concentration and heating rate. Hysteresis loop area of nickel coated short carbon fibers and hybrid filler was compared by using the remanence and coercitivity values. In the testing, hybrid filler was well ahead than nickel coated short carbon fibers. It showed that magnetic hysteresis heating contribution was higher in hybrid filler. IR thermal images also showed that the magnetic hysteresis heating mechanism was dominant in nickel coated short carbon fiber and hybrid filler. However, the magnetic hysteresis heating mechanism was more enhanced in hybrid filler.

Susceptor sheet based inductive heating for joining of non-conductive and non-magnetic composites materials is very good solution. In fiber filled susceptor sheets, heating is based on joule losses and junction losses. Due to nickel coating, magnetic hysteresis heating also contributes to the heating rate. Fibers were unidirectionally aligned and were interconnect between layers that made a dense network. In hybrid filled susceptor sheets, magnetic hysteresis heating was the dominant heating mechanism. Overall, heating was obtained due to several junctions by dielectric and contact resistance as well as intrinsic resistance.

Nickel coated short carbon fiber filled susceptor sheets offer a solution to joining of non-conductive thermoplastic composites. The addition of multi-walled carbon nano-tubes with nickel coated short fibers further increases the heating rate allowing processing time to be further reduced.

6. Summary

A susceptor sheet for induction heating application of non-conducting and non-magnetic thermoplastic composites was developed. Induction heating is a contact-less joining technique. Heat can be generated by an alternating electromagnetic field by joule losses and magnetic hysteresis. Heat is generated by intrinsic resistance of the filler material by joule losses. Ferromagnetic materials generate heat by magnetic hysteresis.

Induction heating depends on fillers properties as well as processing parameters. Experimental work was performed varying filler and filler concentration that has an effect on the electrical, thermal and magnetic properties and can affect the heating properties. On the other hand, process parameters like coil current, frequency and coupling distance can affect only the heating properties.

A good and homogeneous heating with 24°C/ sec heating rate was achieved with nickel coated short carbon fibers with a filler concentration of 15wt.-%. Polypropylene (PP) was used as the matrix and testing was performed at 30A and 456 kHz. Susceptor sheet thickness was 500µm. For a further increase in the heating rate, multi-walled carbon nanotubes were added and optimized at 3wt.-%. With the combination of 15wt.-% nickel coated short carbon fiber and 3wt.-% multi-walled carbon nanotubes, the heating rate was enhanced to 40°C/ sec. Polypropylene was used as the matrix and testing was performed at 30A and 337 kHz. Susceptor sheet thickness was 1mm. The addition of multi-walled carbon nanotubes enhanced the heating by making an effective conductive network.

Nickel coated graphite particles were well below the electrical percolation due to their low aspect ratio; therefore, heating was mainly from magnetic hysteresis. Nickel coated short carbon fiber and nickel coated graphite particles were combined to make a hybrid filler. The heating rate of the hybrid filler was slower than just nickel coated short carbon fibers. Susceptor sheet thickness in NiCGP/ PP, NiCSCF/ PP and NiCSCF/ NiCGP/ PP was 500µm.

Electrical conductivity and magnetic properties were influenced heating mechanism therefore their contribution was estimated. At 20wt.-% of nickel coated short carbon fibers, electrical conductivity was 7340 S/m. While electrical conductivity of hybrid filler (18-6wt.-% concentration) was 4009 S/m. The higher heating of nickel coated short carbon fiber may be due to the higher electrical conductivity. Magnetic properties were evaluated by hysteresis loop. Due to low coating thickness, nickel coated short carbon fibers were soft magnetic materials. Remanence and coercivity of nickel

coated short carbon fibers and hybrid filler were compared. Hybrid filler was well ahead in heating compared to nickel coated short carbon fibers. This shows that the magnetic hysteresis heating contribution was higher in hybrid filler.

Inducting heating has different heating mechanisms that depend on the filler's intrinsic resistance and structure. Magnetic hysteresis depends on hysteresis loss area. Heating due to joule losses and junction losses are dependent on the fiber and its distribution. Unidirectional short fiber showed well interconnected networks as well as head-tail junctions that contributed in heating. Nickel coating further added heating due to magnetic hysteresis. Therefore heating from nickel coated short carbon fiber was a combination of all heating mechanisms.

An IR thermal camera was used to measure temperature, and its images also describe the heating mechanisms. Joule losses showed heating at the outer region of coil; however, magnetic hysteresis concentrated heating on the center.

At lab scale, susceptor sheets were prepared by the addition of MWNTs and permalloy flakes with fibers separately. Heating of MWNTs/ NiCSCF filled polypropylene susceptor sheet was fast and homogeneous. The addition of small amount of MWNTs with fibers enhanced the heating rate. It is comparable with high filler concentrations of fibers and hybrid fillers filled susceptor sheet. However permalloy with fibers was good and homogeneous in heating.

7. References

[1]   Hull, D.: An introduction to composite materials, Cambridge University Press , 1981.

[2]   Harper, C. A.: Handbook of plastics, elastomers and composites, New York, 2002.

[3]   Leach, D. C.: "Continuous fibre reinforced thermoplastic matrix composites," Adv Compo, pp. 43-109, 1984.

[4]   Chang, I. Y.; Lees, J. K.: "Recent developments in thermoplastic composites: a review of matrix systems and processing methods," J Thermoplast Comp Mater , pp. 277-96, 1989.

[5]   Chawla, K. K.: Composite Materials: Science and Engineering, New York: Springer, 2012.

[6]   Burton, R.: Noising head. Aerospace Manufacturing, 2006

[7]   Räckers, B.: Verbundwerkstoffe im Airbus A380; in Kunststoffe im Automilbau, Mannheim, 2006.

[8]   Schlarb, A. K.: "Glassmattenverstärke thermoplaste, eine werkstoffklasse mit zukunft," Plastverarbeiter, 48, 10, pp. 87-90, 1997.

[9]   Bigg, J. R.; Preston, D. M.: "Stamping of thermoplastic matrix composites," Polymer Composites, 10, 4 , pp. 261-268, 1989.

[10]   O'Brien, K.; Kasturi, S. M. A.:"A computational analysis of the heating of glass mat thermoplastic (GMT) sheets by dual beam microwave sources," Polymer composites, 15, 3 , pp. 231-239, 1994.

[11]   Bigg, D. M.: "Processing-property relationship for pet sheet composites," Makromol. Chem., Makromol. Symp. 70/71, pp. 245-254, 1993.

[12]   Jacob, A.: Reinforced plastics, 45, 28, 2001.

[13]   Friedrich, H. E.; Leichtbau in der fahrzeugtechnik, Springer, 2013.

[14]   Hou, M.; Ye, L.; Mai, Y.-W.: "An experimental study of resistance welding of carbon fibre fabric reinforced polyetherimide (CF Fabric/PEI) composite material," Appl Compos Mater , pp. 35-49, 1999.

[15]   Neitzel, M.; Mitschang, P.: Handbuch Verbundwerkstoffe, München: Carl Hanser-Verlag, 2004.

[16]   Mitschang, P.; Blinzler, M.; Wöginger, A.: "Processing Technologies for continuous fiber reinforced thermoplastics with novel Polymer Blends," Composite science and technology, 63, 14 , pp. 2099-2110, 2003.

[17]   Vinson, J.: "Mechanical Fastening of Polymer Composites," *Polymer Engineering and Science 29,* pp. 1332-1339, 1989.

[18]   Kinloch, A. J.: Adhesion and Adhesives, Chapman and Hall

[19]   Lee, L.-H.: Adhesive Bonding, Plenum Press, 1991.

[20] Griese, R. A.; Silverman E. M.: "Joining methods for graphite/PEEK thermoplastic composites," *SAMPE J 25 (5),* pp. 34-38, 1989.

[21] Beevers, A.: "Welding: the way ahead for thermoplastics?," *Engineering ; 231:ACE11-2.,* 1991.

[22] Grimm. R. A.: "Welding processes for plastics," *Adv Mater Process ;147:27-30,* 1995.

[23] Stokes, V. K.: "Joining methods for plastics and plastic composites: an overview," *Polym Engng Sci 29:,* pp. 1310-24, 1989.

[24] Schwartz, M. M.: "Joining of composite materials," *ASM Int ,* pp. 35-88, 1994.

[25] Grimm, R. A.: "Fusion welding techniques for plastics," *Weld J ; 69: ,* pp. 23-8, 1990.

[26] Mitschang, P.; Rudolf, R.; Neitzel, M.: "Continuous Induction Welding Process, Modelling and Realisation," *Journal of thermoplastic composite materials, vol 15,* 2002.

[27] Van Ingen, J. W.; Buitenhuis, A.; Van Wijngaarden, M.; Simmons, F.: "Development of the Gulfstream G650 Induction welded thermoplastic elevators and rubber" International SAMPE Symposium and Exhibition; SAMPE 2010.

[28] Lauster, F.: Elektrowärmetechnik, Stuttgart: B.G. Teubner Verlagsgesellschaft, 1963.

[29] Rudnev, V.; Loveless, D.; Cook, R.; Black, M.: Handbook of induction heating. Marcel Dekker AG, Basel, 2003.

[30] Ibeh, C. C.: Thermoplastic Materials – Properties, Manufacturing Methods, and Applications, CRC Press , 2011.

[31] Rotheiser, J.: Joining of plastics – handbook for designers and engineers, Hanser-Verlag, 1999.

[32] Benatar, A.; Grewell, D. A.; Park, J.: Plastics and composites Welding Handbook, Hanser-Verlag, 2003.

[33] Ehrenstein, G. W.: Handbuch Kunststoff-Verbindungstechnik, Munich: Hanser-Verlag, 2004.

[34] Ageorges, C.; Ye, L.: Fusion Bonding of Polymer Composites, London : Springer , 2002.

[35] Gutowski, T. G.: Advanced composite manufacturing., New York: Wiley, 1997.

[36] Macguire, D. M.: "Joining thermoplastic composites," *SAMPE J. 25 (1),* pp. 11-4, 1989.

[37] Bayerl, T.; Duhovic, M.; Mitschang, P.; Bhattacharyya, D.: "The heating of polymer composites by electromagnetic induction – A review," *Composites: Part A 57,* pp. 27-40, 2014.

[38] Wool, R. P.; O'Connor, K. M.: "Time dependence of crack healing", Journal of polymer science, *Polymer letters Edition 20, issue 1,,* pp. 7-16, 1982.

[39] Kegel, K.: Elektrowärme – Theorie und Praxis, Essen: W. Girardet, 1974.

[40] Maxwell, J. C.: A Dynamical Theory of the Electromagnetic Field, Philosophical Transactions of the Royal Society of London, 1865.

[41] Haimbaugh, R. E.: Practical induction heat treating, ASM International, 2001.

[41] Bosse, G.; Wiesemann, G.: Grundlagen der Elektrotechnik II – Das magnetische Feld und die elektromagnetische Induktion, Düsseldorf: VDI-Verlag, 1996.

[43] Border, J.; Salas, R.: "Induction Heated Joining of Thermoplastic Composites without Metal Susceptors," *34th International SAMPE Symposium, May 8-11,* pp. 2569-2578, 1989.

[44] Kagan V. A.; and Nichols, R. J.: "Benefits of induction welding of reinforced thermoplastic welding of reinforced thermoplastics in high performance applications," *Journal of reinforced plastics and composites vol. 24, 13,* pp. 1345-1352, 2005.

[45] Yarlagadda, S.; Kim, H. J.; Gillespie, J. W. Jr.:"A Study on the Induction Heating of Conductive Fiber Reinforced Composites," *Journal of Composite Materials, 36, Issue 4,* pp. 401-421, 2002.

[46] Gillespie, J. W. Jr.; McCulough R. L.; Fink B. K.: "Induction heating of cross-ply carbon-fiber composites," *In ANTEC 92,* pp. 2106-9, 1992.

[47] Fink, B. K.; McCullough R. L.; Gillespie, J. W. Jr.: "A model to predict the through-thickness distribution of heat generation in cross-ply carbonfiber composites subjected to alternating magnetic fields," *. Comp Sci Technol ;55,* p. 119–30, 1995.

[48] Kim, B.-J.; Choi, W.-K.; Um, M.-K.; Park, S.-J.: "Effects of nickel coating thickness on electric properties of nickel/carbon hybrid fibers," *Surface & Coatings Technology 205 ,* p. 3416–3421, 2011.

[49] Suwanwatana, W.; Yarlagadda, S.; Gillespie, J. W. Jr.: "Hysteresis heating based induction bonding of thermoplastic composites," Composites Science and Technology 66, pp. 1713-1723, 2006.

[50] Svoboda, J.: Magnetic methods for the treatment of minerals, Amsterdam: Elsevier, 1987.

[51] Yarlagadda, S.; Fink, B. K.; Gillespie J. W. Jr.: "Resistive susceptor design for uniform heating during induction bonding of composites," J Thermoplast Comp Mater ;11, pp. 321-37, 1998.

[52] Meyer, E.: "Die Eisenverluste in elektrischen Maschinen (Dissertation)," ETH Zürich, Zürich, 1932.

[53] Bosse, G.; Wiesemann, G.: Grundlagen der Elektrotechnik II – Das magnetische Feld und die elektromagnetische Induktion, Düsseldorf: VDI-Verlag, 1996.

[54] Ahmed, T. J.; Stavrov, D.; Bersee, H. E. N.; Beukers, A.: "Induction welding of thermoplastic composites—an overview," Composites Part A: Applied Science and Manufacturing 37, 10, pp. 1638-1651, 2006.

[55]   Rudolf, R.; Mitschang, P; Neitzel, M.: "Induction heating of continuous carbon-fibre-reinforced thermoplastics," Comp Part A: Appl Sci Manufact , 31, pp. 1191- 1202, 2000.

[56]   Göktürk, H. S.; Fiske, T. J.; Kaylon, D. M.: "Effects of Particle shape and size distributions on the electrical and magnetic properties of nickel/ Polyethylene composites," Journal of Applied Polymer Science, 50, pp. 1891-1901, 1993.

[57]   Yamashita, S.; Hatta, H.; Sugano, T.; Murayama, K.: "Fiber Orientation control of short fiber composites: Experiement," Journal of Composite Materials, 23, pp. 23-32, 1989.

[58]   Bhattacharya, S. K.: Metal-filled Polymers (Properties and Applications), New York: Marcel Dekker, 1986.

[59]   Mamunya, Ye. P.; Muzychenko, Yu. V.; Pissis, P.; Lebedev, E. V.; Shut, M. I.: Percolation phenomena in polymers containing dispersed iron. Polym. Eng. Sci. 42 , pp. 90-100, 2002.

[60]   Kasap, S. O.: Principles of electronic materials and devices, Korea: Mc Graw-Hill , 2002.

[61]   Singh, J.: Quantum Mechanics: Fundamentals and Applications to Technology, New York: Wiley, 1997.

[62]   Clingerman, M. L.: Development and Modeling of Electrically Conductive Composite Materials, Michigan Technological University (Dissertation), 2001.

[63]   Demain, A.; Issi, J.-P.: "The effect of fiber concentration on the thermal conductivity of a Polycarbonate/ pitch-based carbon fibers composites," Journal of Composite Materials, 27, pp. 668-86, 1993.

[64]   Donnet, J.-B.; Bansal, R. C.; Wang, M.-J.: Carbon Black, New York: Marcel Dekker, Inc, 1993.

[65]   Grossiord N.; Loos, J.; Laake, L. C. van.; Maugey, M.; Zakri, C.; Koning, C.; Hart, A. J.: "High conductivity polymer nanocomposites obtained by tailoring the characteristics of carbon nanotube fillers," *. Adv Funct Mater ;18 (20),* pp. 3226-34, 2008.

[66]   Yu S.; Wong W. M.; Hu X.; Juay Y. K.: "The characteristics of carbon nanotube-reinforced poly(phenylene sulfide) nanocomposites," *Journal of Applied Polymer Science 113,* pp. 3477-83, 2009.

[67]   Zhang, Y.; Zou, Y.-W.; He, Y.: "Influence of graphite particles size and its shape on performace of carbon composites bipolar plate," *Journal of Zhejiang University Science, 6A,* pp. 1080-1083, 2005.

[68]   Yi, J. Y.; Choi, G. M.: Percolation behavior of conductor-insulator composites with varying aspect ratio of conductive fiber. *Journal of Electroceramics, 3:4, ,* pp. 361-369, 1999.

[69]   Dani, A.;   Ogale, A. A.: "Electrical percoaltion behavior of short fiber composites: experimental characterization and modeling," *Composites Science and Technology, 56, 8 ,* pp. 911-920, 1996.

[70] Blunk, R. H.; Lisi, D. J.; Yoo, Y.; Tucker III, C. L.: "AIChE Journal, 49," pp. 18-29, 2003.

[71] Drubetski, M.; Siegmann, A. N. M.: "Electrical properties of hybrid carbon black/carbon fiber polypropylene composites," *Journal of Material Science 42, 1,* pp. 1-8, 2007.

[72] Stucks A. D.; Parrott, J. E.: Thermal Conductivity of Solids, London: Pion Limited, 1975.

[73] Berman, R.: Thermal Conduction in Solids, Oxford: Claredon, 1976.

[74] Bird, R. B.; Stewart, W. E.; Lightfoot, E. N.: Transport Phenomena, New York: Wiley, 1960.

[75] Pierson, H. O.; Handbook of carbon, graphite, diamond and fullerenes: properties,processing and applications, New Jersey: Noyes Publications, 1993

[76] G., Wypych.; Handbook of fillers: physical properties of fillers and filled materials, Toronto, ChemTech Publishing, 2000

[77] Tekce, H. S.; DilekKumlutas, Tavman, I. H.: "Effect of Particle Shape on Thermal Conductivity of Copper Reinforced Polymer Composites," *Journal of reinforced plastics and composites, Vol. 26, No. 1,* 2007.

[78] King, Julia A.; Hauser, Rebecca A.; Tomson, Amanda M.; Wescoat, Isabel M.: Synergistic Effects of Carbon Fillers in thermally conductive liquid crytal polymer based resins, Journal of COMPOSITE MATERIALS, Vol. 42, No. 1, 2008

[79] Egelkraut, S.; Maerz, M.; Ryssel, H.: "Polymer bonded soft magnetic particles for planar inductive devices," in *Integrated Power Systems (CIPS), 5th International Conference*, 2008.

[80] Zhu, L.; Xie, D.; Ma, J.; Shao, J.; Shen, X.: "Fabrication of polydimethylsiloxane composites with nickel particles and nickel fibers and study of their magnetic properties.," *. Smart Mater. Struct. 22 ,* 2013.

[81] Hao, C.; Li, X.; Wang, G.: "Magnetic alignment of nickel-coated carbon fibers," *, Materials Research Bulletin 46,* pp. 2090-2093, 2011.

[82] Gray, D.: American Institute of Physics Handbook, New York: McGraw-Hill, 1972.

[83] Svoboda, J.: Magnetic Techniques for the Treatment of Materials, Amsterdam: Elsevier, 1987.

[84] Zinn, S.; Semiatin, S. L.: "Elements of induction heating – design, control, and applications," in *ASM International*, Metal Park, 1988.

[85] Moser. L.: Experimental analysis and modelling of susceptorless induction welding of high performace thermoplastic polymer composites., Kaiserslautern: IVW GmbH, 2012.

[86] Baehr, H. D.; Stephan, K.: Wärme- und Stoffübertragung, Heidelberg: Springer-Verlag, 2010.

[87] Welty, J. R.: Engineering heat transfer, New York: Wiley, 1974.

[88] Yang, H.-A.; Lin, C.-W.; Peng, C.-Y.; Fang, W.: "On the selective magnetic induction heating of iron scale structures," *J Micromech Microeng 16,* pp. 1314-20, 2006.

[89] Dutz, S.; Hergt, R.; Mürbe, J.; Müller, R.; Zeisberger, M.; Andä, W.; Töpfer, J.; Bellemann, M. E.: "Hysteresis losses of magnetic nanoparticle powders in the single domain size range," *J Magn Magn Mater 308,* pp. 305-12, 2007.

[90] Bayerl, T.: "Application of particulate susceptor for the inductive heating of polymer-polymer composites," Kaiserslautern, IVW GmbH, 2012.

[91] Suwanwatana, W.; Yarlagadda, S.; Gillespie, J. W. Jr.: "An investigation of oxidation effects on hysteresis heating of nickel particles," *J Mater Sci 38,* pp. 565-73, 2003.

[92] Suwanwatana, W.; Yarlagadda, S.; Gillespie, J. W. Jr.: "Hysteresis heating based induction bonding of thermoplastic composites," *Composites Science and Technology 66 ,* pp. 1713-1723, 2006.

[93] Noll, A.: Effektive Multifunktionalität von monomodal, bimodal und multimodal mit Kohlenstoff-Nanoröhren, Graphit und kurzen Kohlenstofffasern gefülltem PPS, Kaiserslautern, 2012.

[94] Chang, T. E.; Jensen, L. R.; Kisliuk, A.; Pipes, R. B.; Pyrz, R.; Sokolov, A.P.: "Microscopic mechanism of reinforcement in single-wall carbon nanotube/polypropylene nanocomposite," *Polymer 46,* pp. 439-44, 2005.

[95] Thostenson, E. T.; Ren, Z.; Chou, T-W.: "Advances in the science and technology of carbon nanotubes and their composites: a review," *Composites Science and Technology 61,* pp. 1899-912, 2001.

[96] Nogales, A.; Brozam G.; Roslaniec, Z.; Schulte, K.: Sics, I.; Hsiao, B. S.; Sanz, A.; Garcia-Gutierrez, M. C.; Rueda, D. R.; Domingo, C.; Ezquerra, T. A.: "Low percolation threshold in nanocomposites based on oxidized single wall carbon nanotubes and poly(butylene terephthalate).," Macromolecules 37, p. 7669–72, 2004.

[97] Lim, S. J.; Lee, J. G.; Hur, S. H.; Kim, W. N.: "Effects of MWCNT and nickel-coated carbon fiber on the electrical and morphological properties of polypropylene and polyamide 6 blends," Macromol. Res. 22, 6, pp. 632-638, 2014.

[98] Noll, A.; Burkhart, T.: "Morphological characterization and modelling of electrical conductivity of multiwalled carbon nanotuebs/ Poly(p-Phenylene Sulphide) nanocomposites obtained by twin screw extrusion," Compos. Sci. Technol., 71, 499, 2011.

[99] Dresselhaus, M. S.; Lin, Y. M.; Rabin, O.; Jorio, A.; Souza Filho, A.G., Pimenta, M. A.; Saito, R.; Samsonidze, Ge. G.; Dresselhaus, G.: "Nanowires and nanotubes," Mat. Sci. Eng. C 23, pp. 129-140, 2003.

[100] Standard DIN EN ISO 3915. [Performance]. 1999.

[101] Rizvi, R.; Naguib, H.: "Piezoresistance characterization of PVDF-MWNT nancomposites," ICCM 19.

[102] "Standard ASTM E1225 – 04".

[103] "Hüttinger Elektronik GmbH + Co. KG: TruHeat HF 5010," in Technical Description. Company publication, no. 24148352 EN, 2010.

[104] Mironov, V. S.; Kim, S. Y.; Park, M.: "Electrical properties of polyethylene composite films filled with nickel powder and short carbon fiber hybrid filler," Carbon Letters Vol. 14, No. 2, pp. 105-109 , 2013.

[105] Weber, M.; Kamal, M. R.:"Microstructure and volume resistivity of composites of isotactic polypropylene reinforced with electrically conductive fibers," Polym. Comp., 18(6) , pp. 726-740, 1997.

[106] Barsoukov, E.; Macdonald, J. R.: Impedance Spectroscopy Theory, Experiment, and Applications, Wiley, 2005.

[107] Goto, Y.: "Dielectric behavior in ferroelectric Pb5Ge3O11 powders," J. Phys. Soc. Jpn 50(2) , pp 538-542, 1981.

[108] Jonscher, A. K.; Reau, J.-M.:"Analysis of the complex impedance data for β-PbF2,"J. Mater. Sci. 13, pp. 563-570, 1978.

[109] Chaki, T. K.; Khastgir, D.; Das, N. C.: "Effect of filler blend composition on the electrical and mechanical properties of conductive EVA based composites,"Polym Comp 8 (6), p. 395, 2000.

[110] Das, N. C.; Chaki, T. K.; Khastgir, D.; Chakraborty, A.: "Effect of processing parameters, applied pressure and temperature on the electrical resistivity of rubber-based conductive composites," Carbon , vol. 40, pp. 807-816, 2002.

[111] http://www.professionalplastics.com/professionalplastics/ThermalPropertiesof PlasticMaterials.pdf

[112] Chauhan, D.; Singhvi, N.; Singh, R.: "Effect of Geometry of Filler Particles on the Effective Thermal Conductivity of Two-Phase Systems," International Journal of Modern Nonlinear Theory and Application, 1, 40-46 , pp. 40-46, 2012.

[113] Serguei, M.; Lebedev, Olga S. Gegle, Serguei N. Tkachenko, "Metal–polymer PVDF/nickel composites and evaluation of their dielectric and thermal properties," *J. Electrostat. 68 122–7,* pp. 122-7, 2010.

[114] Mansour, S. H.; Gomaa, E.; Bishay, I. K.: "Effect of metal type and content on mechanical, electrical and free-volume properties of styrenated polyesters," *J. Mater. Sci. 42,* pp. 8473-80, 2007.

[115] Rusu, M.; Sofian, M.; Rusu, D.: "Mechanical and thermal properties of zinc powder filled high density polyethylene composites," *Polym. Test. 20 ,* pp. 409-17, 2001.

[116] Khaibullin, R. I.; Popok, V. N.; Bazarov, V.V.: "Ion synthesis of iron granular films in polyimide," *Nucl. Instrum. Methods B 191,* pp. 810-4, 2002.

[117] Jamal, E. M. A.; Joy, P. A.; Kurian, P.; Anantharaman, M. R.: "Synthesis of nickel–rubber nanocomposites and evaluation of their dielectric properties," *Mater. Sci. Eng. B 156,* pp. 24-31, 2009.

[118] Bosse, G.; Wiesemann, G.: Grundlagen der Elektrotechnik II – Das magnetische Feld und die elektromagnetische Induktion, Düsseldorf: VDI-Verlag, 1996.

[119] Shengfei, H.; Hui, L.; Xiangxing, C.; Chong, Z.; Zuifang, L.: "The Electrical Conductive Effect of Nickel-coated Graphite/ Two-component Silicone-rubber Sealant," *Journal of Wuhan University of Technology-Mater. Sci. Ed. June ,* 2013.

[120] Anhalt, M. "Magnetische Eigenschaften weichmagnetischer Composite," Dissertation, TU Clausthal,, 2008.

[121] Miller, A. K.: "The nature of induction heating in graphite-fibre, polymer–matrix composite materials.," *SAMPE Journal 26 (4),* pp. 37-54, 1990.

[122] Fink, B. K.; McCullough, R. L.; Gillespie, J. W. Jr.: "A local theory of heating in cross-ply carbon fibre thermoplastic composites by magnetic induction," Composite Materials, University of Delaware, USA. CCM-Report.

[123] Kim, H.; Yarlagadda, S.; Gillespie, J. W. Jr.; Shevchenko, N. B.; Fink, B. K.: "A study on the induction heating of carbon fibre reinforced thermoplastic composites," *Adv. Composite Mater,* vol. 11, No. 1, pp. 71-80, 2002

[124] Border, J.; Salas, R.: "Induction heated joining of thermoplastic composites without metal susceptors," *34th International SAMPE Symposium, 2569-2578,* 1989.

[125] Stacey, F. D.; Banerjee, S. K.: The physical principles of Rock Magnetism, Amsterdam: Elsevier, 1987.

[126] Orfeuil, M.: Electric process heating. Technologies, equipment, applications,, Ohio: Battelle Press, 1987.

[127] Acher, O.; Adenot, A. L.: "Bounds on the dynamic properties of magnetic materials," *Phys. Rev. B, vol. 62, no. 17,* pp. 11324-11327, 2000.

[128] Leuchtmann, P.: Einführung in die elektromagnetische Feldtheorie,, München: Pearson Studium, 2005.

[129] Yarlagadda, S.; Fink, B. K.; Gillespie, J. W. Jr.: "Resistive susceptor design for uniform heating during introduction bonding of composites.," *Journal of Thermoplastic Composite Materials 11 (7),* pp. 321-37, 1998.

[130] Yoshida, S.; Sato, M.; Sugawara, E.; Shimada, Y.: "Permeability and electromagnetic inteference charcteristics of Fe-Si-Al alloy flakes polymer composites," *J. Appl. Phys., vol. 85, no. 8,* pp. 4636-4638, 1999

[131] XR, Xiao; SV, Hao; KN, Street, Development of fusion bonding repairof thermoplastic resin composites, Proceedings of ICCM-8, Honolulu 1991

8. List of Publications

Conferences

[1]   Muddassir, M.; Gurka, M.:Effect of nickel coated carbon fibers and nickel coated graphite particles on induction heating. 20[th]International Conference on Composite Materials, Copenhagen, Denmark, 19-24 July 2015

9. List of Supervised Student Research and Graduation Projects

1. Naik, Rahul: In co-operation of MWCNT with Nickel coated Carbon fiber & Graphite particles to enhance electrical conductivity for Induction Heating, IVW-Bericht 15-016, Institut für Verbundwerkstoffe GmbH, Kaiserslautern, Studienarbeit, 2015

2. Gökkaya, Sebahattin: The effect of Permalloy, and nickel-coated graphite particles to the electrical conductivity and the inductive heatability of thermoplastic composites of polypropylene and nickel-coated carbon fibers. IVW-Bericht 15-083, Institut für Verbundwerkstoffe GmbH, Kaiserslautern, Diplomarbeit, 2015

10. Curriculum Vitae

Personal Data

Name: Muhammad Muddassir

Address: Karachi, Pakistan

Career:

1989 – 1990	Matriculation, Mirpurkhas (Pak)
1990 – 1992	Intermediate (FSc), Mirpurkhas (Pak)
1995 – 2001	NED University of Engineering and Technology, Karachi (Pak) Course of Studies: Chemical Engineering
2001-2006	Assistant Manager (R&D), SUPARCO Karachi (Pak)
2006 – 2007	The University of Sheffield, Sheffield, England Course of Studies: Polymer and Polymer Composites Degree: MSc
2007 – 2012	Manager (R&D), SUPARCO Karachi (Pak)
2012 – Today	Research Associate at Institut für Verbundwerkstoffe GmbH, Kaiserslautern